AD-A166 262 A GAUSSIAN WAVE PACKET METHOD FOR STUDYING TIME DEPENDENT QUANTUM MECHANI..(U) CALIFORNIA UNIV SANTA BARBARA QUANTUM INST S SAWADA ET AL. FEB 86 TR-7 1/1

UNCLASSIFIED N00014-81-K-0598 F/G 20/10 NL

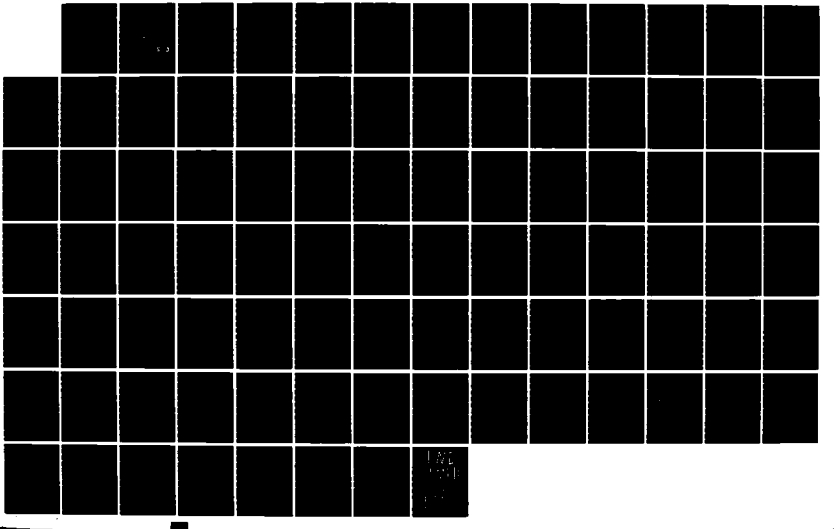

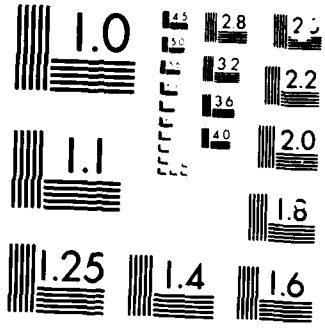

(12)

SECURITY CLASSIFICATION OF THIS PAGE (When Data Entered)

REPORT DOCUMENTATION PAGE		READ INSTRUCTIONS BEFORE COMPLETING FORM
1. REPORT NUMBER: 7	2. GOVT ACCESSION NO.	3. RECIPIENT'S CATALOG NUMBER
4. TITLE (and Subtitle): A GAUSSIAN WAVE PACKET METHOD FOR STUDYING TIME DEPENDENT QUANTUM MECHANICS IN A CURVE CROSSING SYSTEM: LOW ENERGY MOTION, TUNNELING AND THERMAL DISSIPATION		5. TYPE OF REPORT & PERIOD COVERED: Annual Technical Report 6. PERFORMING ORG. REPORT NUMBER
7. AUTHOR(s): Shin-Ichi Sawada and Horia Metiu		8. CONTRACT OR GRANT NUMBER(s): N00014-81-K-0598
9. PERFORMING ORGANIZATION NAME AND ADDRESS: University of California, Quantum Institute, Santa Barbara, CA 93106		10. PROGRAM ELEMENT, PROJECT, TASK AREA & WORK UNIT NUMBERS: NR 056-766/4-21-81 (472)
11. CONTROLLING OFFICE NAME AND ADDRESS: Office of Naval Research, Department of the Navy, Code: 612A: DKB, Arlington, VA 22217		12. REPORT DATE: February 1986 13. NUMBER OF PAGES: 85
14. MONITORING AGENCY NAME & ADDRESS (if different from Controlling Office): Office of Naval Research Detachment Pasadena, 1030 East Green Street, Pasadena, CA 91105		15. SECURITY CLASS. (of this report): unclassified/unlimited 15a. DECLASSIFICATION/DOWNGRADING SCHEDULE

16. DISTRIBUTION STATEMENT (of this Report)

This document has been approve for public release and sale; its distribution is unlimited.

17. DISTRIBUTION STATEMENT (of the abstract entered in Block 20, if different from Report)

This document has been approved for public release and sale; its distribution is unlimited.

18. SUPPLEMENTARY NOTES

Accepted: J. Chem. Phys.

19. KEY WORDS (Continue on reverse side if necessary and identify by block number)

quantum mechanics, thermal dissipation

20. ABSTRACT (Continue on reverse side if necessary and identify by block number)

We explore numerically the behavior of a method of describing the time dependent quantum mechanics of a curve crossing system. The two nuclear wave functions corresponding to the two electronic states are each described by a Gaussian wave packet. The packet describing the incident state mimics the initial wave function, and the other packet is created by the time dependent Schroedinger equation. They are both propagated by using a variational method. The packets interact and we do not assume that they have a small width. Exploratory calculations are made for curve crossing dynamics at low

DD FORM 1 JAN 73 1473 EDITION OF 1 NOV 65 IS OBSOLETE
S/N 0102-LF-014-6601

kinetic energy above the barrier of the lowest adiabatic state, for tunneling, for multiple crossings, and for a curve crossing system which is strongly coupled to a harmonic bath whose motion is described by a mean trajectory classical Langevin method.

OFFICE OF NAVAL RESEARCH

Contract N00014-81-K-0598

Task No. NR 056-766/4-21-81 (472)

Technical Report No. 7

A GAUSSIAN WAVE PACKET METHOD FOR STUDYING TIME DEPENDENT QUANTUM MECHANICS IN A CURVE CROSSING SYSTEM: LOW ENERGY MOTION, TUNNELING AND THERMAL DISSIPATION

by

Shin-Ichi Sawada and Horia Metiu

J. Chem. Phys. accepted (1985)

University of California
Department of Chemistry
Santa Barbara, CA 93106

A Gaussian Wave Packet Method for Studying Time Dependent Quantum Mechanics in a Curve Crossing System: Low Energy Motion, Tunneling and Thermal Dissipation

Shin-Ichi Sawada and Horia Metiu

Department of Chemistry
University of California, Santa Barbara
Santa Barbara, California 93106

ABSTRACT

We explore numerically the behavior of a method of describing the time dependent quantum mechanics of a curve crossing system. The two nuclear wave functions corresponding to the two electronic states are each described by a Gaussian wave packet. The packet describing the incident state mimics the initial wave function, and the other packet is created by the time dependent Schroedinger equation. They are both propagated by using a variational method. The packets interact and we do not assume that they have a small width. Exploratory calculations are made for curve crossing dynamics at low kinetic energy above the barrier of the lowest adiabatic state, for tunneling, for multiple crossings, and for a curve crossing system which is strongly coupled to a harmonic bath whose motion is described by a mean trajectory classical Langevin method.

I. INTRODUCTION

I.1 Description of the problem and its solution.

Several recent papers[1-5] have shown that the Gaussian wave packet (GWP) method, originated by Heller and his coworkers[6] and developed by him and others[6-13], can be very useful in treating atom diffraction,[1] H_2 diffraction,[2] H_2 rotational excitation[2] and H_2 and Br_2 vibrational excitation by collision with a rigid lattice,[3] as well as atom diffraction caused by collision with a surface undergoing thermal motion.[4]

The experience accumulated so far shows that the application of the GWP method to surface science problems is very promising. Satisfactory accuracy can be obtained with a relatively small amount of computer time, and the results are easy to interpret in terms of simple, intuitive, classical-like concepts.

There is however a group of problems for which the application of the GWP method, in the form practiced so far, meets with conceptual difficulties. A good example is the adsorption of a Li atom approaching a metal surface at thermal energies. It is widely believed that this process should be described by a curve crossing model, in which Li sticking is a transition from a neutral to an ionic state. Since the motion of the Li atom is nearly classical it seems profitable to try to describe it by using Gaussian wave packets. A correct GWP description of such a process requires the splitting of the incident packet into two packets, one representing the ion bound to the surface and the other the neutral backscattered into the vacuum. Packet splitting is also required for describing sticking caused by tunneling, by excitation of internal modes of the molecule, by excitation of modes in the solid or by transfer of energy from perpendicular to parallel translational modes. The GWP methods employed so far[1-13] conserve the number of packets and can describe the above processes only if they are suitably modified. In this paper we present such a modification.

To describe the main ideas we consider the case of a Li atom approaching a metal surface. This is characterized by a wave

function of the form

$$\psi(x,R;t) = G_1(R;t)\Phi_1(x,R;t) + G_2(R,t)\Phi_2(x,R;t) \ , \quad (I.1)$$

where $\Phi_1(x,R)$ is the ionic state and $\Phi_2(x,R)$ is the neutral one; $G_1(R;t)$ and $G_2(R;t)$ are the nuclear wave functions associated with the electronic states Φ_1 and Φ_2; R and x represent all the nuclear and electronic coordinates, respectively. The GWP method assumes then that G_1 and G_2 are Gaussian wave packets of the kind used by Heller:[6]

$$G_i(R;t) = \exp\{(i/\hbar)[\alpha_i(t)(R-R_i(t))^2+P_i(t)(R-R_i(t)+\gamma_i(t)]\} \quad (I.2)$$

If a neutral Li atom approaches the surface, we have initially $G_1(R;t)\equiv 0$, while the parameters in $G_2(R;t)$ are determined by the properties of the incident atom (i.e. direction of incidence, kinetic energy, etc.) The approach of the Li atom to the surface can be described by the usual GWP method, up to the point where the transition to the ionic curve starts taking place. This transition is equivalent to the birth of a second packet, namely $G_1(R;t)$. As the time evolves the two packets interact with each other and build up the correct ionization probability $|G_1(R;t)|^2$.

To handle this situation the GWP procedure must be extended in several ways. First, we must find a way of creating G_1, at the proper moment; we use for this a short time Green's function which generate G_1 from G_2, through the coupling between the ionic and the neutral states. Once the new packet is created, it must interact with the initial one, so that their joint evolution leads to the correct ionization probability. This is achieved by using the minimum error method.[10] Finally, we do not assume that the packets are narrow throughout the interaction region since this approximation exagerates the classical character of the Li^+ motion and leads to errors.[8,11]

I.2 Applications

The resulting MEM split Gaussian wave packet (MEM-SGWP) method can be used to explore several physical and computational issues pertinent to the above model. First we investigate whether the split packets behave reasonably and whether SGWP is numerically stable; then we examine several simplified versions of the theory to see whether they work well. Numerical studies meant to answer such questions are presented in Section III.2.

A more subtle and uncertain matter is whether SGWP can generate tunneling behavior, that is, whether an incident packet whose energy is below the height of the barrier on the lowest adiabatic potential, can be split to create a packet behind the barrier. The customary GWP method will not permit tunneling since the center of the incident packet moves on a classical trajectory. Calculations demonstrating tunneling behavior are presented in Section III.3.

Further numerical calculations (Section III.4) attempt to establish when a two state description is necessary and what are the consequences of this necessity. Even in those cases (e.g. charge transfer) where a two diabatic state description is convenient it does not always follow that a two state description is also needed in the equivalent adiabatic representation. We expect to need two adiabatic states when the energy of the incident packet is comparable with gap between the states. In such cases the "transmission" of the wave function, through the region where the two adiabatic states are closest to each other, is impaired as if the upper state helps "reflect" the incident packet. Calculations showing that SGWP generates such behavior are presented in Section III.4.

In a one dimensional system the creation of a packet on the ionic state does not lead to binding: the ionic packet oscillates in the well and splits into an outgoing neutral packet and an ionic packet whenever it goes through the crossing region. Repeated occurrence of this process makes the amplitude of the nuclear ionic state go to zero. The above sequence is the GWP

description of a predissociation process. The calculations presented in Section IV show that a multiple crossing SGWP model leads to such behavior.

Finally in Section V we explore the curve crossing behavior of a neutral atom which is ionized upon approaching a moving lattice. The manner in which the thermal lattice motion modifies the behavior of the packets is described by coupling the MEM-SGWP equations to a mean trajectory classical Langevin equation describing lattice motion. In surface science such a model is relevant with regard to sticking of alkali, which is believed to require a two state description; previous work on adsorption-desorption dynamics[14,15] considered one energy surface only. The calculation is also relevant to the problem of tunneling in systems subject to thermal noise, which has received a lot of attention lately.[16]

All the calculations presented here are exploratory and intend to test the qualitative behavior of SGWP. We plan to study the accuracy of the method once we develop an exact procedure for solving the problems described above.

I.3 Other methods

Most of the existing work applying curve crossing models to surface science problems[17-32] has often been concerned with high kinetic energy phenomena, where sticking is not an issue and classical approximations of varying quality are fairly adequate. Here we are especially concerned with the limit of very low kinetic energy where single classical trajectory methods are not likely to be useful and quantum effects (both for the electronic excitation and perhaps the motion of the light atom) are important.

There are a number of approaches, other than GWP, that might be usefully applied to the problem of interest here. The mean trajectory approximation (MTA)[28-29, 32-39] uses one classical trajectory to describe the motion of the nucleus. The two state aspects of the problem are partly incorporated by using in the classical equation an average potential energy which includes

contributions from both the ionic and the neutral surfaces, in proportion to their instantaneous occupation (see Section III for details). Recent calculations[39] show that at low kinetic energies the method leads to unphysical behavior.

WKB theory has been extended to curve crossing problems[40-43] and its main limitation, as far as surface science is concerned, is the difficulty of extending it to three dimensions.

The multiple trajectory method of Tully and Preston[44] is frequently critized because it neglects interference effects; since these are likely to be washed out by thermal averaging (when coupling to phonons is included) this is not a significant flaw here. A potentially important limitation is that it will miss quantum effects for light particles.

Another fruitful line of research was originated by attempts to implement and/or simplify the semi-classical method developed in several elegant papers of Pechukas.[45] Straight applications of Pechukas' method led to inefficient numerical codes and numerical instabilities.[46] The simplifications introduced by George and Miller[47] offer some remarkable insights in the physics of the problem, but have not yet reached the computational simplicity characterizing the GWP approach.

Finally Herman and Freed's implementation[48a] of early work of Laing and Freed[49b] leads to an interesting method which however seems rather difficult to apply, especially for many dimensions.

In this context SGWP has several appealing features: it is easy to use in three dimensions; it is computationally efficient; and it provides an intuitive classical-like description of time dependent quantum mechanical process.

II. THE MODEL

II.1 The Hamiltonian

We consider a system described by two diabatic[49] electronic states $\Phi_i(x,R)$, $i = 1,2$ and the Hamiltonian matrix

$$H_{ij}(R) = \int dx \Phi_i(x,R) H(x,R) \Phi_j(x,R) \ , \qquad (II.1)$$

with

$$H_{ii}(R) = W_o\{\exp[-2\alpha(R-R_o)] + (-i)^j \exp[-\alpha(R-R_o)]\} + (-1)^{i-1}\Delta\epsilon/2 \qquad (II.2)$$

and

$$H_{ij} = (\beta\Delta\epsilon/2) \exp\{-\alpha^2(R-Re)^2\} \qquad (II.3)$$

The "ionic curve" H_{11} is a Morse potential whose asymptotic energy (i.e. the energy for $R\to\infty$) is not zero, as customary, but $\Delta\epsilon/2$. The asymptotic energy gap between the two states (i.e. the "ionization potential") is $\Delta\epsilon$. The binding energy of the ion to the surface is U_o and β is a constant characterizing the strength of the coupling between the states. The off diagonal element H_{12} peaks at $R=R_c$ which is the position where H_{11} and H_{12} cross.

The values of the parameters used in the calculations presented here are listed in Table I. The corresponding Hamiltonians are called Hamiltonian I and II. In Figs. 1, and 4 we plot the diabatic potential surfaces, the adiabatic ones and the coupling H_{12} for these Hamiltonians.

Since Φ_i, i=1,2 are diabatic states the coupling between them takes place through H_{12}; therefore, for simplicity, we ignore other coupling terms and set[49]

$$\int dx \ \Phi_i(\infty,R)^* \frac{\partial^n}{\partial R^n} \Phi_j(x,R) = \delta_{ij}\delta_{no} \ . \qquad (II.4)$$

Using the wave function (I.1) and the conditions (II.4) in the time dependent Schrodinger equation leads to

$$i\hbar\partial G_i(R,t)/\partial t = (K + H_{ii}(R))G_i + H_{ij}G_j \ , \qquad \text{(II.5)}$$

where K is the kinetic energy operator. We solve this equation under the assumption (which is the essence of Heller's method) that the functions G_i have the form (I.2) and maintain it at all times; the effect of the collision is to change the parameters appering in (I.2). In the present work we derive differential equations and initial conditions for α_i, R_i, P_i and γ_i and solve them numerically for the problems specified in Section I.

II.2 The initial conditions

II.2.a. The creation of a new packet

Consider, for illustration, the case when the colliding particles are initially in the electronic state 2. The parameters of the packet $G_2(R;t)$ are determined by the initial conditions, which also set $G_1(R;t) \equiv 0$.

Since all Heller-like methods conserve the number of Gaussians, we must make a modification that will split the incident packet into a "neutral" and an "ionic" one. To achieve such splitting we use the formal solution of Eq. (II.5):

$$|G_1(t)\rangle = |G_1(t_o)\rangle - (i/\hbar)\int_{t_o}^{t} dt' \exp(-(i/\hbar)[K+H_{11}](t-t'))H_{12}|G_2(t')\rangle \qquad \text{(II.6)}$$

Here t_o is the time at which the packet $|G_2(t_o)\rangle$ begins to overlap spatially with H_{12}. This is the last time step in the integration of the differential equation (II.5) for which we can maintain $|G_1(t_o)\rangle = 0$. In the next time step we must create a new packet $|G_1(t_o+\tau)\rangle$ whose functional form is determined from (II.6). By using a very small value for τ we can replace the integral with $\tau \exp(-(i/\hbar)[K+H_{11}]\tau)H_{12}|G_2(t_o)\rangle$ and the exponential operator with its short time limit.[50] This gives

$$G_1(R;t_o+\tau) = -(i\tau/\hbar)(m/2\pi i\hbar\tau)^{1/2}$$

$$\int dR' \exp\{(i/\hbar)[(m/2\tau)(R-R')^2 - H_{11}(R')]\}$$

$$H_{21}(R')G_1(R;t_o) \qquad (II.7)$$

Generally the function $G_1(R;t_o+\tau)$ is not a Gaussian. However, since τ is arbitrarily small we can use - with arbitrary accuracy- the stationary phase approximation which replaces $H_{11}(R')$ with it's second order expansion in powers of $(R-R')$. Since in the present model $H_{21}(R')$ and $G_1(R';t_o)$ are both Gaussians, the use of the above expansion allows us to perform the integral in (II.7) analytically; this gives for $G_1(R;t_o+\tau)$ a Gaussian.

We can summarize this whole procedure by stating that we generate G_1 from G_2 by using first order perturbation theory with respect to the small parameter τH_{12}, and a stationary phase approximation with respect to the large parameter $ml^2/\hbar\tau$, where l is a length over which the potential H_{11} changes. Both approximations are arbitrarily accurate since τ is arbitrarily small.

II.2.b <u>The initial parameters of the incident packet</u>

Since in all GWP methods the parameters of the Gaussian wave packets evolve according to first order differential equations, the theory is not defined unless it provides a prescription for the choice of the initial conditions. In the GWP method this simple requirement can become a delicate and ambiguous matter.

In general, the time dependent theory of collisions uses an initial wave function which mimics the pre-collision state prepared by the experimental set up. This causes difficulties for the GWP theories since it is unlikely that anyone would want to do - at least in the foreseable future - experiments in which the initial state is a narrow wave packet. To understand why this is the case we consider how an idealized experiment of this kind might be done. We can prepare a wave packet by measuring the position of the "projectiles" (i.e. the incident molecules) before they reach the surface. To do this we must intersect the projectiles beam with a probe beam designed to overlap with it in

a very small volume l^3. In such an arrangement the deflection of a probe particle at the time t_o signals the fact that a projectile was present in the volume l^3. The state of that projectile can be adequately described by a packet of width l, whose center was located in the probe volume at t_o. The packet thus formed continues to travel towards the surface, collides with it and is scattered into the detector; the particles in a plane state - which went undisturbed through the volume - have the same fate. The detector registers the arrival of both the packet and the plane wave and cannot distinguish between them. To measure only the arrival of the deflected wave packets we must lower the flux of incident projectiles to the point that whenever a projectile scattered by the surface is detected in coincidence with the deflection of a probe particle we can be fairly certain that we are dealing with packet scattering.

Since there is a very low probability that such difficult experiments will be performed we must decide what is the experimental significance of these GWP calculations. One point of view[10] is that in all experiments - other than the one described above - the packets have no reality. They are merely "pieces" of the wave function, introduced for computational convenience, and only the coherent sum of such packets - which represents the total wave function - has any meaning. Therefore the choice of the initial parameters in each Gaussian G_α should be made so that $\Sigma\, G_\alpha$ best fits the initial wave function.[10]

Another point of view is that a Gaussian wave packet state is a limiting case in quantum mechanics, which we might call corpuscular (as opposed to wave like), which provides a reasonable description of a semi-classical time dependent processes. This is the point of view which, for the sake of simplicity, is adopted here.

Unfortunately this interpretation does not provide a prescription for choosing the initial values of all packet's parameters. We can choose $R_2(t=0)$ so that the packet is just

outside the interaction zone; we can select $P_2(t=0)^2/2m$ to give the initial energy (there is a slight error involved in doing this); we can choose a normalized packet and thus have $\exp\{-2Im\gamma_2/\hbar\}(\hbar\pi/2Im\alpha_2)^{1/2} = 1$. Since the initial phase of the packet is irrelevant we can choose $Re\gamma_2(t=0)=0$. We are thus left with two unknown parameters, $Re\alpha_2(t=0)$ and $Im\alpha_2(t=0)$.

To get the calculation started one customarily follows Heller[6] who recommends a choice of parameters that would give a narrow minimum uncertainty wave packet at the most important point on the trajectory. In potential scattering this point is the turning point.[6] In the present case there is some ambiguity since we can choose either the crossing point or the turning point, which are both important. We have selected the former on the subjective belief that the transfer from one curve to another is the most important event in the present system. Therefore we use the equations of motions for $Re\alpha(t)$ and $Im\alpha(t)$ to select the initial values $Re\alpha(t=0)$ and $Im\alpha_2(t=0)$ that will give $Re\alpha_2(t_c)=0$ and a small width $l_2(t_c) = (\hbar/2Im\alpha_2(t_c))^{1/2}$, at the time t_c at which the center of the packet G_2 reaches the crossing position R_c. Specifically we chose $Re\alpha_2(t_c)=0$ and a large value for $Im\alpha_2(t_c)$ and perform a backward propagation from R_c to the initial position $R_2(0)$, by using the equations of motion for $Re\alpha_2$ and $Im\alpha_2$ on the surface $H_{22}(R)$, without any coupling to the state 1.

We note that we see no compelling a priori reason to follow Heller's recommendations. There is some a posteriori justification since in the past[1-6] such choices led to accurate results which were stable with respect to variations of the initial values chosen for $\alpha(t=0)$.[1-4,6] We find that the same stability exists in the present system but we do not necessarily expect this to be the case for new problems of a different character. At this time we regard this ambiguity as a temporary nuisance which can be avoided by using GWP-s to fit the initial wave function that is prepared experimentally.

II.3 <u>The propagation of the wave packets</u>

Once the parameters of the initial G_2 packet are chosen and

the new G_1 packet is created we must select a scheme for their propagation. The simplest Heller scheme[6] assumes that the packets remain narrow throughout the collision. and move independently. Skodje and Truhlar,[8] and Heather and Metiu[9] have shown that the first assumption does not work well for packets which, like G_1, are trapped in an anharmonic well. The second assumption - which is reasonable for the problems that were of interest to Heller[6] - is untenable in the present case, since the amplitude of the packet G_1 must grow at the expense of that of G_2; this cannot be achieved if the packets are decoupled.

For these reasons we are using for the propagation a variational procedure[10] which we call the minimum error method (MEM) which does not make the assumptions mentioned above. The only approximation is that in the course of time the wave functions G_1 and G_2 remain Gaussians.

In working with other systems Sawada, Heather, Jackson and Metiu[10] have shown that sometimes the use of one Gaussian per electronic state does not offer enough flexibility in the variational wave function; improved accuracy can be obtained by using nuclear wave functions which are sums of Gaussians coupled to each other. We have developed such a method for the curve crossing problem and preliminary numerical tests show it to be rather expensive. Therefore at this time we prefer to use the present one-Gaussian-per-electronic-state model.

The variational equations obtained by using the minimum error method are given in the Appendix. The equations are transformed by using Heller's P-Z method[6] and the resulting differential equations are solved by using a fourth order Runge-Kutta method with variable step size.

II.4. Numerical details and the units.

All the calculations presented here were carried out with the Hamiltonians defined by Eqs. (II.1-3) and the parameters given in Table I. We use a "natural" system of units with α^{-1} for length, $(\alpha v_o)^{-1}$ for time and $\hbar\alpha v_o^{-1}$ for mass; the parameter α^{-1} controls the range of the potentials (see Eqs. II. (2-3)) and v_o

is the initial velocity. The latter is the expectation value of the velocity operator $-(i\hbar/M)\partial/\partial R$ for the initial wave packet and it is equal to $P_2(t)/M$, where $P_2(t)$ is the momentum of the packet G_2 (see Eq. I.2). An important quantity is Massey's parameter $\lambda = \Delta\epsilon/\hbar\alpha v_o$, which is the asymptotic energy gap $\Delta\epsilon$ (i.e. the ionization potential) in the energy units $\hbar\alpha v_o$.

The matrix elements H_{ij} corresponding to the parameters given in Table I are shown in Figs. 1, 4 and 8, together with the corresponding adiabatic states. On the same figures we have indicated by arrows the kinetic energies of the incident packets used in the present calculations. These are labelled by the values of the Massey parameter λ, whose inverse is proportional to the incident velocity. Note that for a particle in a GWP state G_2 the kinetic energy $\langle G_2|(-\hbar^2/2m)\partial^2/\partial R^2|G_2\rangle$ differs from the classical energy $P_2(t)^2/2m$ of the center of the packet. The difference, denoted $\Delta P_2^2/2m$, is shown in Table II, which also shows the values of λ, of $P_2^2/2m$ and the difference between the kinetic energy of the incident packet and the height of the barrier on the lowest adiabatic state. Note that $\Delta P_2^2/2m$ is very small compared to the "classical" kinetic energy of the packet $P_2(t=0)^2/2m$, because we use a spatially broad packet which has a narrow spread in the momentum space.

III. PACKET SPLITTING FOR ONE CROSSING

III.1 The behavior of SGWP method and its comparison with MTA and LHA.

In this section we report calculations with the Hamiltonian I, defined by Eqs. (II.1-3) and the parameters listed in Table I. The matrix elements H_{ij} as well as the corresponding adiabatic states are shown in Fig. 1. We examine the behavior of the packets generated by the split GWP method and compare them to that given by simplified versions of the theory.

Since we compare the present calculations (MEM) with the mean trajectory approximation (MTA) and the local harmonic approximation (LHA) we describe them briefly here. MTA assumes the wave function[28]

$$\psi(x,R;t) = G(R;t)[c_1(t)\Phi_1(x,R) + c_2(t)\Phi_2(x,R)] \ , \qquad \text{(III.1)}$$

where G is a GWP of the form (I.2). One can show[28] that the center of the Gaussian G moves according to Newton's equation with the force $-\Sigma\ \Sigma\ c_i^*(t)c_j(t)\partial H_{ij}(R)/\partial R$. While this force depends on the instantaneous populations of the two states and the phase difference between the corresponding amplitudes, it is unable to generate a nuclear motion which has a "two trajectories" character. This shortcoming is important only at low incident kinetic energy.

The local harmonic approximation (LHA) uses one packet for each electronic state and assumes[6] that G_1 and G_2 are narrow throughout the collision so that the integrals in which they are involved can be computed by the method of steepest descent or the stationary phase approximation. This simplifies the differential equations which give the evolution of the parameters in G_1 and G_2 and speeds up their integration. Physically the use of narrow Gaussian amounts to taking a semiclassical limit.

In all the calculations presented here we assume that the initial state is neutral. The packet G_2 is constructed as discussed in Section II.2b and the packet G_1 is created as

described in Section II.2a.

In Fig 2 we show how the centers of the two packets move, for various incident kinetic energies of G_2. The time evolution of the corresponding state occupation probabilities is shown in Figs. 3.

Let us examine in detail Fig. 2a which illustrates the motion of the two packets. At the initial time the center of the packet G_2 is located at $R_2 = 10$, and that of the newly created G_1 is at $R_1 = 8.2$. The new packet is closer to the crossing point located at R_c=5 (see Fig. 1)) than the incident one, but they are both far from it. After about 5 time units the packet G_1 catches up with G_2. In all the calculations carried out so far the new packet G_1 is created closer to the crossing point and G_2 catches up with it because its energy of (i.e. $\langle G_2|-\hbar^2\nabla^2/2m|G_2\rangle$) at the moment of G_1's birth is larger than that of G_1. At the time 6.5 the packet G_2 reaches its turning point, i.e. its center turns around and moves away from the surface. Note that the turning point of the center (at R=5.4) is not the classical turning point. This behavior is different from that given by the simplest version of Heller's theory - which makes the local harmonic approximation (LHA) - in which the center of the packet moves classically and turns at the classical turning point. As shown by Heather and Metiu[11] if LHA is not made the center of the packet does not move classically and behaves like a "fuzzy ball" which turns upon collision with a repulsive potential before its center reaches the wall. Furthermore, the coupling between Gaussians introduces a new force in the equation of motion for $R_2(t)$, which has no classical analog.[10,12] This can also affect the trajectory and the location of the turning point.[12]

While the packet G_2 turns around and leaves the scene of the action, the center of G_1 is accelerated towards the wall of the potential H_{11}, turns around at $R_1 \simeq 1.2$, is trapped in the well and oscillates in it. The motion of this packet does not have to be classical[11] but it happens to resemble classical motion. In the cases in which the energy of G_1 exceeds the dissociation

energy of H_{11} the packet escapes from the surface.

The Figs. 2b-d correspond to different kinetic energies of the incident packet and show the same general behavior: the split packets move in a nearly classical fashion on the two surfaces.

By comparison the mean trajectory approximation fairs poorly. The packet G representing the incoming particle manages to penetrate above the ionic well and for a brief period it moves similarly to G_2. However when it reaches the crossing point for the second time it changes its behavior to resemble G_1. This happens because at t=5 the effective potential $V_{eff} = \Sigma\ \Sigma\ c_i(t)^* c_j(t) H_{ij}(R)$ switches from resembling H_{22} to resembling H_{11} ($|c_2|^2$ becomes small and $|c_1|^2$ grows, as seen in Fig. 3a.) At the time t=11 the behavior is reversed because $|c_2|$ starts growing rapidly again and $V_{eff} \sim H_{22}$.

Since packet trajectories are not observables we should judge the usefulness of MTA by comparing its predictions for the occupation probabilities to those of MEM-SGWP. This is done in Figs. 3a-d. The results obtained with MTA are consistently poor. We note that a detailed numerical analysis of MTA shows that at low kinetic energies MTA has rather unphysical behavior.[33]

The LHA approximation for the split Gaussians does give trajectories which are, qualitatively speaking, well behaved. However the asymptotic values of the transition probability are different from those of MEM-SGWP as shown in Table III.

We have found that all the results reported here are stable with respect to the choice of the initial width of G_2 and of the point where G_1 is first created. If G_1 is created too early (i.e. at a distance which is too far from the point where H_{12} starts being different from zero) subsequent propagation makes it disappear (i.e. its amplitude goes to zero). If it is started too late (i.e. in the crossing region) the results are strongly dependent on the starting point. If G_1 is created in a strip of about 1.5Å, located far from the crossing point but in a region where H_{12} is not exactly zero, its properties are independent on the point of creation. In all cases we find that immediately

after the G_1's appearance the parameters in the Gaussians undergo fast transient changes and then settle to a smooth and physically reasonable evolution.

III.3 Tunneling within SGWP

In this section we study systematically how the packets behave as the energy of the incident packet changes from being above to being below the barrier on the lowest adiabatic state. The calculations are carried out with the Hamiltonian II defined by Eqs.(II.1-3) and the parameters given in Table I. The value of β is 0.3 and the mass is that of Li. The matrix elements $H_{ij}(R)$ are plotted in Fig. 4 together with the potential energies of the corresponding adiabatic states. The incident kinetic energies are labelled by the values of λ and are indicated on the graph. The difference between the incident kinetic energy and the top of the barrier on the lowest adiabatic state is given in Table II.

The trajectories followed by the MEM-SGWP packets is shown in Figs. 5a-f. The general behavior parallels that already seen in the sequence shown in Fig. 2. In the first three calculations (i.e. λ = 100, 110, 120) the kinetic energy is above the barrier and in the last three (Figs. (6d-f)) it is below. The trajectories are only slightly modified as the incident energy is slightly lowered, with no apparent trauma when the energy gets below the barrier. The lowest energy curve is somewhat peculiar since both packets turn around. This is not acceptable behavior for the ionic packet G_1, but it is not cause for concern: the amplitude of the misbehaving packet is completely negligible!

It is more interesting, from the point of view of tunneling, to monitor the total energies of each packet as a function of time. At this point it is necessary to make a few remarks concerning the energy in the SGWP theory.

The total energy of the system is

$$H(t)=N(t) \int dxdR\ \psi^*(x,R;t)H\ \psi(x,R;t) \qquad \text{(III.1)}$$

with the normalization

$$N(t) \equiv \int dx \int dR \psi^*(x,R;t)\psi(x,R;t) = \sum_i \int dR G_i^*(R;t)G_i(R;t). \quad \text{(III.2)}$$

By using (I.1) in Eq. (III.1) we can write

$$H(t)=N(t)^{-1}\sum_i \int dR G_i^*(K+H_{ii}(R))G_i+N(t)^{-1}2Re\int dR G_1^*(R;t)H_{12}(R)G_2(R;t) \quad \text{(III.3)}$$

The terms in the sum represent the results that would be obtained in a state selected energy measurement (e.g. $E_1(t)$ is obtained if the energy of the ionic component is measured). The last term in (III.3) is an energy contribution due to quantum interference between the nuclear wave functions.

In Figure 6 we plot the time evolution of the energies

$$E_i(t) = \int dR G_i^*[K+H_{ii}(R)]G_i / \int dR G_i^* G_i \quad \text{(III.4)}$$

which differ from the terms appearing in the sum in Eq. (III.3) only through normalization. We believe that plotting $E_i(t)$ as a function of time gives a feeling for the rate of energy exchange between the packets; furthermore the position of $E_1(t)$ and $E_2(t)$ with respect to the barrier on the lower adiabatic states can be used as an indication whether tunneling takes place.

In Fig.6a we show the evolution of $E_i(t)$ for λ=100. This corresponds to a kinetic energy above the barrier on the lowest adiabatic state and below the energy of the upper adiabatic state (see Fig. 5). The energy of the newly formed packet G_1 at the time of formation (i.e. t=7 is much higher than that of the incident packet. This does not cause any problem with energy conservation. To show this we write the total energy as

$$E(t) = \sum_{i=1}^{+} \mathcal{P}_i(t)E_i(t) + N(t)^{-1}2Re\int dR G_1^* H_{12} G_2 \quad \text{(III.5)}$$

where

$$\mathcal{P}_i(t) = \int dR G_i^* G_i / \sum_{i=1}^{2} \int dR G_i^* G_i \quad \text{(III.6)}$$

is the probability that the particle is in the state i. The total

energy E(t) is conserved at all times even when $E_1(t)$ is very large, because when $E_1(t)$ grows, $\mathcal{P}_i(t)$ becomes small; furthermore the interference term can also compensate some of the changes in $E_1(t)$ to keep E(t) constant. The same kind of reasoning explains how it is possible that total energy is conserved in the asymptotic channels (i.e. bound G_1 and unbound G_2) even though the packet energies E_i are changed by the collision.

We note several interesting results concerning the energy of the packets. In all our calculations the energy of the newly formed packet G_1 is above the asymptotic value $H_{11}(R\to\infty)$. Thus the center of the packet is not placed, when it is created, in a classically forbidden region of the diabatic state $H_{11}(R)$. In fact, in all cases in which the packet G_1 manages to penetrate in the region above the ionic well it does so without going through a classically forbidden region. We emphasize that in our propagation scheme we do not use a quadratic expansion of the potential and do not assume independent Gaussians. Thus neither the motion of the center of the packet (i.e. the evolution of $R_i(t)$ and $P_i(t)$) nor the energy of the packet are classical, so there is no a priori reason to expect that the trajectory of $E_i(t)$ is at all times in a classically allowed region. Moreover tunneling is so much associated, in our mind, with barrier penetration that the above result is somewhat surprising.

It is interesting to note that in Fig. 6f, corresponding to the lowest incident kinetic energy, the packet G_1 cannot penetrate behind the adiabatic barrier. The $E_1(t)$ curve comes down towards the H_{11} surface and it is turned around by it. It appears that the particle emerges from the surface in an ionic state, but this is not the case. As shown in Fig. 7 the probability that G_1 exits - for the kinetic energy used in Fig. 6f - is initially very small and it goes to zero; in contrast in the cases 6a-e, in which tunneling takes place, the probability $\mathcal{P}_1(t)$ grows to finite values (see Fig. 7).

III.4 Two states versus one state representation

Several problems in surface science are conveniently

represented in terms of a two state model. An obvious example is alkali adsorption on metals where the adsorbed alkali is ionic and the incident one is neutral. The two state character of the system is revealed by desoprtion experiments in which both ions and neutrals are observed. Another example is H_2 dissociative adsorption, which can be thought of as a transition from a H_2-Me state to a 2H-Me state (Me means metal surface).[51] In this case no 2H desorption has been observed to suggest that a 2H-Me state is involved in dynamics. Therefore while one might prefer to use a two diabatic state description of H_2 scattering or desorption it is not at all clear that a two adiabatic states description is necessary.

It is therefore of interest to establish some criteria whether one or two state descriptions are necessary. A reasonable condition can be obtained by comparing the gap between the two lowest adiabatic states with the kinetic energy of the incoming particle: if the latter is much smaller only one state is needed. Of course, when the two surfaces are unknown, which is generally the case, one would like to have some observable effects which signal the presence of the second state. In order to see if such effects exist we carried out calculations with a Hamiltonian in which the adiabatic surfaces are similar to those used in the previous section (Fig. 4), but the gap between them is smaller (Fig. 8). This is obtained by using the Hamiltonian II defined by Eqs. (II.1-3) and the parameters of Table I with β=0.1 instead of β=0.3.

In Fig. 9 we show the energies $E_1(R(t))$ and $E_2(R(t))$ of the ionic and neutral packets, respectively. The incident kinetic energies are labelled by the Massey parameter λ; the corresponding kinetic energy and the difference between it and the height of the barrier are given in Table II. The values of λ are chosen to give the same values for the barrier height minus the kinetic energy as those used in the previous section.

The most interesting result is that lowering the upper adiabatic state, to get it closer to the bottom one, leads to

higher neutral population. This happens as if the upper state helps reflect the incident packet. This effect can be seen by comparing the probabilities shown in Fig. 10 to those shown in Fig. 7.

IV SPLIT GWP METHOD WITH MULTIPLE CROSSINGS

The calculations presented so far have split the incident packet once, when it approached the curve crossing region. As a result the newly formed packet G_1 oscillates in the ionic state forever. In reality the trapped packet G_1 splits off a neutral packet whenever it approaches the curve crossing point and as a result the amplitude of the ionic packet dwindles, and a succession of outgoing neutral packets are created. This behavior is the GWP description of the "predissociation" of the ionic state.

In order to test whether SGWP generates such behavior we carried out the SGWP calculation shown schematically in Fig. 11: in Fig. 11(a) packet 2 is split to generate packet 1; after that packet 2 is turned around and leaves the surface while 1 moves in the ionic well (Fig. 11b); when packet 1 approaches the crossing region again, we use SGWP to generate a new neutral packet 2'; this leaves the surface, while 1 turns back towards it; this succession is repeated until the amplitude of 1 becomes negligible.

An idealized time of flight (TOF) measurement applied to this process will give peaks corresponding to the arrival times of the successive neutral packets, separated by a time comparable with the period of the motion of G_1 in the ionic well. Such a result corresponds to an experiment in which the incident state is a packet that is well localized in space. If the experiment is carried out with an incident state which is close to a plane wave we must describe it by using a train of several incident packets; the succession of emerging neutral packets will then be continuous in time. Moreoever since the time resolution of TOF detectors is poor, as compared to the period of the motion in the ionic well, the time "granularity" given by GWP is not a practical shortcoming.

The results of this multiple splitting calculation are shown in Fig. 12. The Hamiltonian is that described in Fig. 1, $\lambda = 42$ and $\beta = 0.3$. The trajectories of the centers of various packets

are plotted in Fig. 12a. We see that the ionic packet G_1 is formed at t=0 and reaches the crossing point at t ~ 6; later G_2 turns around and leaves the surface, while G_1 oscillates in the ionic well. As G_1 moves away from the surface a new neutral packet G_2' is created at t ≃ 9, before G_1 reaches the crossing point. Immediately G_2' leaves the surface while G_1 continues to oscillate, creating G_2'' when it approaches the crossing point again. The probability that the particle is ionic is shown in Fig. 12b. Clearly the creation of G_2' and G_2'' diminishes $P_1(t)$, as expected. It is not surprising that MTA give very poor results for this case.

We found this procedure to be rather stable with respect to the precise point where the packets are split. If the splitting is done too early the amplitude of the new packet goes to zero; if it is done too late the result depends on the splitting point. There is a strip of about 1A width, ahead of the crossing region, in which splitting can be done without affecting the results.

V. THE EFFECT OF DISSIPATION BY PHONONS

V.1 Introductory Remarks

The problem of curve crossing or tunneling in quantum systems coupled to a heat bath is a topic of much current interest;[16] one would like to formulate a theory which predicts the manner in which energy dissipation and dephasing by thermal fluctuations change tunneling rates. The present model is also relevant -in surface science- to the problem of sticking induced by curve crossing followed by inelastic interactions between the incident particle and the lattice. Both phonons and electron hole pair excitations may be important and both can be treated by a model in which the incident particle is coupled strongly to independent bosons.[31a]

In this section we describe a theory in which the lattice motion is coupled to the quantum degrees of freedom through a mean trajectory approximation. This permits us to combine the GWP quantum dynamics of the particle with a classical Langevin[14a,52] equation describing the motion of the lattice. Other models which couple curve crossing dynamics to stochastic variables simulating a heat bath have been presented in the literature.[53]

V.2 The model

We consider a particle colliding with a one dimensional atom chain (Fig. 13). The Hamiltonian is

$$H = -(\hbar^2/2M)\partial^2/\partial R^2 - (\hbar^2/2m)\partial^2/\partial r^2 - (\hbar^2/2m)\sum_i \partial^2/\partial q_i^2 + H(r,R,x) + V_L(r,\{q_i\}) \quad . \tag{V.1}$$

The lattice atoms are divided here into two groups: the primary atoms whose coordinates are denoted r and the secondary atoms having the coordinates q. The concrete example used here has only one primary atom. The independence of the electronic Hamiltonian H(r,R,x) on the positions of the secondary atoms implies that only the atoms in the primary zone interact with the incident particle. We assume that the lattice is harmonic (i.e.,

the lattice potential energy $V_L(r,\{q_i\})$ is quadratic) but do not linearize the interaction between the incident particle and the primary zone atoms.

V.3 The Hartree approximation

We make now the Hartree approximation, which assumes a wave function of the form

$$\psi = X_L(r,\{q_i\};t)[G_1(R,t)\Phi_1(R,r,x) + G_2(R,t)\Phi_2(R,r,x)] \quad (V.2)$$

where Φ_i are the electronic wave functions (1 is neutral and 2 is ionic), G_1 and G_2 are the nuclear wave functions of the incident particle, and X_L is the wave function of the lattice.

Using the minimum error method[10] and the properties (II.4) of the electronic wave functions leads to[54]

$$i\hbar\partial G_i/\partial t = -(\hbar^2/2m)\partial^2 G_i/\partial R^2 + \langle H_{ii}\rangle_L G_i + \langle H_{ij}\rangle_L G_j \quad (V.3)$$

for i =1 or 2 and $j \neq i$, and to

$$i\hbar\partial X_L/\partial t=-(\hbar^2/2m)\partial^2 X_L/\partial r^2-(\hbar^2/2m)\Sigma\partial^2 X_L/\partial q_i^2+[V_L(r,\{q_i\})+V_{eff}(r)]X_L \quad (V.4)$$

Here

$$\langle H_{ij}\rangle_L \equiv \int X_L^*(r,\{q_i\})H_{ij}(R,r)X_L(r,\{q_i\})dr\prod_{i=1}^{N} dq_i \quad (V.5)$$

$$V_{eff}(r) = \sum_{i=1}^{2}\sum_{j=1}^{2} \int G_i(R)^* H_{ij}(R,r)G_j(R)dR \quad (V.6)$$

and

$$H_{ij}(R,r) = \int \Phi_i^*(R,r,x)\, H(R,r,x)\Phi_j(R,r,x)dx. \quad (V.7)$$

Because we made the Hartree approximation the primary atom interacts with the incoming particle through the effective potential (V.6). This is the sum of the ionic potential $H_{11}(R,r)$

averaged over the distribution $G_1^*(R,r;t)G_1(R,r;t)$ (which is proportional to the probability that the particle is an ion located at R) plus the neutral potential $H_{22}(R,r)$ averaged over the distribution $G_1^*(R,r;t)G_1(R,r;t)$ (which is proportional with the probability that the particle is neutral and is located at R) plus the interference term $2Re\int dR G_1^*(R,r;t)\ H_{12}(R,r)\ G_2(R,r;t)$.

To do better than the Hartree approximation we would have to use the wave function

$$\psi(R,r\{q\},x;t) = X_L(\{q_i\}) \sum_{i=1}^{2} G_{1,i}(r,R;t)\Phi_i(R,r,x) \qquad (V.8)$$

which incorporates the correlated quantal motion of the primary zone atoms and that of the incident particle; the Hartree approximation is made for the secondary lattice atoms only.

It is instructive to think under what conditions we can hope that the Hartree approximation is satisfactory. This approximation simplifies the force exerted by the incident atom on the primary atom, by averaging it over the state of the incident particle. If the particle state $\Sigma\ G_i\ \Phi_i$ is predominantly ionic than the force exerted on the primary atom resembles that caused by the ion; in the opposite case the interaction resembles that exerted by the neutral. In the intermediate case the force is the average of the ionic and neutral forces, with the corresponding quantum weights. For the present problem one may assume that the lattice-atom energy transfer and dephasing are most efficient at the moment of the impact and that the repulsive part of the potential is most important. Since the repulsive walls for ion and neutral are similar it may not be essential that the effective potential mixes them in exactly the right way. On the other hand, if electron hole pair excitations and the polarization of the electron-gas (i.e. "image effect") are important we might want to use the non-Hartree wave function Eq (V.8). This will treat the coupling of the ion to the electron gas on a different footing than the coupling of the neutral.

V.4 The mean trajectory approximation for lattice motion

The equations (V.3-6) can be further simplified by assuming that: (a) the lattice wave function is, throughout the collision, Gaussian in the variables q and r; and that (b) the mean square displacement of the variable r in this Gaussian state is very small. Assumption (b) allows us to perform the integral in Eq. (V.5) by the steepest descent method, to obtain

$$\langle H_{ij} \rangle_L = H_{ij}(R, r(t)) \ , \qquad (V.9)$$

where r(t) is the mean position of the primary atom at time t:

$$r(t) = \int dr \prod_{i=1}^{N} dq_i \ X_L^*(r,\{q\};t) \ \ rX_L(r,\{q\};t). \qquad (V.10)$$

Due to Eq. (V.9) and (V.3) the wave functions G_1 and G_2 no longer depend on the lattice wave function, but only on the mean primary atom position r(t). From Heller's work[6] we know that if the Hamiltonian is harmonic in the variables $\{q_i\}$, and the Gaussian wave function X_L is narrow with respect to r, then it follows that r(t) and $q_i(t)$ satisfy classical equations of motion:

$$m\ddot{r}(t) = -\partial V_{eff}/\partial r(t) - m\omega^2(r(t)-q_1(t)) \ , \qquad (V.11)$$

$$\omega_i^{-2} m\ddot{q}_i(t) = q_{i-1}(t) - 2q_i(t) + q_{i+1}(t), \quad i=1,2,... \qquad (V.12)$$

with

$$q_0(t) \equiv r(t)$$

The mean trajectory approximation decouples thus the wave functions G_i, i=1,2 from the wave function X_L; the only lattice information that is needed is the time evolution of the center of the packet representing the primary lattice atom; the latter moves classically on a mean potential which is the average interaction between the incident particle and the primary atoms over the

particle wave function.

To assess the validity of the mean trajectory approximation we must quantify the demand that the Gaussian X_L is narrow. Since this assumption is used to justify the integration of (V·5) by the Laplace method, the width $l(t)$ of the Gaussian $g(r)=\int X_L^*(r,q_1..q_N)X_L(r,q_1..q_N)\prod dq_i$ must be smaller than the length L over which the function $H_{ij}(r,R)$ changes with r. Furthermore, for r(t) to move classically under the influence of the potential $V_{eff}(r(t))$ we must have[10,11] $l^2(t)<<4[\partial V_{eff}(r(t))/\partial r(t)]^{-1}[\partial^3 V_{eff}(r(t))/\partial r(t)^3] \equiv \eta(t)$. An order of magnitude estimate of the width $l(t)$ of the Gaussian $g(r)$ is the mean displacement of the primary atom $l^2 \sim (\hbar/m\omega)\coth[\hbar\omega/2k_BT]$.

As a side remark we note that this expression for l^2 does not lead to a divergence, in the present theory, for $\omega\to 0$. Indeed as $\omega\to 0$ and $l^2\to\infty$ the Gaussian $g(r)$ tends to $l\delta(r-r(t))$. Since in the present theory the wave function appears everywhere in integrals over frequency the quantity $l(\omega)$ is multiplied with the density of states, leading thus to expressions containing $\int d\omega\rho(\omega)l(\omega)$. Since $\rho(\omega) = 3\omega^2/\omega_D^2$ (for a Debye model) $l(\omega)\rho(\omega)$ is proportional to ω as $\omega\to 0$. Thus in the $\omega\to 0$ limit the integrals through which $l(\omega)$ appears in the theory are well behaved.

We can summarize the conditions under which the Gaussian $g(r)$ is sufficiently narrow by requiring

$$(\hbar/m\omega)\coth(\hbar\omega/2k_BT)<<\max[L(t)^2,\eta(t)^2] \equiv \lambda^2.$$

In the high temperature limit $\hbar\omega/k_BT<<1$ and $\coth(\hbar\omega/2kT)\to 2k_BT/\hbar\omega$. Thus the condition $(2\hbar^2/m\lambda^2)<<k_BT$ ensures the validity of the mean trajectory approximation in the high temperature limit. This result makes sense, since in the high temperature limit the important frequency in the system is $k_BT/\hbar$. We can use it to form the action $A \equiv m\lambda^2 k_BT/\hbar$ by using λ as a typical length of the potential. Then a classical trajectory limit should be valid if $\hbar/A<<1$, which leads to the high temperature condition obtained

above.

V.5 A summary of the equations

After we made the mean trajectory approximation for the motion of the primary atom and took the classical limit for the motion of all the lattice atoms, the nuclear wave functions G_i satisfy

$$i\hbar\partial G_i(R,t)/\partial t=-(\hbar^2/2M)\partial^2 G_i(R,t)/\partial R^2+H_{ii}(R,r(t))G_i(R,t) + H_{ij}(R,r(t))G_j(R,t) \quad , \; i,j=1,2 \text{ and } i\neq j. \tag{V.13}$$

These equations are solved by the MEM-SGWP method.

To compute r(t) we use the Eqs. (V.11-13) and the Langevin equation method proposed by Adelman and Doll.[52] The version implemented here is the ghost atom method developed by Garrison and Adelman[55] and Shugard, Tully, and Nitzan.[56] This solves

$$m\ddot{r}(t) = -\partial V_{eff}/\partial r(t)-m\omega^2(r-r_g) \tag{V.14}$$

and

$$m\ddot{r}_g(t) = -m\omega^2(r_g-r)-m\omega_g^2 r_g - m\gamma dr_g/dt+F(t) \tag{V.15}$$

In choosing the friction coefficient γ and the ghost atom frequency ω_g we follow Garrison and Adelman.[55] The fluctuating force has the correlation function

$$\langle F(t)F(0)\rangle = 2mk_BT\gamma\delta(t) \quad , \tag{V.16}$$

which assumes the high temperature (i.e. classical) limit when the thermal average is performed. Some quantum effects can be put back into the theory by replacing $2k_BT$ with $\hbar\omega\coth(\hbar\omega/2k_BT)$. The qualitative effect of using the expression (V.16) is that at low temperature (i.e. $\hbar\omega/k_BT > 1$) it produces more noise than the real quantum system does. Furthermore, Eq. (V.16) does not give different weights to energy loss (i.e. Stokes) and energy gain (i.e. anti-Stokes) processes. This should introduce very large

errors at the lowest temperatures where the Stokes processes have high intensity and that of anti-Stokes processes is almost zero. As Tully's extensive work has demonstrated the method based on Eq. (V.16) should be reliable at high temperatures (i.e. $\hbar\omega << k_B T$).

V.6 Illustrative numerical results

We present results of several calculations carried out by solving Eqs. (V.13-16). The lattice parameters are $\omega_D = 1.43 \times 10^{-3}$ a.u. and the mass of Ni. The projectile mass is that of Na and the matrix $H_{ij}(R, r(t))$ is defined by Eqs. (II.1-3) with R replaced with R-r(t); the values of the parameters are those listed in Table I under Hamiltonian I. The coupling strength is $\beta = 0.3$ and the incident kinetic energy is given by $\lambda = 43$ (the kinetic energy is $mv_0^2/2 = 89.9\lambda^{-2}$ eV).

In Figs. 13a we show the trajectory followed by the packets (one crossing only) in the case when the lattice is rigid. The effect of allowing the lattice to move, at T=0K is shown in Fig. 13b, where the amplitude of the ionic packet decays as a result of phonon excitations. The zero point energy of the lattice was included in the classical Langevin equation. In Fig. 13c we show the energy $E_1(t)$ of the ionic packet (see Eq. (III.4)) as a function of the packet position. The arrows indicate the flow of time. The behavior of the system at non-zero temperatures is shown in Figs. 14a and b. At lower temperature ($T = \Theta_D$, where Θ_D is Debye temperature) the ion is quickly equilibrated, and phonon absorption is seen; however the amplitude does not decay as continuously as in Fig. 13a at T=0. For $T = 5\Theta_D$ (Fig. 14b) the ion has not settled to a low amplitude even after three oscillations in the well.

These calculations illustrate the fact that the addition of a thermal dissipative channel drives the Gaussian wave function in a manner that resembles classical mechanics. The computation is rather inexpensive and we estimate that it is possible for three dimensional models.

VI. Conclusions

We have presented a Guassian wave packet theory, for a curve

crossing system, which has one packet per electronic state. The most interesting feature of the theory is that it permits tunneling, in the sense that a packet incident in a barrier splits into one packet reflected by the barrier and one which penetrates behind it. The procedure for multiplying the number of packets in the course of propagation is general and should be useful in numerous other applications of the GWP method to phenomena in which wave function splits spontaneously, in the course of the collision, into spatially disjoint pieces.

Another new development is the discussion of various approximations involved in coupling the curve crossing system whose properties are described within a GWP formulation to a many-body classical system, such as a lattice. The use of Hartree approximation permits an approximate but self-consistent treatment of this problem. The classical limit for the motion of the many-body system is not necessary; the use of the GWP method to propagate the bath variables quantum mechanically is feasible, as demonstrated recently by Singer and Smith.[58]

The numerical studies presented here explored the stability of the method and studied the qualitative behavior of the packets. We are now developing an exact method for solving this problem and hope to report soon a comparison between the results obtained with SGWP and the exact ones. If the SGWP method turns out to have satisfactory accuracy than it can be used for three-dimensional studies for which exact calculations are much more difficult.

We had two reasons for undertaking this study. First, we were curious about the behavior of the packets in a strongly non-classical situation, such as a two state system at energies for which tunneling plays an important role. Second, we are searching for a method of doing very inexpensive three-dimensional curve crossing calculations for a quantum system imbedded in a classical heat bath; since the behavior of the bath must be generated by repeated use of classical molecular dynamics the ability to calculate the quantum part cheaply (but reliably) is of paramount importance. The GWP method seems a natural candidate for this

task.

Acknowledgements: This work was supported in part by the Office of Naval Research and the National Science Foundation (through CHE82-06130). We thank K. Singer for sending us his unpublished work and Eric Heller for useful discussions.

REFERENCES

1. (a) G. Drolshagen and E. Heller, J. Chem. Phys. 79, 2072 (1983); G. Drolshagen and E. Heller, Surface Sci., 139, 260 (1984). (b) B. Jackson and H. Metiu, J. Chem. Phys., 82, 5707 (1985).

2. B. Jackson and H. Metiu, J. Chem. Phys. (in press).

3. R. Heather and H. Metiu, Poster at the 1985 Conference on Dynamics of Molecular Collisions, Snowbird, Utah, July 14-19, 1985.

4. B. Jackson and H. Metiu, J. Chem. Phys., 83, 1952 (1985).

5. There are a number of interesting papers concerning surface scattering which use Gaussian wave packets but do not employ Heller like propagation methods: P.M. Agrawal and L.M. Raff, J. Chem. Phys., 77, 3946 (1982); A.T. Yinnon and R. Kosloff, Chem. Phys. Lett., 102, 216 (1983); R.B. Gerber, A.T. Yinnon and R. Kosloff, Chem. Phys. Lett., 105, 523 (1984); R. Kosloff and C. Cerjan, J. Chem. Phys., 81, 3722 (1984).

6. (a) E.J. Heller, J.Chem. Phys., 62, 1544 (1975); (b) E.J. Heller, ibid. 65, 1289 (1976), 65, 4979(1976); 67, 3339(1977); 75, 2923 (1981); (c) M.J. Davis and E.J. Heller ibid. 71, 3383(1979); E.J. Heller, Acc. Chem. Res. 14, 368 (1981); K.C. Kulander and E.J. Heller, J. Chem. Phys., 69, 2439 (1978); E.J. Heller, ibid., 68, 2066 (1978); 68, 3891 (1978); S.Y. Lee and E.J. Heller, ibid., 71, 4777 (1979); R.C. Brown and E.J. Heller, ibid., 75, 186 (1981); S.Y. Lee and E.J. Heller, ibid., 6, 3035 (1982); M. Blanco and E.J. Heller, ibid., 78, 2504 (1983); D.J. Tannor and E.J. Heller, ibid., 77, 202 (1982); E.J. Heller, R.L. Sundberg and D. Tannor, ibid., 6, 1882 (1982).

7. R.D. Coalson and M. Karplus, Chem. Phys. Lett., 90, 301 (1982); J. Chem. Phys., 79, 6150 (1983).

8. R.T. Skodje and D.G. Truhlar, J. Chem. Phys., 80, 3123 (1983).

9. D. Thirumalai, E.J. Bruskin and B.J. Berne, J. Chem. Phys., J. Chem. Phys., 83, 230 (1985).

10. S. Sawada, R. Heather, B. Jackson and H. Metiu, J. Chem. Phys., 83, 3009 (1985).

11. R. Heather and H. Metiu, Chem. Phys. Lett., 118, 558 (1985).

12. R. Heather and H. Metiu, J. Chem. Phys., (in print).

13. R.G. Littlejohn, Phys. Rep. (in press).

14. (a) J.C. Tully in Many body phenomena at surfaces, eds. D. Langreth and H. Suhl, (Academic Press, New York, 1984), p. 377; J.C. Tully, Annu. Rev. Phys. Chem., 31, 319 (1980); (b) J.C. Tully Surface Sci., 111, 461 (1981); E.K. Grimmelmmann, J. C. Tully and E. Helfand, J. Chem. Phys., 74, 5300 (1981); J.E. Adams and J.D. Doll, J. Chem. Phys., 74, 1467, 5332 (1981).

15. (a) S.Efrima, C. Jedrzejek, K.F. Freed, E. Hood and H. Metiu, J. Chem. Phys., 79, 2436 (1983); E. Hood, C. Jedrżejek, K.F. Freed and H. Metiu, ibid., 81, 3277 (1984); (b) Z.W. Gortel, H.J. Kreutzer and R. Teshima, Phys. Rev. B 22, 512 (1980); Z.W. Gortel, J.H. Kreuzer and D. Spaner, J. Chem. Phys., 72, 234 (1980); H.J. Kreutzer and R. Teshima, Phys. Rev. B24, 4470 (1981); H.J. Kreutzer, Int. J. Mass. Spectrom. Ion Phys., 53, 273 (1983); (c) T.F. George, J. Chem. Phys., 86, 10 (1982); J.C. Lin and T.F. George, Surf. Sci., 107, 417 (1981); 108, 340 (1981).

16. A.O. Caldeira and A.J. Leggett, Ann. Phys., 149, 374 (1983); S. Chakravarty and A.J. Leggett, Phys. Rev. Lett., 52, 5 (1984); H. Grabert, U. Weiss and P. Hanggi, Phys. Rev. Lett., 52, 2193 (1984); R.Silbey and R.A. Harris, J. Chem. Phys., 80, 2615 (1984), J.A. Bray and M.A. Moore, Phys. Rev. Lett., 49, 1545 (1982); B. Carmelli and D. Chandler, J. Chem. Phys., 82, 3400 (1985).

17. R. Brako and D.M. Newns, Vacuum 32, 39 (1982); Surface Sci., 108, 253 (1981); Solid State Commun. 33, 713 (1980).

18. J.K. Norskov, D.M. Newns, and B.I. Lundgvist, Surf. Sci., 80, 179 (1979).

19. K. Schönhammer and O. Gunnarsson, Phys. Rev. B22, 1629 (1980); B24, 7084 (1981); Surf. Sci., 117, 53 (1982).

20. J.C. Tully, Phys. Rev. B16, 4324 (1977).

21. T.B. Grimley, V.C. Jyothi Basu and K.L. Sebastian, Surf. Sci., 124, 305 (1983).

22. N.D. Lang, Phys. Rev. B27, 2019 (1983); M.L. Yu and N.D. Lang, Phys. Rev. Lett., 50, 127 (1983).

23. B. Kasemo, E. Tornqvist, J.K. Norskov, and B.I. Lundqvist, Surf. Sci., 89, 554 (1979).

24. J.W. Gadzuk and H. Metiu, Phys. Rev. B22, 2603 (1980); S. Holloway and J.W. Gadzuk, Surf. Sci., (in press); J.W.

Gadzuk and J.K. Norskov, J. Chem. Phys., 81, 2828 (1984).

25. W. Bloss and D. Hone, Surf. Sci., 72, 277 (1978).

26. H. Mueller and W. Brenig, Z. Phys. B34, 165 (1979); W. Brenig, Z. Phys. B23, 361 (1976); B36, 81 (1979); B36, 227 (1980); B48, 127 (1982); J. Phys. Soc. Japan 51, 1914 (1982).

27. E. Hood, F. Bozso and H. Metiu, Surf. Sci., (in press).

28. S. Sawada, A. Nitzan and H. Metiu, Phys. Rev. B32, 851 (1985).

29. A.E. DePristo, Surface Sci., 137, 130 (1984); R.F. Grote and A.E. DePristo, Surf. Sci., 131, 491 (1983); A.M. Richard and A.E. DePristo, Surf. Sci., 134, 338 (1983).

30. D. Kumamoto and R. Silbey, J. Chem. Phys., 75, 5164 (1981).

31. (a) K.M. Leung, G. Schon, P. Rudolph and H. Metiu, J. Chem. Phys., 81, 3307 (1984); (b) H. Metiu and G. Schon, Phys. Rev. Lett., 53, 13 (1984).

32. J.A. Olson and B.J. Garrison, Nucl. Inst. Meth. (in press); J. Chem. Phys. (in press).

33. M.H. Mittelman, Phys. Rev. 122, 499 (1961).

34. G.D. Billing, Chem. Phys. Lett., 30, 391 (1975); Chem. Phys. 70, 223 (1982).

35. J.T. Muckerman, I. Rusinek, R.E. Roberts and M. Alexander, J. Chem. Phys., 65, 2416 (1976).

36. S.D. Augustin and H. Rabitz, J. Chem. Phys., 69, 4195 (1978).

37. D.J. Diestler, J. Chem. Phys., 78, 2240 (1983).

38. J. Olson and D. Micha, Int. J. Quantum Chem., 22, 971 (1982); P.K. Swarminathan and D.A. Micha, Int. J. Quantum Chem., 16, 377 (1982).

39. S. Sawada and H. Metiu, Surface Sci., (submitted).

40. B.C. Eu, J. Chem. Phys., 52, 1882(1970); 55, 560 (1971); 56, 2507 (1972).

41. M.S. Child, J. Mol. Spectrosc., 53, 280 (1974).

42. J.S. Cohen, Phys. Rev., A13, 85, 99 (1976).

43. O. Atabeck, R. Lefebvre and M. Jacon, J. Chem. Phys., 81, 3874 (1984).

44. R.K. Preston and J.C. Tully, J.Chem. Phys., 54, 4297 (1971); J.C. Tully and R.K. Preston, ibid., 55 562 (1971).

45. P. Pechukas, Phys. Rev. 181, 174 (1969); P. Pechukas and J.P. Davis, J. Chem. Phys., 56, 4970 (1972); J.T. Hwang and P. Pechukas, ibid., 56, 4970 (1972).

46. A.P. Penner and R. Wallace, Phys. Rev. A7, 1007 (1973); A9, 1136 (1974); A11, 149 (1975).

47. The key work is W.H. Miller and T.F. George, J. Chem. Phys. 56, 5637,5668 (1972). Numerous applications and improvements were made by T.F. George. For more recent papers from his group are J.M. Yuan, T.F. George, B.M. Skuse, R.L. Jaffe, A. Komornicki and K. Morokuma, Israel J. Chem. 19, 337 (1980) and J.R. laing, J.M. Yuan, I.H. Zimmerman, P.L. DeVries and T.F. George, J. Chem. Phys., 66, 2801 (1977).

48. (a) M.F. Herman, J. Chem. Phys., 76, 2949 (1982); 79, 2771 (1983); 81, 754, 764 (1984); 82, 3666 (1985); M.F. Herman and K.F. Freed, 78, 6010 (1983). (b) J.R. Laing and K.F. Freed, Phys. Rev. Lett., 34, 849 (1975); K.F. Freed, Chem. Phys. 10, 393 (1975); J.R. Laing and K.F. Freed, ibid., 19, 91 (1977).

49. T.F. O'Malley, Adv. Atom. Mol. Phys., 7, 223 (1971); H. Metiu, J. Ross and G. Whitesides, Angew. Chem. (Int. Ed.) 18, 377 (1979); J.C. Tully in Dynamics of Molecular Collisions, ed. W.H. Miller (Plenum, New York, 1976); K.S. Lam and T.F. George, in Semi-Classical Methods in Molecular Scattering and Spectroscopy, ed. M.S. Child (D. Reidel, Dordrecht, 1980) pp 179; E.E. Nikitin, Theory of Elementary Atomic and Molecular Processes in Gases, (Clarendon Press, Oxford, 1974).

50. R.P. Feynman and A.R. Hibbs, Quantum Mechanics and Path Integrals, (McGraw Hill Co., New York, 1965).

51. J.E. Lennard-Jones, Trans. Farad. Soc., 68, 202 (1932).

52. S.A. Adelman and J.D. Doll, J. Chem. Phys., 64, 2375 (1976); S.A. Adelman and B.J. Garrison, ibid., 65, 3751 (1976); S.A. Adelman and J.D. Doll, Acc. Chem. Res., 10, 378 (1977); S.A. Adelman, Adv. Chem. Phys., 44, 143 (1980); J.D. Doll, in Aerosol Microphysics edited by W.H. Marlow (Springer, New York, 1980).

53. M. Tsukada, J. Phys. Soc. Jpn., 51, 2927 (1982); H. Ueba, Phys. Rev. B31, 3915 (1985); B. Martire and R.G. Gilbert, Chem. Phys., 56, 241 (1981); D.P. Ali and W.H. Miller, J. Chem. Phys., 78, 6640 (1983).

54. This is a tedious calculation in which a number of terms which lead to phase factors in the wave function must be removed in order to obtain Eqs. (V.3-7). Direct substitution of (V.2) in the time dependent Schrodinger equation leads to the same results.

55. B.J. Garrison and S.A. Adelman, Surf. Sci., 66, 253 (1977).

56. M. Shugard, J.C. Tully and A. Nitzan, J. Chem. Phys., 71, 1630 (1979); J.C. Tully, ibid., 73, 1975 (1980).

57. H. Metiu and S. Sawada, unpublished.

58. K. Singer and W. Smith, Semi-classical many-particle dynamics with Gaussian wave packets, Daresbury Laboratory Preprint, Oct. 1985.

APPENDIX

The Equations used for the MEM-SGWP propagation of the packets are:[57]

$$\dot{\gamma}_i - P_i\dot{R}_i = i\hbar\alpha_i/m - P_i^2/2m + \{[V_{ii}(2)+V_{ij}(2)]\, M_i(2) - [V_{ii}(0)+V_{ij}(0)]M_i(4)\}B_i \tag{A.1}$$

$$\dot{\alpha}_i + 2\alpha_i^2/m = B_i\{M_i(2)[V_{ii}(0) + V_{ij}(0)] - M_i(0)\,[V_{ii}(2) + V_{ij}(2)]\} \tag{A.2}$$

$$\dot{P}_i = -V_{ii}(1)M_i(2)^{-1} + (M_i(2)\mathrm{Im}\alpha_i)^{-1}\ \mathrm{Im}[\alpha_i^* V_{ij}(1)] \tag{A.3}$$

$$\dot{R}_i = P_i/m + \{2\mathrm{Im}\alpha_i\ M_i(2)\}^{-1}\ \mathrm{Im}\ V_{ij}(1) \tag{A.4}$$

where

$$M_i(n) = \int G_i(R)^*(R-R_i(t))^n G_i(R)\ , \tag{A.5}$$

$$V_{ij}(n) = \int G_i(R)^*(R-R_i(t))^n H_{ij}(R)G_j(R)dR\ , \tag{A.6}$$

$$B_i = \{M(4)M_i(0) - M(2)^2\}^{-1} \tag{A.7}$$

and $i=1,2$, $j=1,2$, $i\neq j$.

Also note that

$$-V_{ii}(1)M_i(2)^{-1} = -\int dR G_i^* G_i(\partial H_{ii}/\partial R)/\int dR G_i^* G_i = -\frac{\partial}{\partial R_i}\{\int dR G_i^* H_{ii}\ G_i/\int dR G_i^* G_i\} \tag{A.8}$$

and that

$$B_i\{M_i(2)V_{ii}(0)-V_{ii}(2)M_i(0)\} = -(1/2)\frac{\partial^2}{\partial R_i^2}\{\int dG_i^* H_{ii} G_i/\int dR G_i^* G_i\} \tag{A.9}$$

Table I. The values of the parameters used in Eqs. (II.1-3) to define the Hamiltonians.

	Hamiltonian I		Hamiltonian II	
	atomic units	other	atomic units	other
U_o	0.025H[a]	0.68 eV	0.184H[a]	5.0 eV
$\Delta\epsilon$	0.005H[a]	0.136 eV	0.147H[a]	4.0 eV
α^{-1}	2.5 a[b]	1.32 Å	2.5 a[b]	1.32Å
R_o	5.0 a[b]	2.64 Å	5.0 a[b]	2.64Å
R_c	12.5 a[b]	6.6 Å	9.0 a[b]	4.75Å
β	0.1 or 0.3	0.1 or 0.3	0.1 or 0.3	0.1 or 0.3
m	42300[c]	22.991[c]	12,800a.u.[d]	6.94[d]

(a) Hartree

(b) a is Bohr radius

(c) the mass of Na

(d) the mass of Li

Table II. The energies of the incident packets. For the definition of column headings see the text.

			Incident energy-barrier height	
λ^a	$P_2/2m$	$\Delta P_2/2m$	β=0.3	β=0.1
90	2.91	1.39×10^{-2}	---	9.21×10^{-1}
100	2.35	1.76×10^{-2}	7.60×10^{-1}	3.70×10^{-1}
110	1.95	1.42×10^{-2}	3.48×10^{-1}	-4.16×10^{-1}
120	1.63	1.17×10^{-2}	3.50×10^{-2}	-3.54×10^{-1}
130	1.39	9.82×10^{-3}	-2.10×10^{-1}	-5.99×10^{-1}
140	1.20	8.34×10^{-3}	-4.05×10^{-1}	-9.49×10^{-1}
150	1.05	7.25×10^{-3}	-5.60×10^{-1}	---
---	eV	eV	eV	eV

(a) Massey parameter (Section II.4)

Table III. The probability that a particle starting in the state 2 emerges in state 1 (one crossing only).

	$\beta = 0.3$				$\beta = 0.1$		
λ	LHA-SGWP	MEM-SGWP	MTA		LHA-SGWP	MEM-SGWP	MTA
40	0.954	0.655	1.0	35	0.429	0.404	0.807
41	0.979	0.588	1.0	36	0.409	0.382	0.888
42	0.954	0.500	1.0	37	0.372	0.334	0.978
43	0.887	0.404	1.0†	38	0.341	0.286	1†
44	0.750	0.308	1.0†	39	0.370	0.235	1†
45	0.622	0.219	1.0†	40	0.395	0.180	1†

† The packets turn around before reaching the curve crossing region.

FIGURE CAPTIONS

Fig. 1. The diabatic potentials $H_{ii}(R)$, i = 1,2 (see Eqs. II.2), the coupling $H_{ij}(R)$ (dash-dotted line, right hand side scale) and the adiabatic potentials $H^a_{ii}(R)$, (dashed lines) i=1,2. The parameters are those for Hamiltonian I in Table I, with β=0.3. The adiabatic and diabatic potentials overlap everywhere except in the crossing region.

Fig. 2. The trajectories of the centers R_1 (dashed line) and R_2 (full line) of the ionic and neutral packets, respectively, obtained by MEM-SGWP. The dash-dotted line is the MTA result. The Hamiltonian I with β=0.3 (see Table I for parameter values and Fig. 1 for plots) was used for all calculations. The Massey parameters for the incident G_2 packets are: (a) λ=37; (b) λ=38; (c) λ=42 and (d) λ=43. The kinetic energy is $mv_0^2/2 = 3.30\ \lambda^{-2}$ Hartree = $89.9\ \lambda^{-2}$ eV.

Fig. 3. The time evolution of the probability that a neutral particle approaching the wall remains neutral. The full lines are the results obtained with MEM-SGWP and the dashed lines those given by MTA. The parameters are those used in Fig. 2.

Fig. 4. The adiabatic potentials $H_{11}(R)$ and $H_{22}(R)$ (full lines) and the diabatic coupling $H_{12}(R)$ (dashed - dotted line), given by Eqs. (II.1-3) and the parameters for Hamiltonian II of Table I, with β=0.3. The diabatic curves H^a_{11} and H^a_{22} are the dashed lines. They differ from the diabatic curves only in the crossing region. The arrows on the right hand side indicate the kinetic energy of the incident packets.

For conversion from the Massey parameter λ to the kinetic energies see Table II.

Fig. 5. The trajectories $R_1(t)$ and $R_2(t)$ of the centers of the ionic (full lines) and neutral (dashed lines) packets G_1 and G_2, respectively. The calculations are for the Hamiltonian II defined by Eqs. (II.1-3) and the parameters given in Table I, with β=0.3. The incident Massey parameters are: (a) λ=100; (b) λ=110; (c) λ=120; (d) λ=130; (e) λ=140; (f) λ=150. The calculations (a) - (c) correspond to kinetic energies above the barrier, the others are below. For conversion of λ to kinetic energies see Table II.

Fig. 6. The adiabatic energy surfaces H^a_{11} and H^a_{22} (dash-dotted lines) and the packet energies $E_1(t)$ and $E_2(t)$ defined by Eq. (III.4)). The calculations are for the Hamiltonian II defined by Eqs. (II.1-3) and the parameters given in Table I with β=0.3. The distance R is the position of the center of the corresponding packet. The arrows on the curves indicate the flow of time. Various curves correspond to (a) λ=100; (b) λ=110; (c) λ=120; (d) λ=130; (e) λ=140; λ=150.

Fig. 7. The probability that a particle starting in the neutral state 2 ends up in the state 1. Various curves correspond to different Massey parameters λ. The correspondence between λ and the incident kinetic energy is given in Table II.

Fig. 8. The matrix elements $H_{ii}(R)$ (full lines) and H_{ij}(dashed-dotted lines) defined by Eqs. (II.1-3) and the parameters for Hamiltonian II given in Table I. The value of β is 0.1. The adiabatic energy curves H^a_{ii} are also given. The incident kinetic energies

used in subsequent calculations, labeled by the values of λ (see Table II for conversion) are marked on the graph.

Fig. 9. The adiabatic energy surfaces of Fig. 8 (dashed-dotted lines) and the energies $E_1(R(t))$ and $E_2(R(t))$ of the ionic and neutral packets, respectively (see Eq. (III.4) for definition). (a) λ=90; (b) λ=100; (c) λ=110; (d) λ=120; (e) λ=130; (f) λ=140. The Massey parameter λ indicates the incident kinetic energy (see Table II).

Fig. 10. The probability $P_1(t)$ that a neutral particle is ionized, for the Hamiltonian shown in Fig. 8 the curves corresponding to different incident kinetic energies are labelled by λ. For the relationship between λ and kinetic energy see Table II.

Fig. 11. Schematical representation of successive splitting of packets. See the text for explanation.

Fig. 12. The behavior of the Gaussian packets when multiple splitting is performed. The calculation is done with Hamiltonian I (see Eqs. (II.1-3) and Table I), β=0.3 and λ=42 ($mv_0^2/2 = 89.9\ \lambda^{-2}$). (a) The evolution of the centers of the neutral packets R_2, R_2', R_2'' and that of the ionic packet R_1. (b) the probability $P_1(t)$ that the system is ionic.

Fig. 13. Schematic representation of the lattice atom system and its parameters.

Fig. 14. The results of a calculation using the Hamiltonian I (Table I) λ=43 ($mv_0^2/2 = 89.9\ \lambda^{-2}$ eV) and β=0.3, coupled through a mean trajectory Langevin equation

to a Ni lattice with ω_D=1.43x10^{-3} a.u. (a) The motion of the centers of the ionic (R_1) and neutral (R_2) packets for a rigid lattice; (b) the same for a lattice at T=0K (c) the energy of the above packets at T=0K.

Fig. 15. Same as Fig. 13b except that: (a) T=Θ_D; and (b) T=5Θ_D, where Θ_D is the Debye temperature.

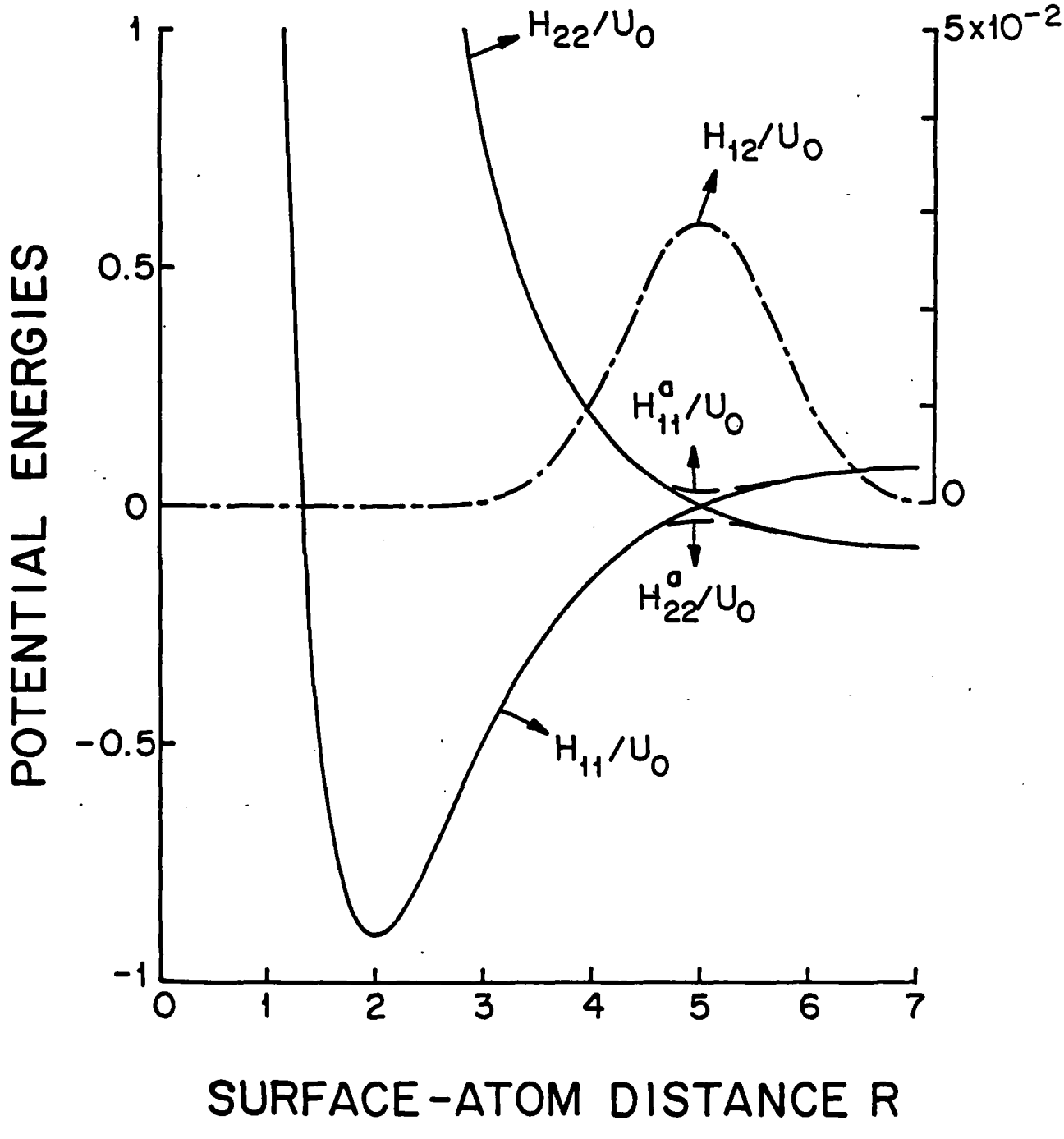
POTENTIAL ENERGIES
SURFACE-ATOM DISTANCE R
H_{22}/U_0
H_{12}/U_0
H_{11}^a/U_0
H_{22}^a/U_0
H_{11}/U_0
5×10^{-2}
1
0.5
0
-0.5
-1
0
1
2
3
4
5
6
7

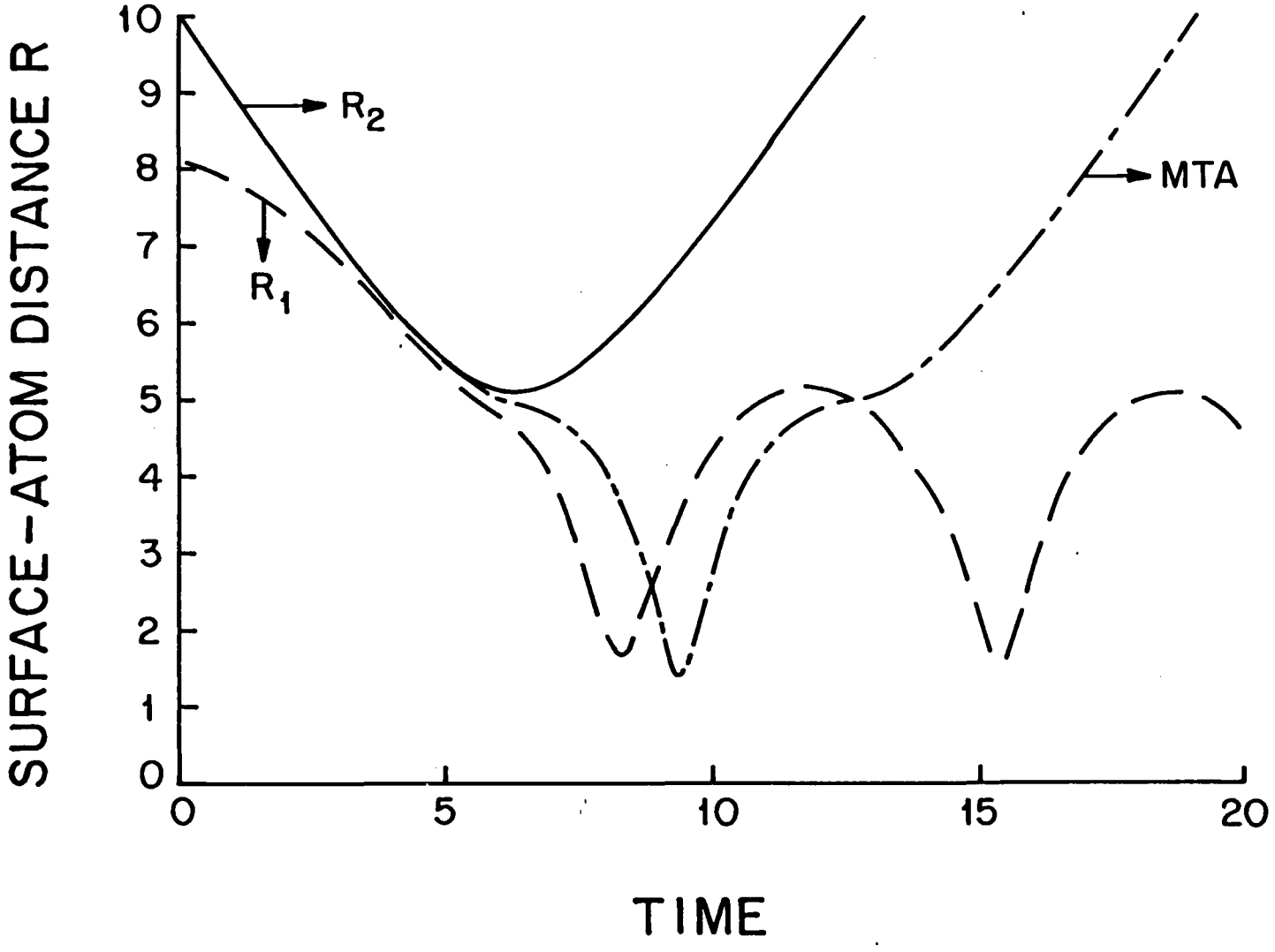
SURFACE-ATOM DISTANCE R
10
9
8
7
6
5
4
3
2
1
0
R_2
R_1
MTA
0
5
10
15
20
TIME

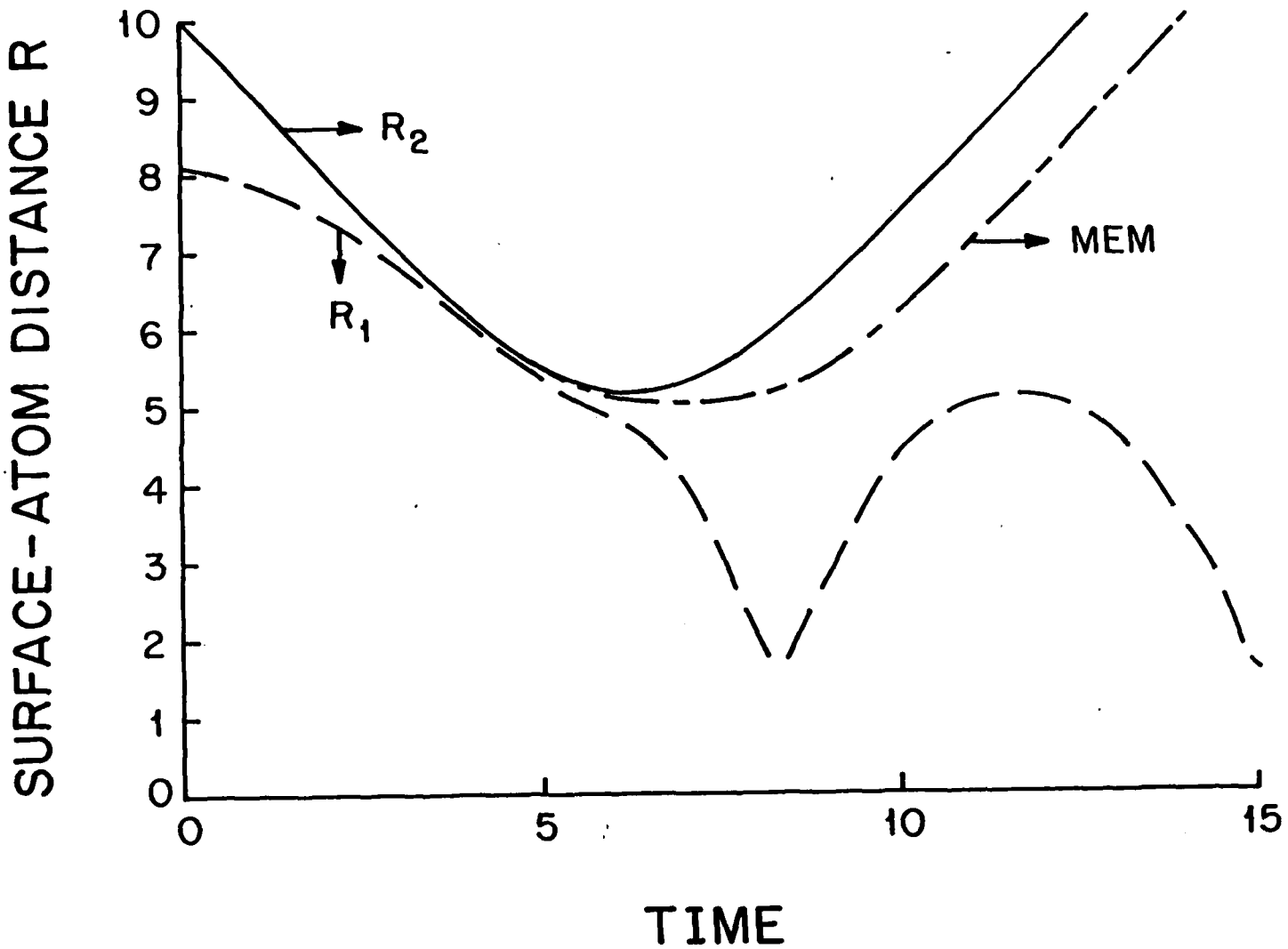
SURFACE-ATOM DISTANCE R
10
9
8
7
6
5
4
3
2
1
0
0
5
10
15
TIME
R2
R1
MEM

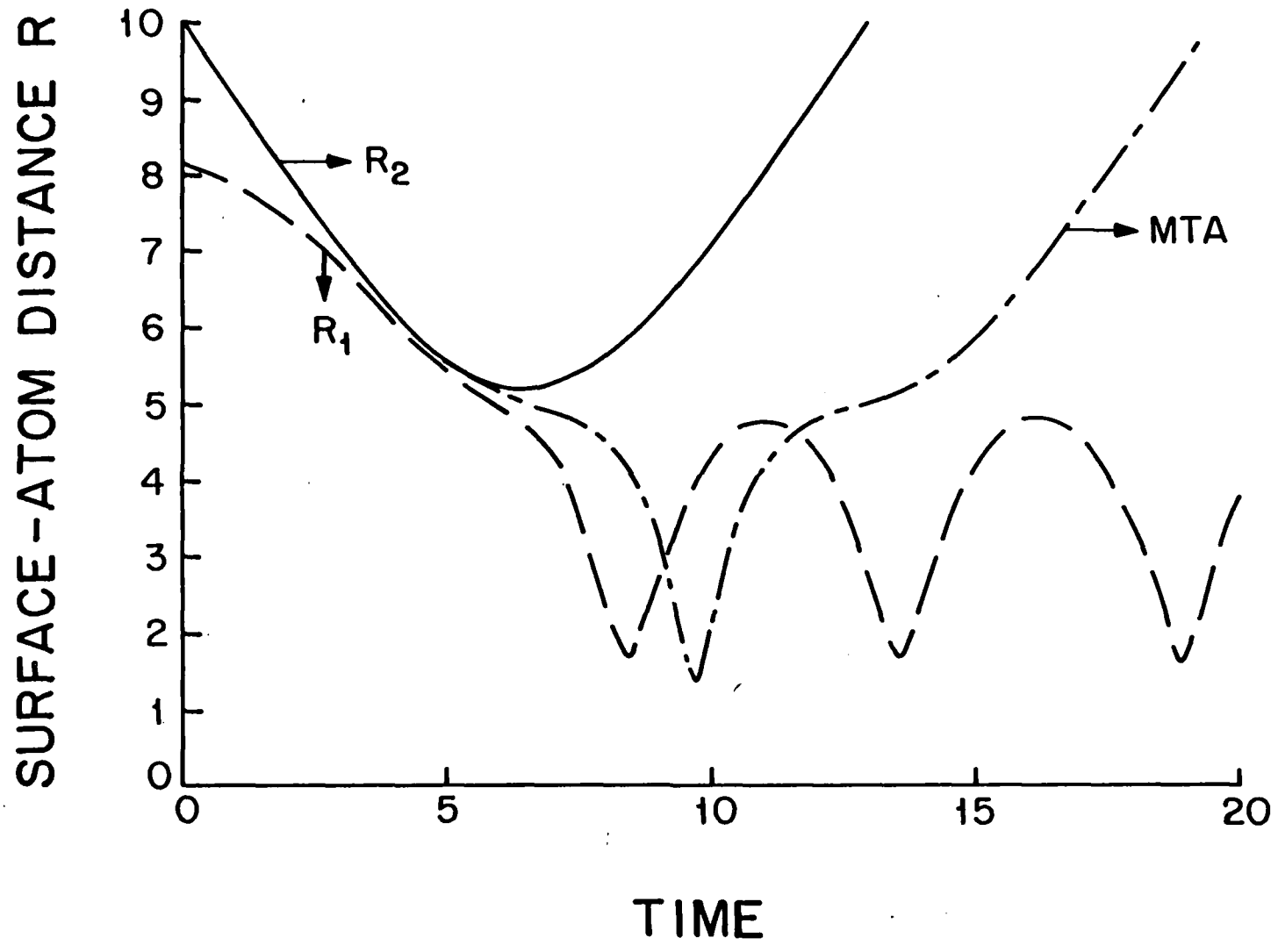
SURFACE-ATOM DISTANCE R
10
9
8
7
6
5
4
3
2
1
0
0
5
10
15
20
TIME
R2
R1
MTA

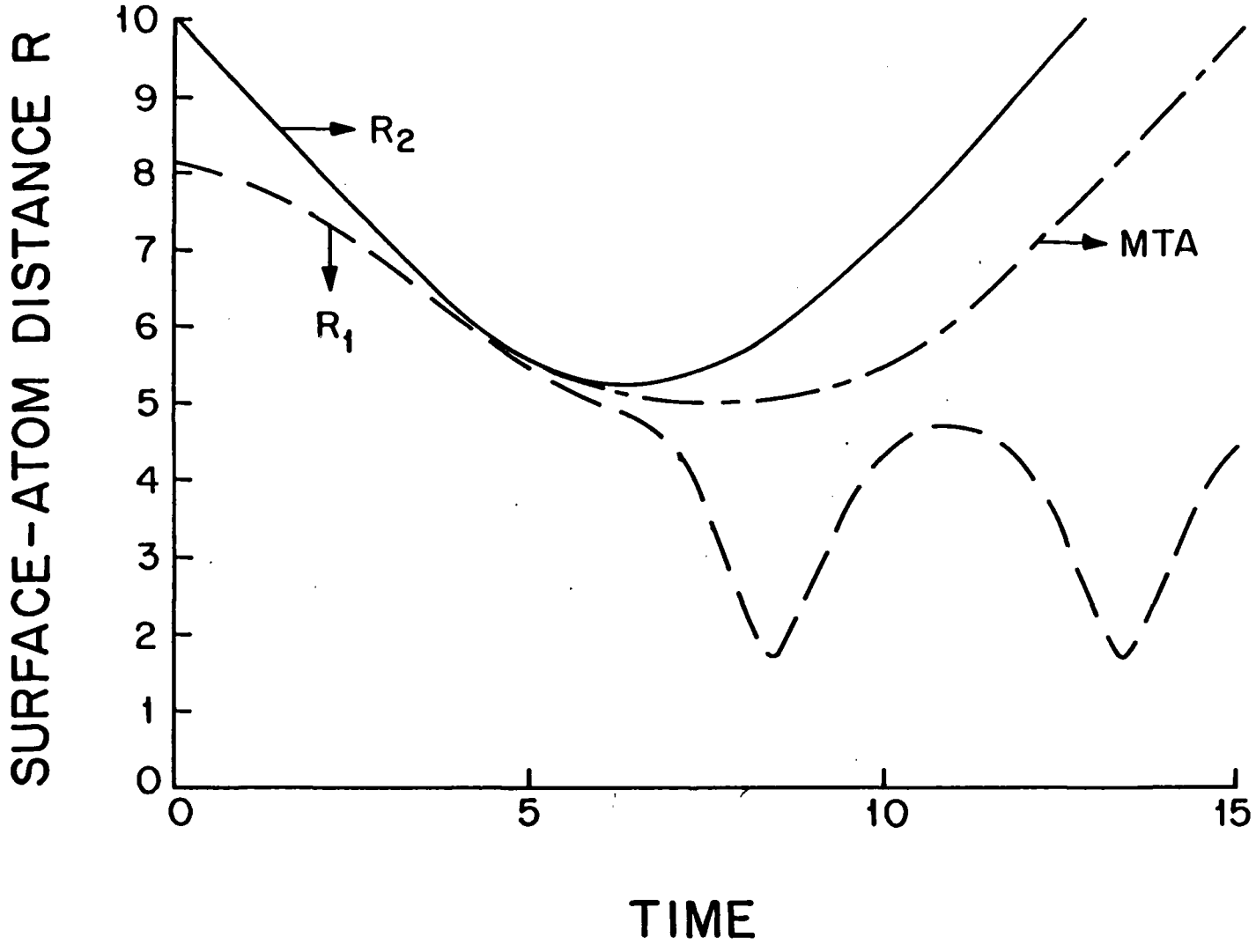
SURFACE-ATOM DISTANCE R
10
9
8
7
6
5
4
3
2
1
0
0
5
10
15
TIME
R_2
R_1
MTA

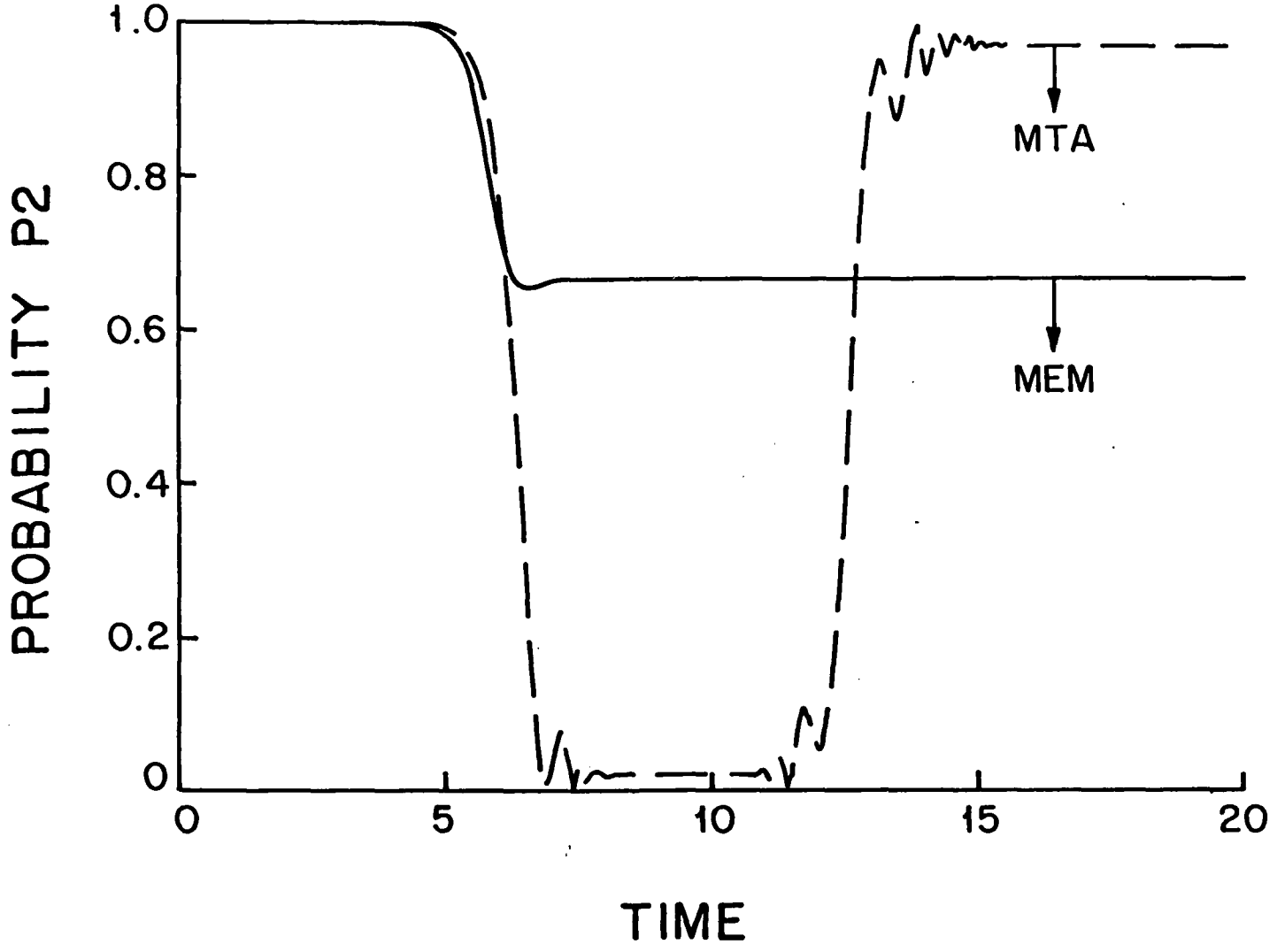
1.0
0.8
0.6
0.4
0.2
0
PROBABILITY P2
0
5
10
15
20
TIME
MTA
MEM

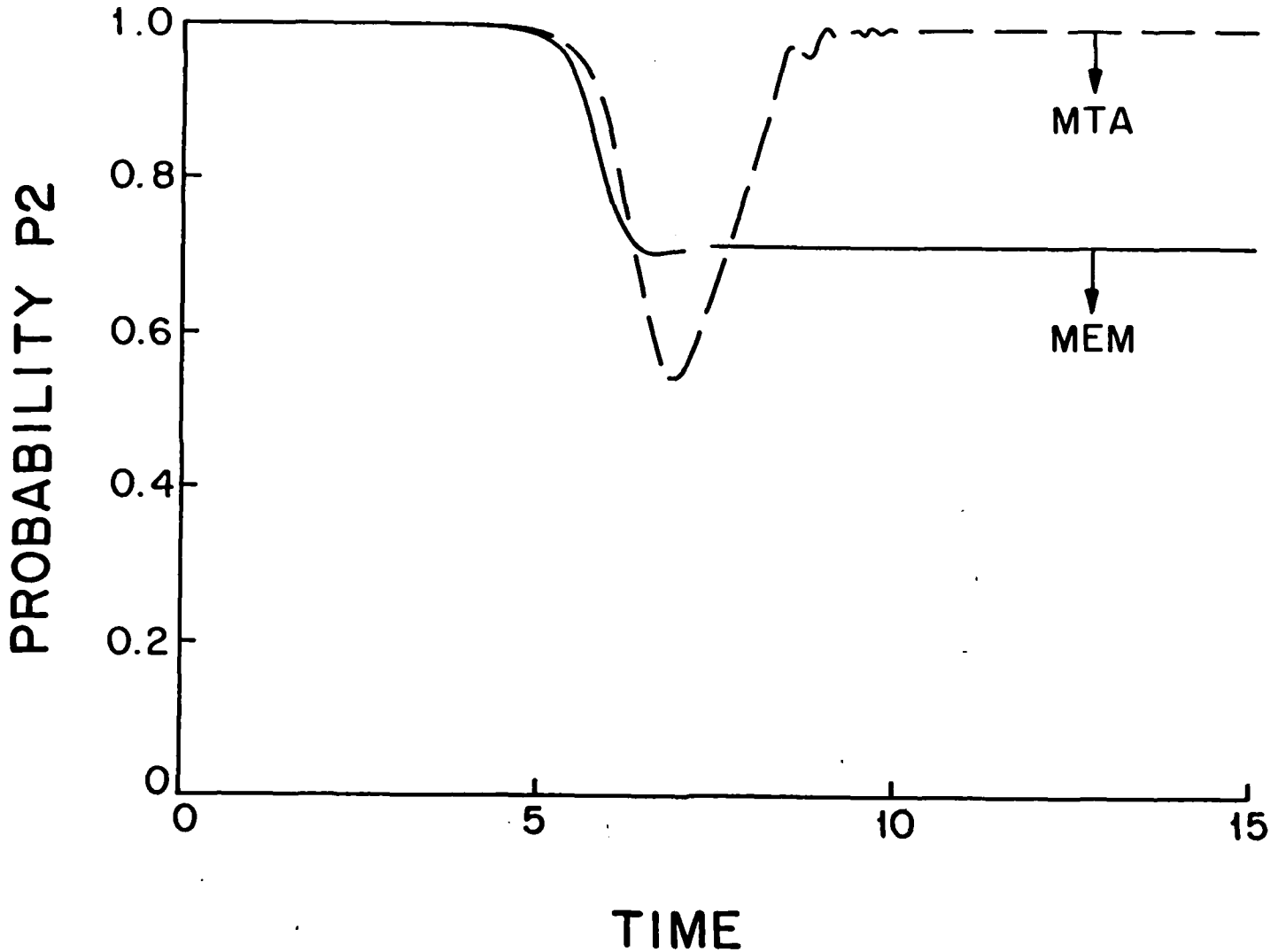
1.0
0.8
0.6
0.4
0.2
0
PROBABILITY P2
0
5
10
15
TIME
MTA
MEM

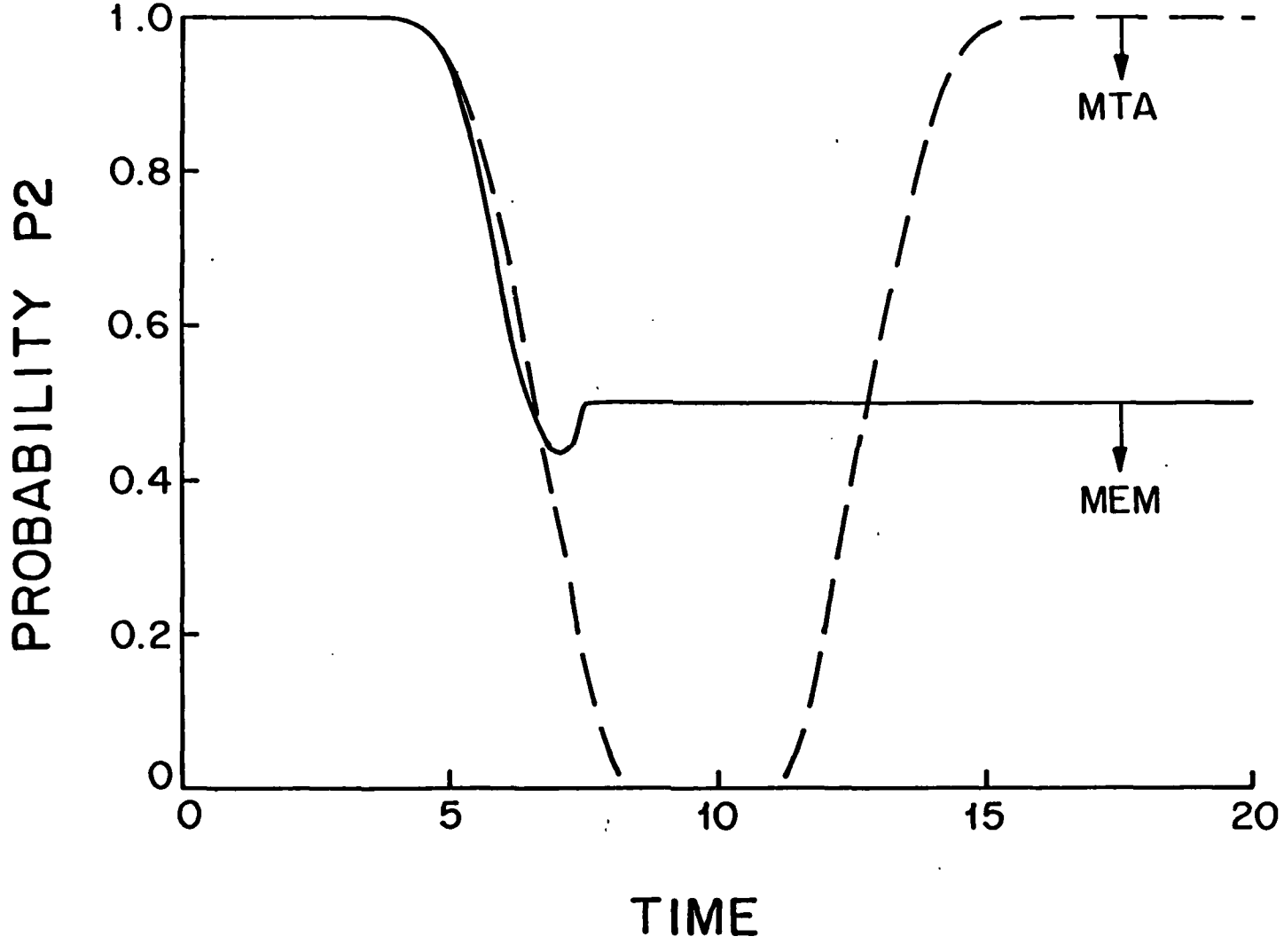
1.0
0.8
0.6
0.4
0.2
0
PROBABILITY P2
0
5
10
15
20
TIME
MTA
MEM

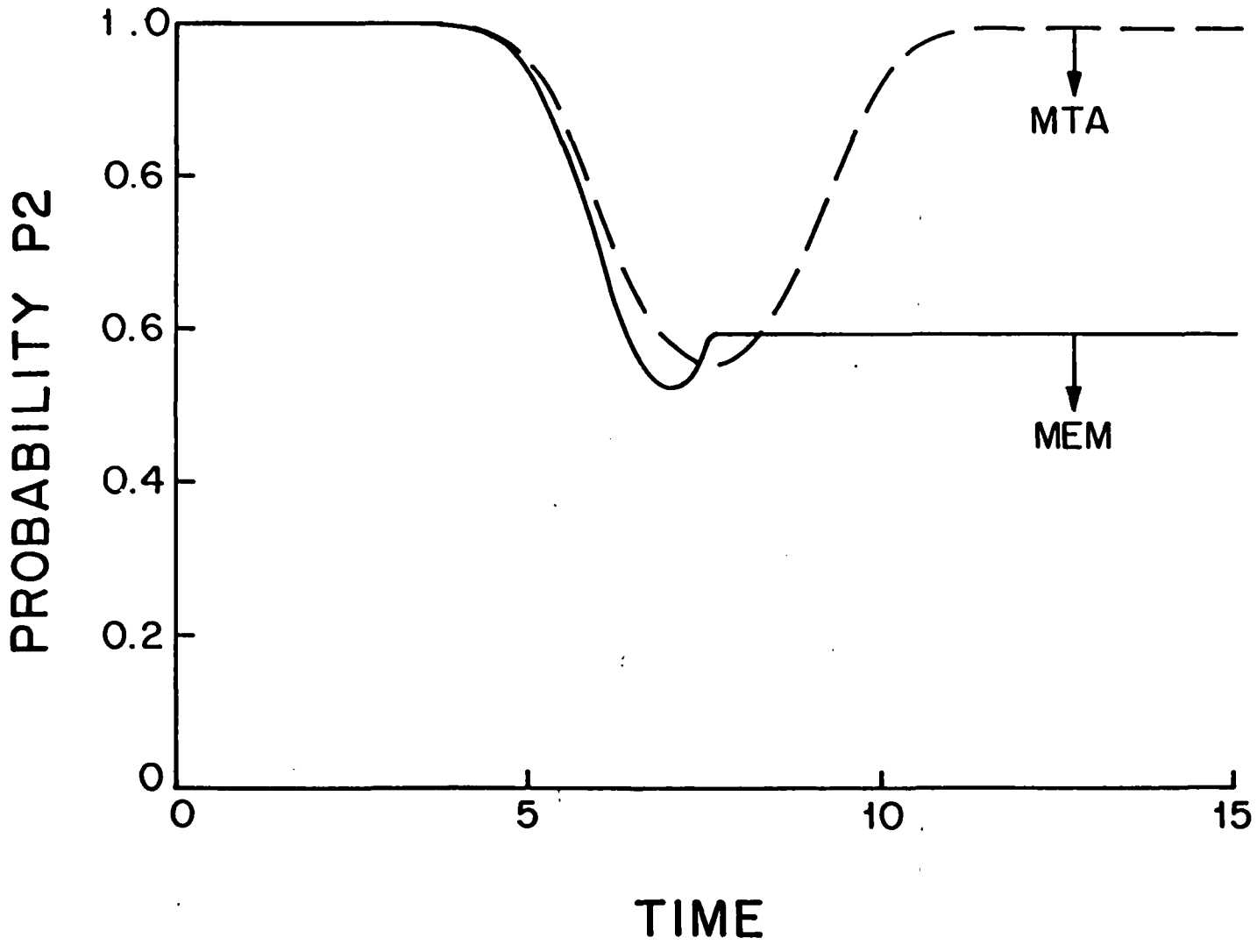
1.0
0.6
0.6
0.4
0.2
0
PROBABILITY P2
0
5
10
15
TIME
MTA
MEM

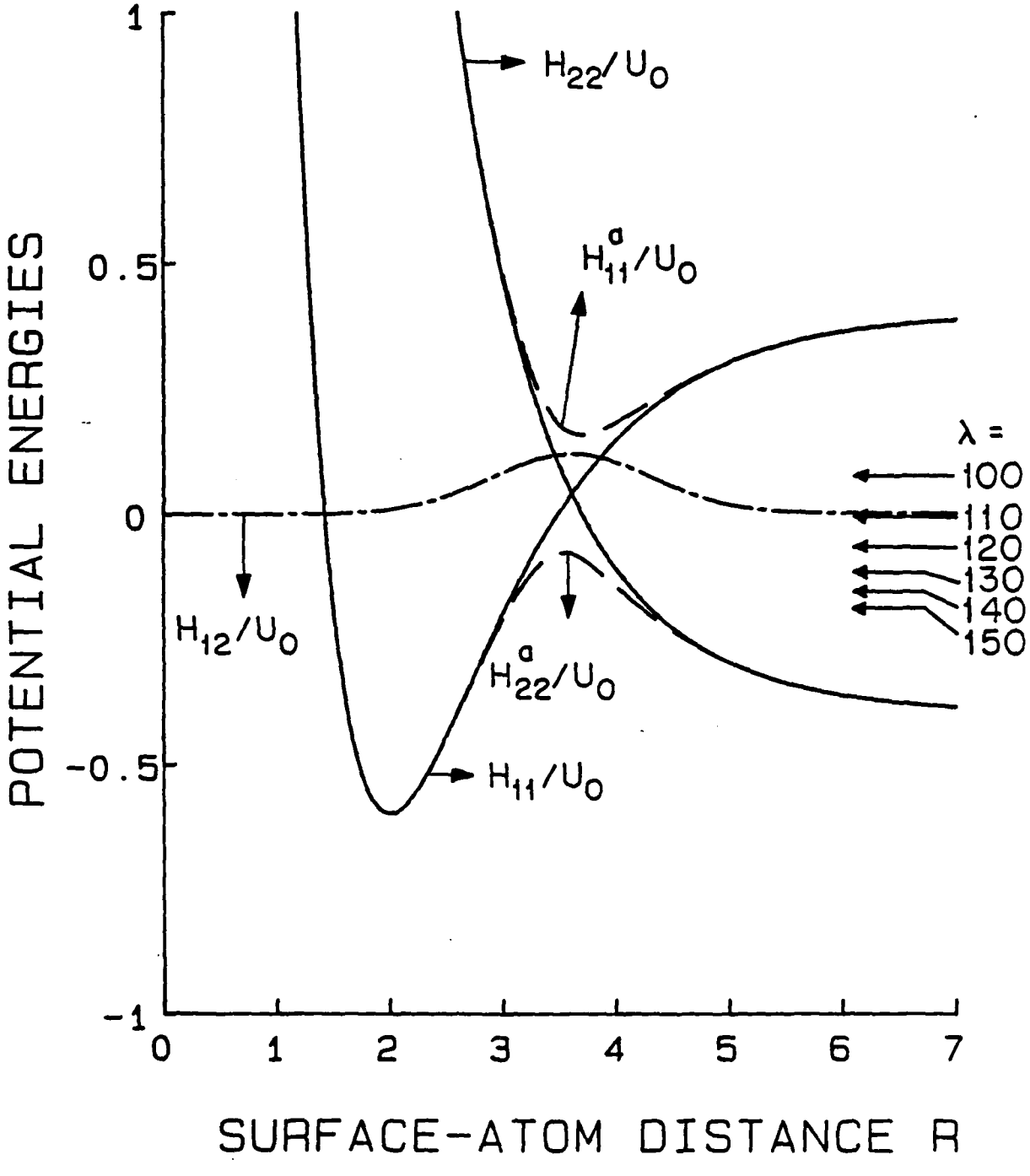
POTENTIAL ENERGIES
1
0.5
0
-0.5
-1
0
1
2
3
4
5
6
7
SURFACE-ATOM DISTANCE R
H_{22}/U_0
H_{11}^a/U_0
H_{12}/U_0
H_{22}^a/U_0
H_{11}/U_0
λ =
100
110
120
130
140
150

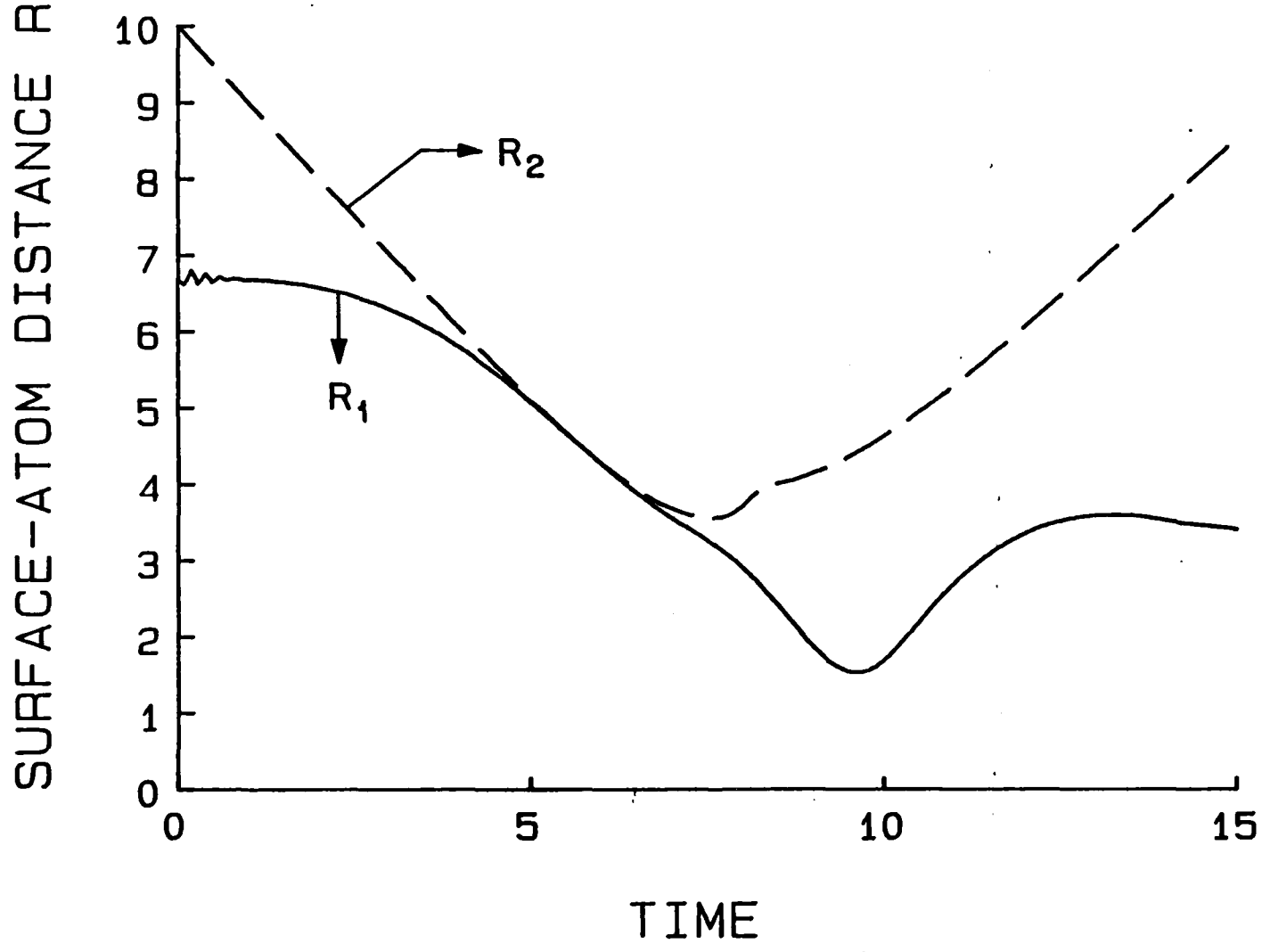
SURFACE-ATOM DISTANCE R
10
9
8
7
6
5
4
3
2
1
0
0
5
10
15
TIME
R_2
R_1

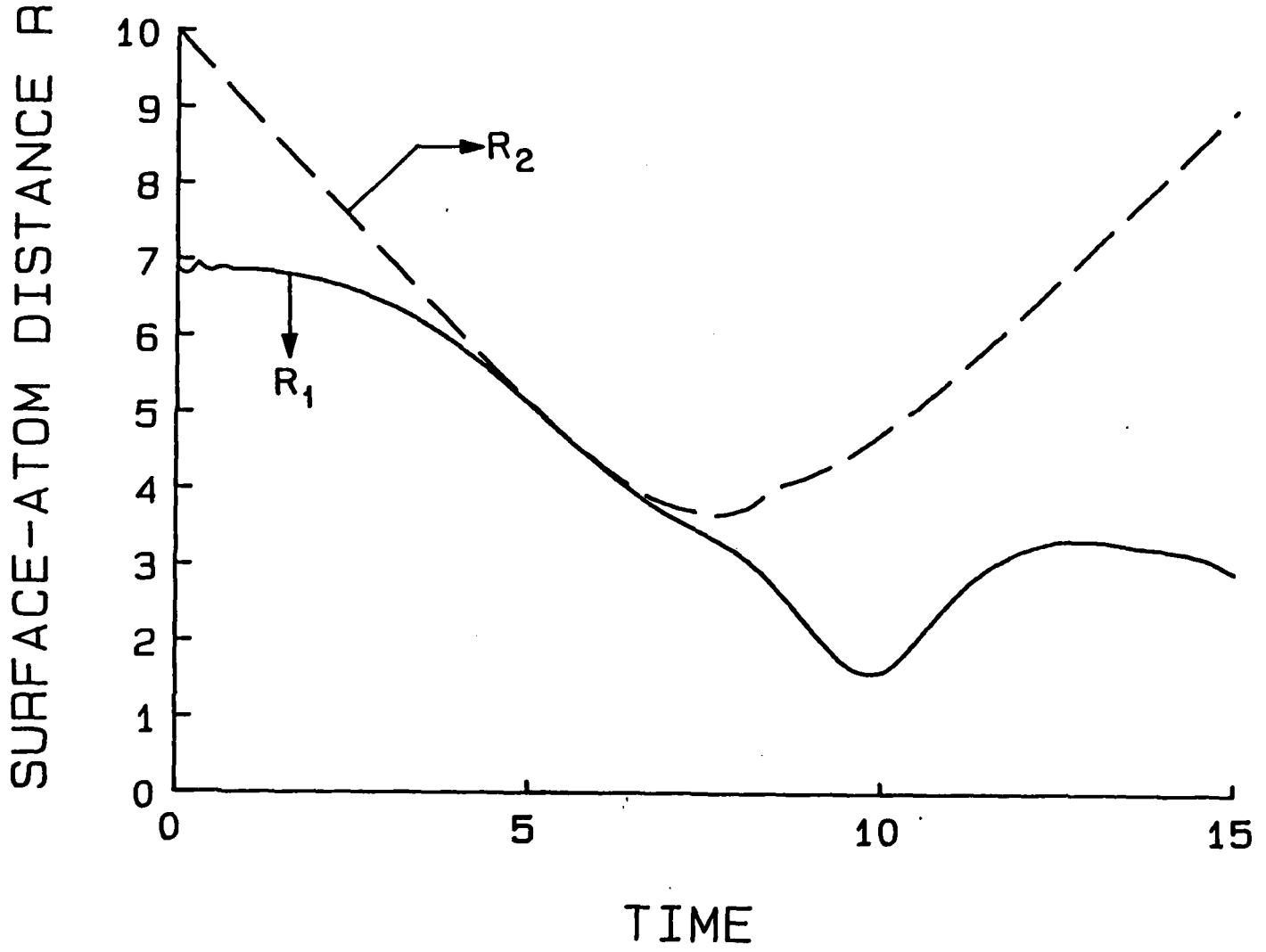
SURFACE-ATOM DISTANCE R
10
9
8
7
6
5
4
3
2
1
0
R_2
R_1
0
5
10
15
TIME

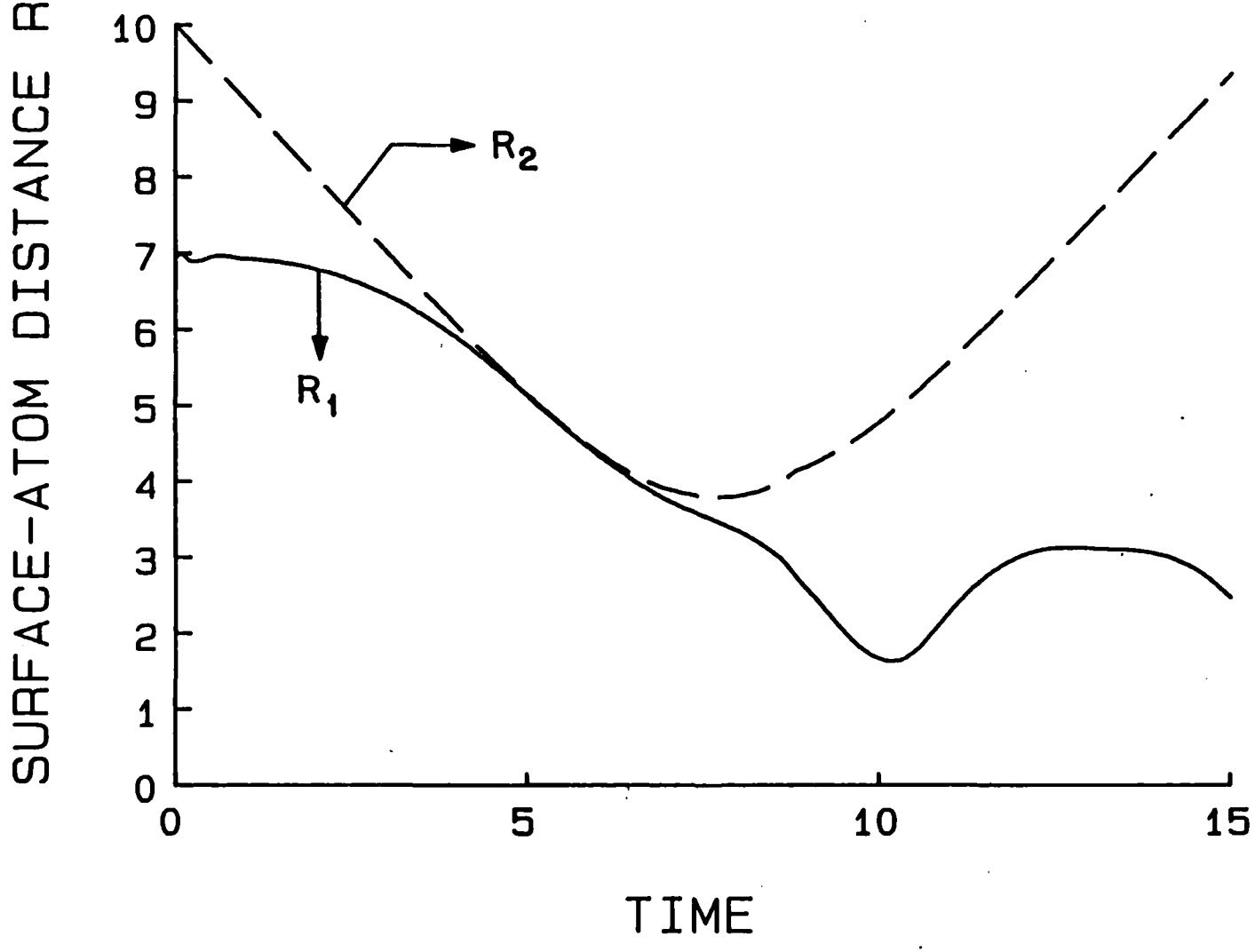
SURFACE-ATOM DISTANCE R
10
9
8
7
6
5
4
3
2
1
0
0
5
10
15
TIME
R_2
R_1

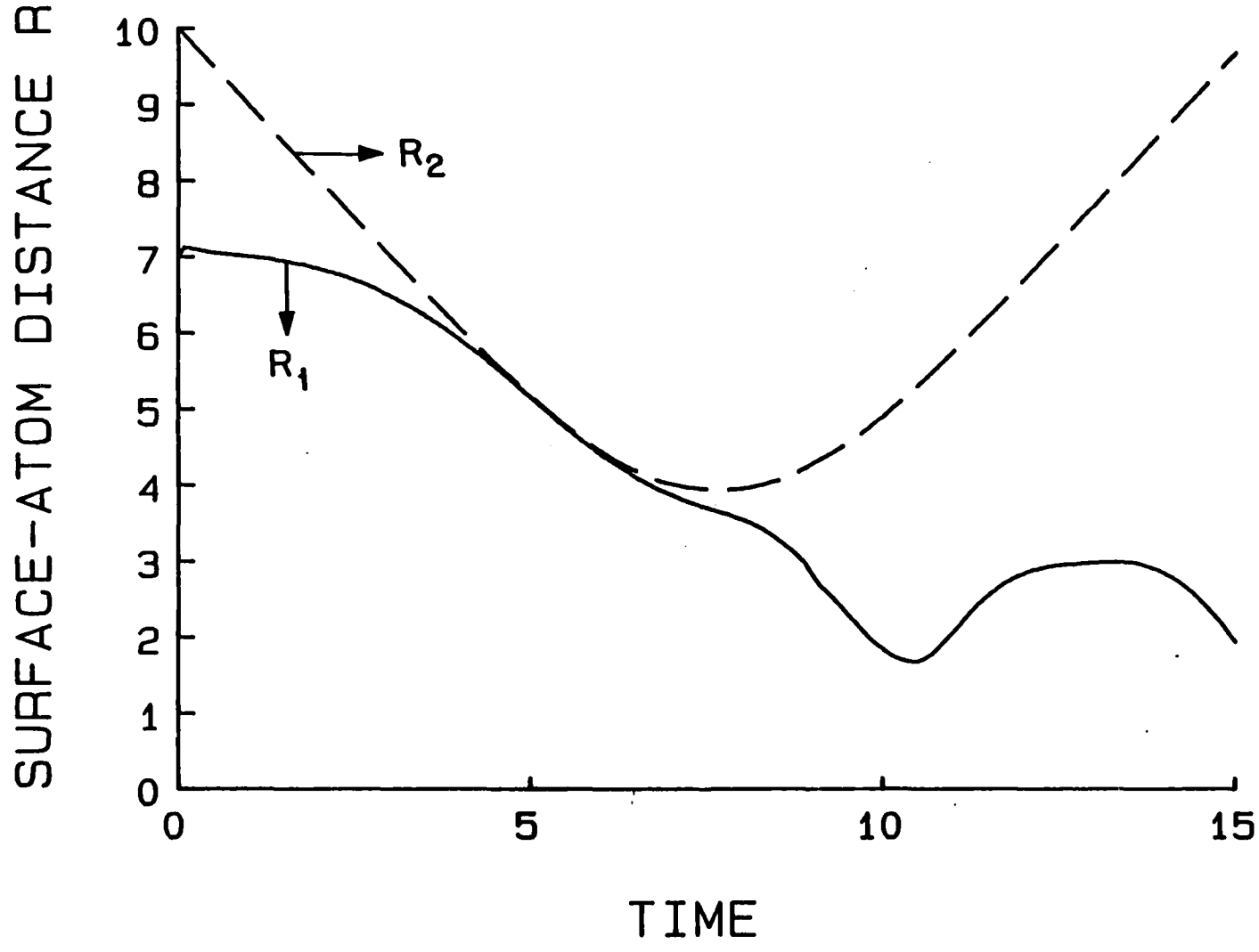
SURFACE-ATOM DISTANCE R
10
9
8
7
6
5
4
3
2
1
0
0
5
10
15
TIME
R_2
R_1

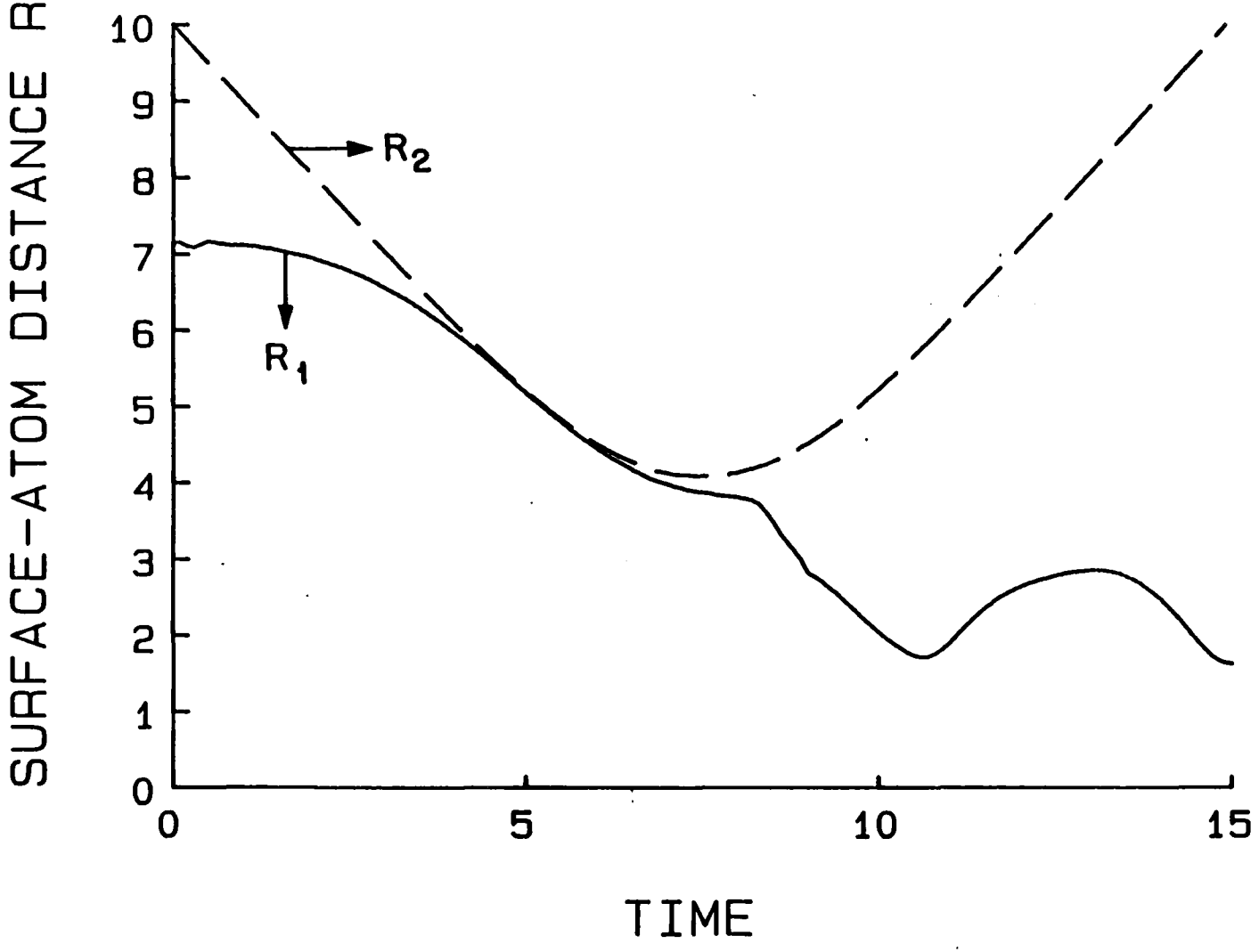
SURFACE-ATOM DISTANCE R
10
9
8
7
6
5
4
3
2
1
0
0
5
10
15
TIME
R_2
R_1

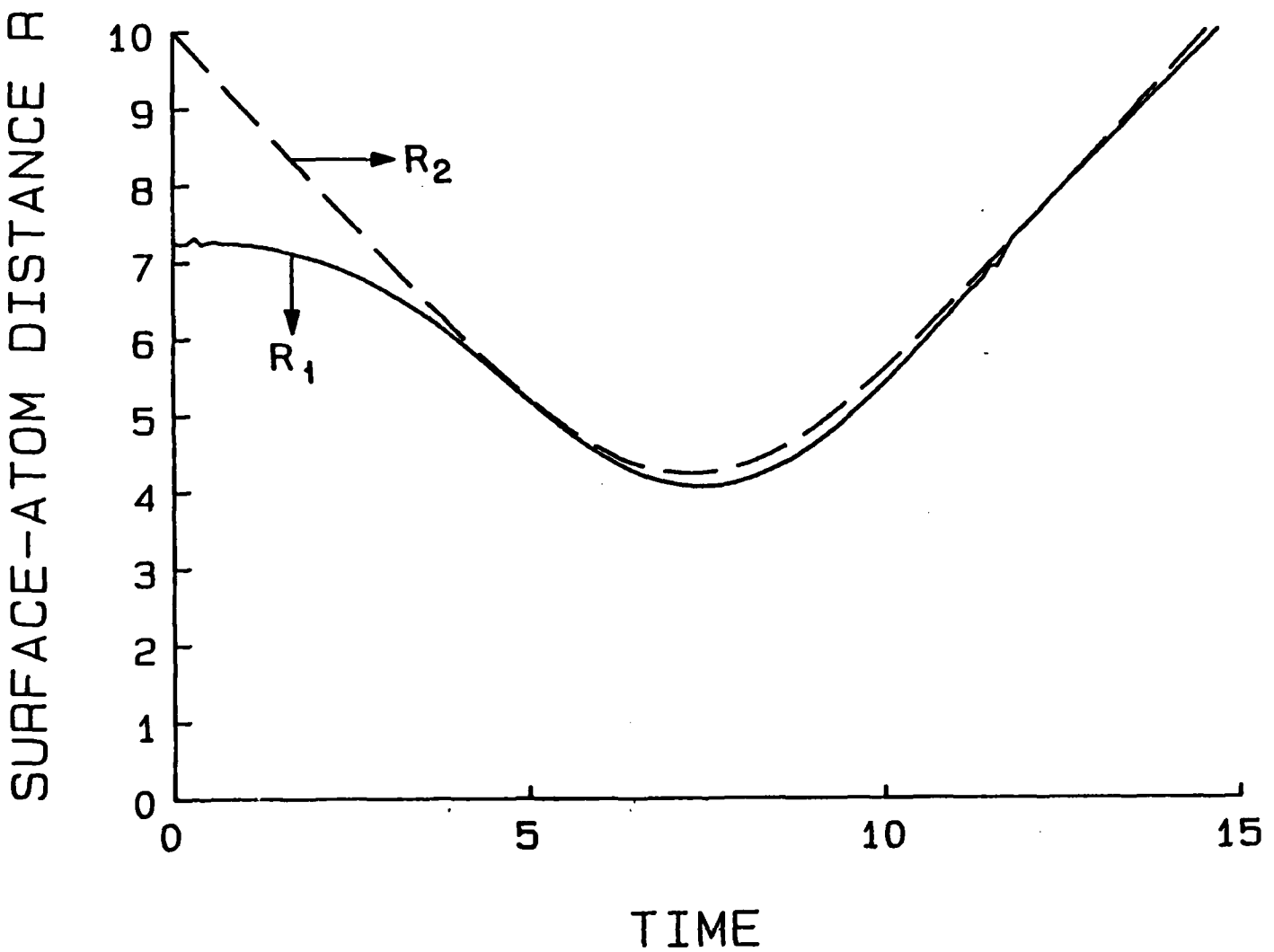
SURFACE-ATOM DISTANCE R
10
9
8
7
6
5
4
3
2
1
0
0
5
10
15
TIME
R_2
R_1

SURFACE-ATOM DISTANCE R
0
1
2
3
4
5
6
7
-1
-0.5
0
0.5
1
ENERGIES
E_2/U_o
E_1/U_o

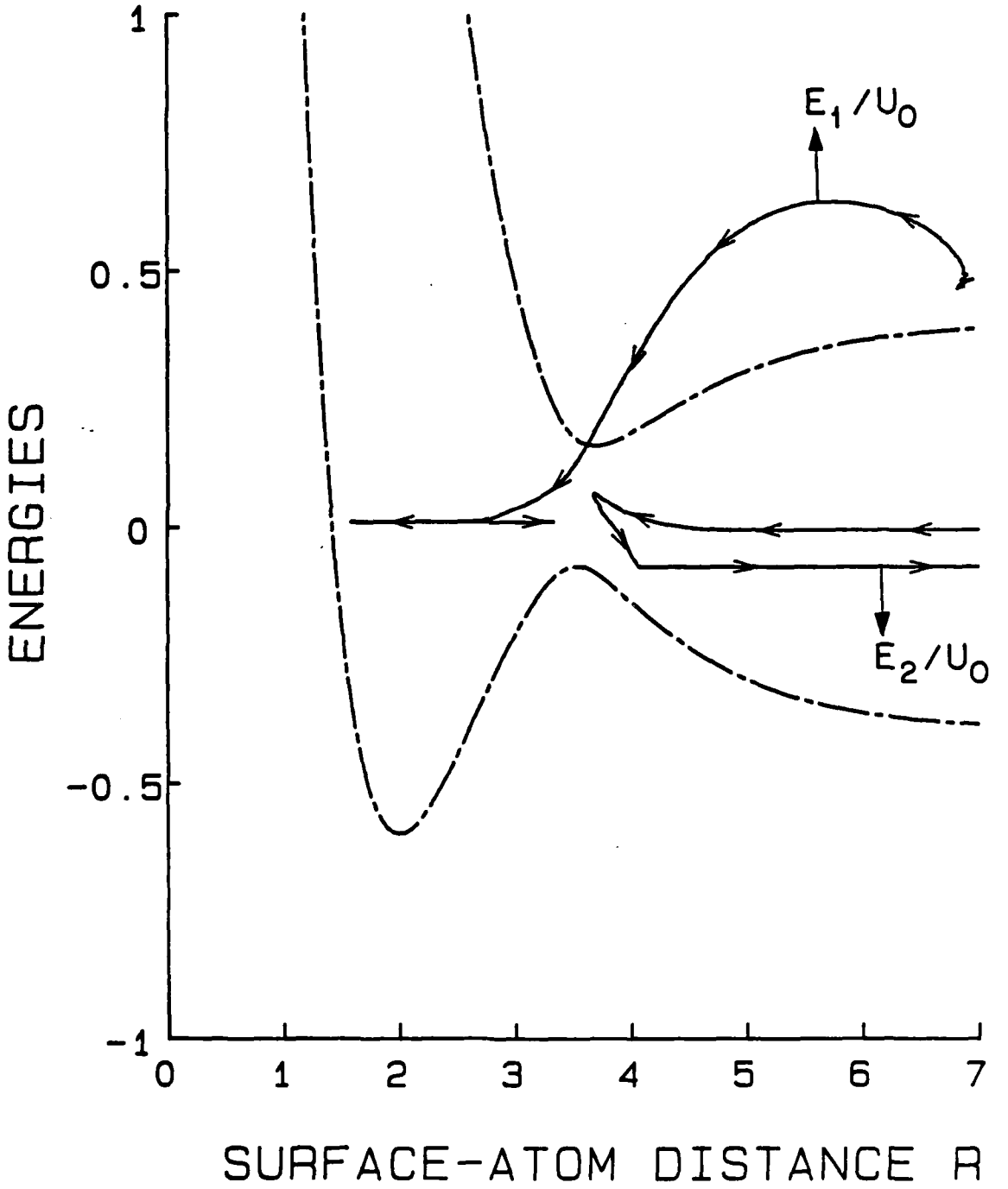
1
0.5
0
-0.5
-1
ENERGIES
E_1/U_0
E_2/U_0
0
1
2
3
4
5
6
7
SURFACE-ATOM DISTANCE R

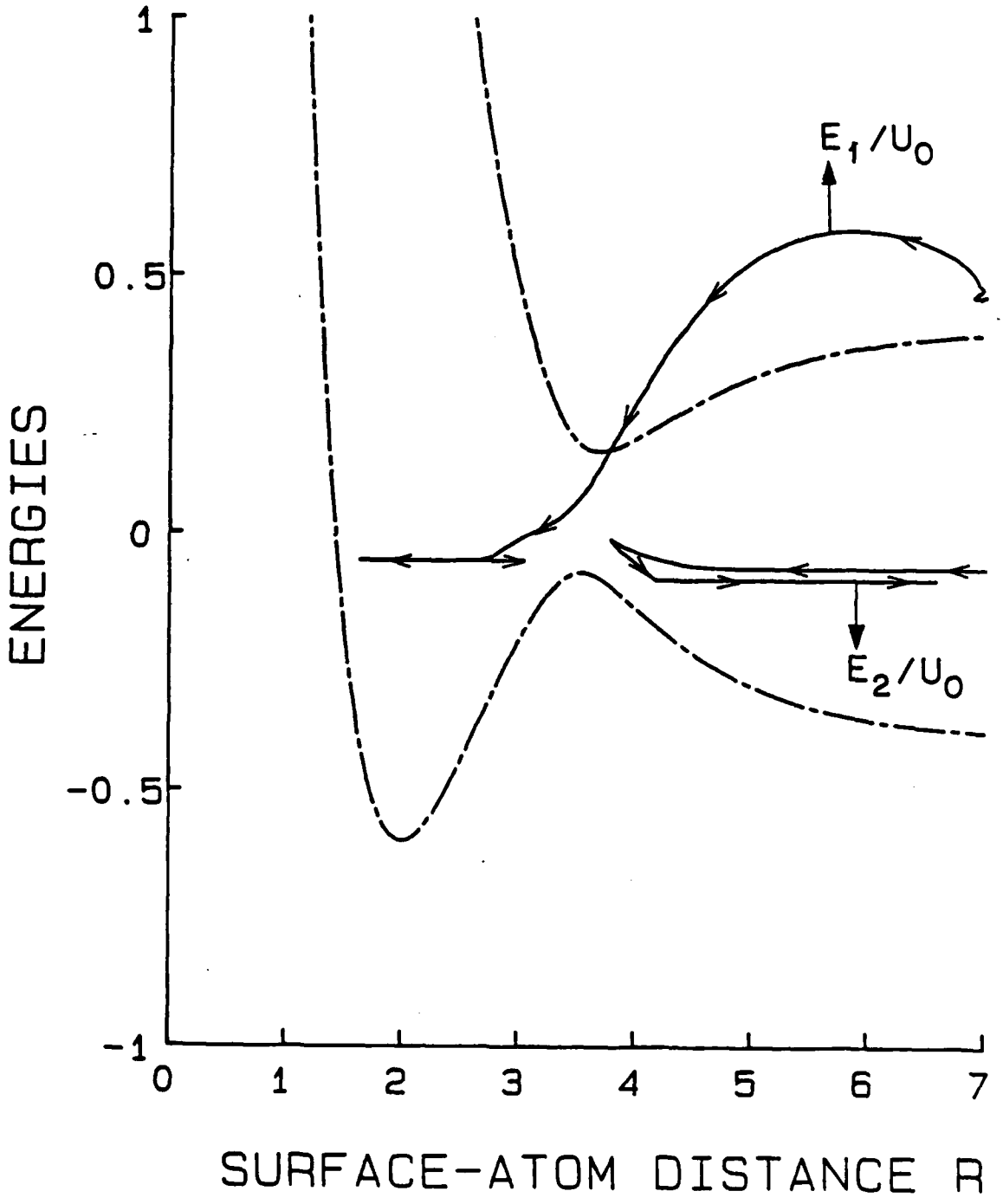
1
0.5
0
-0.5
-1
ENERGIES
E_1/U_0
E_2/U_0
0
1
2
3
4
5
6
7
SURFACE-ATOM DISTANCE R

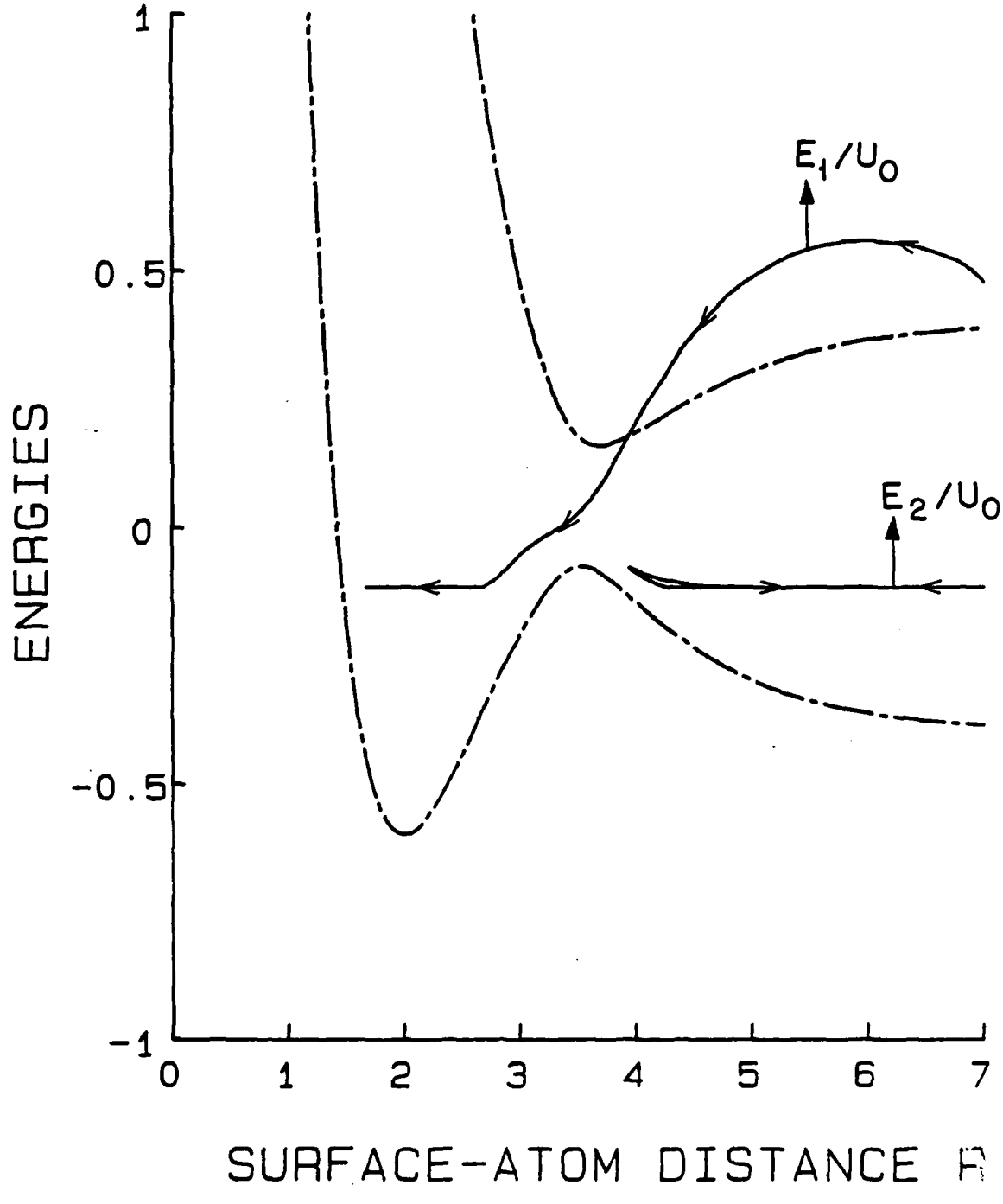
1
0.5
0
-0.5
-1
ENERGIES
E_1/U_0
E_2/U_0
0
1
2
3
4
5
6
7
SURFACE-ATOM DISTANCE R

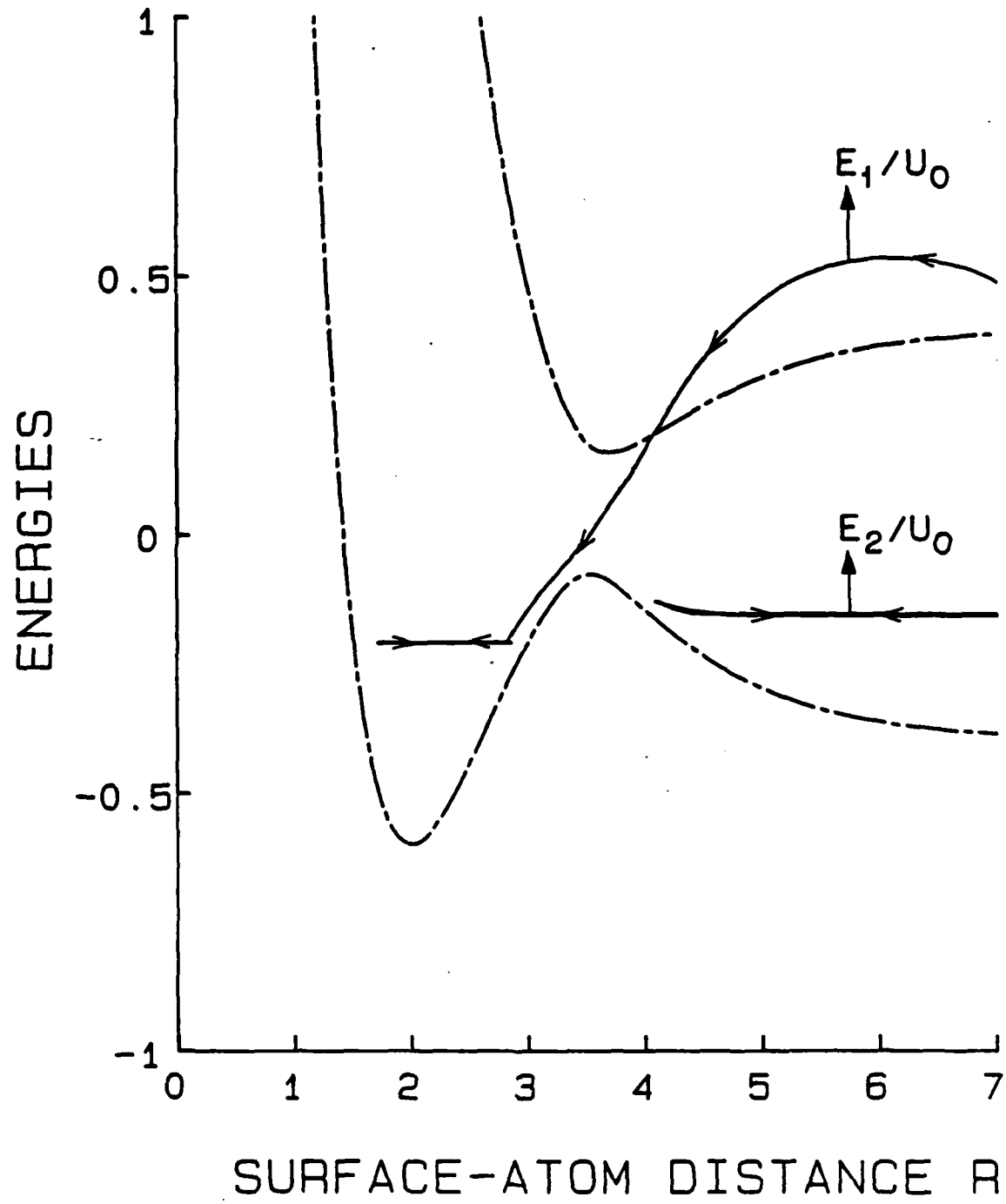
1
0.5
0
-0.5
-1
ENERGIES
E_1/U_0
E_2/U_0
0
1
2
3
4
5
6
7
SURFACE-ATOM DISTANCE R

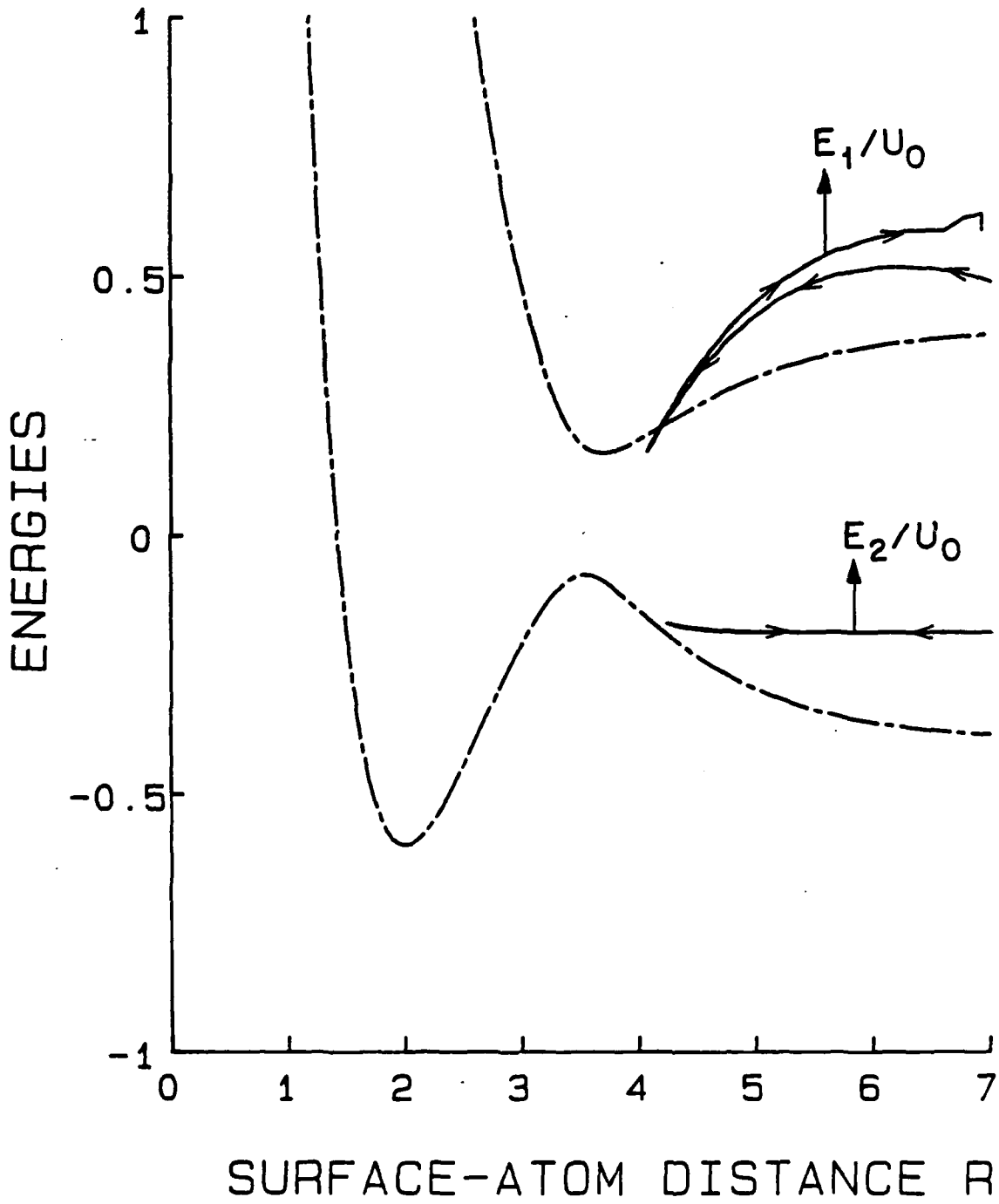
1
0.5
0
-0.5
-1
ENERGIES
E_1/U_0
E_2/U_0
0
1
2
3
4
5
6
7
SURFACE-ATOM DISTANCE R

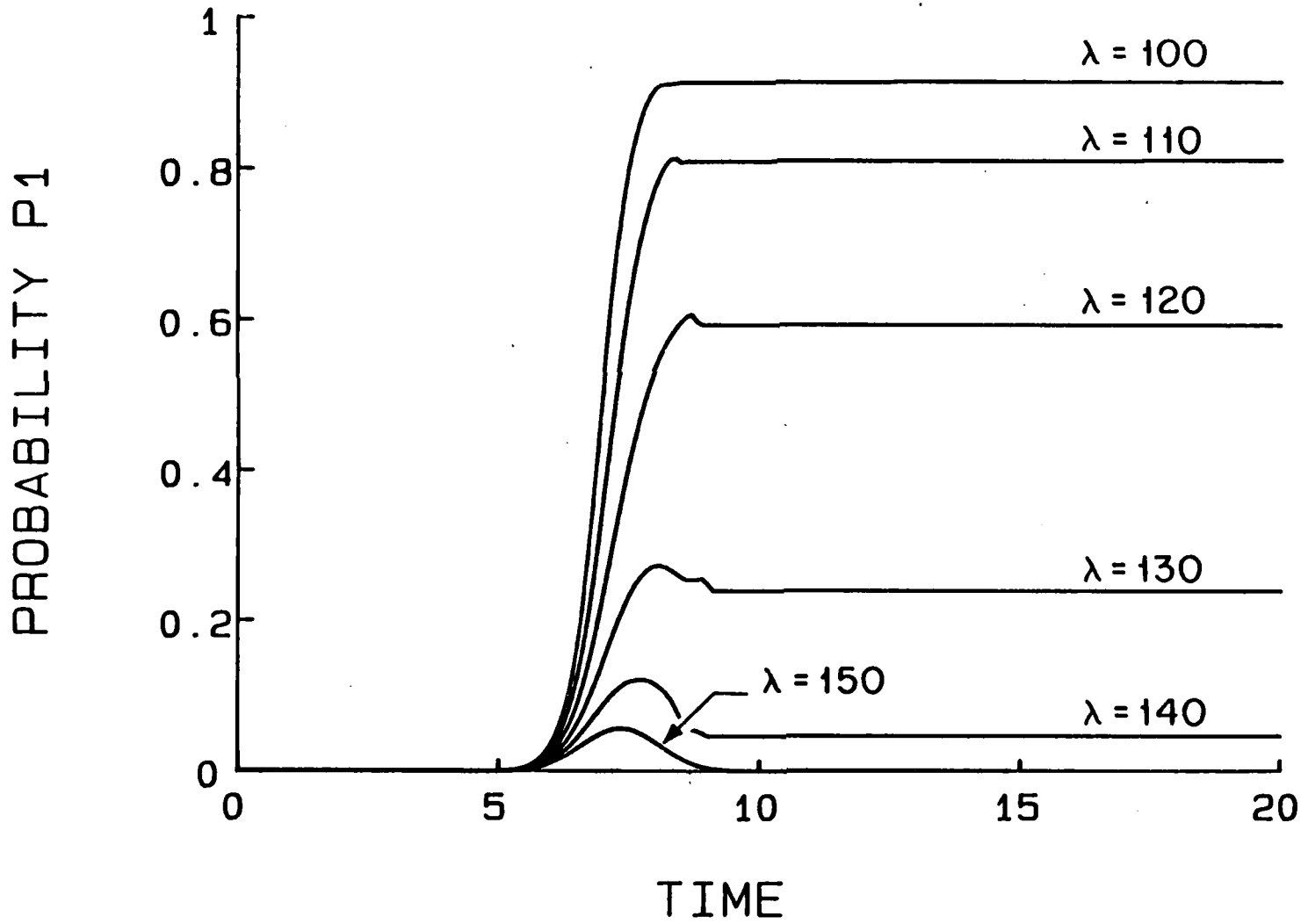
PROBABILITY P1
1
0.8
0.6
0.4
0.2
0
0
5
10
15
20
TIME
λ = 100
λ = 110
λ = 120
λ = 130
λ = 140
λ = 150

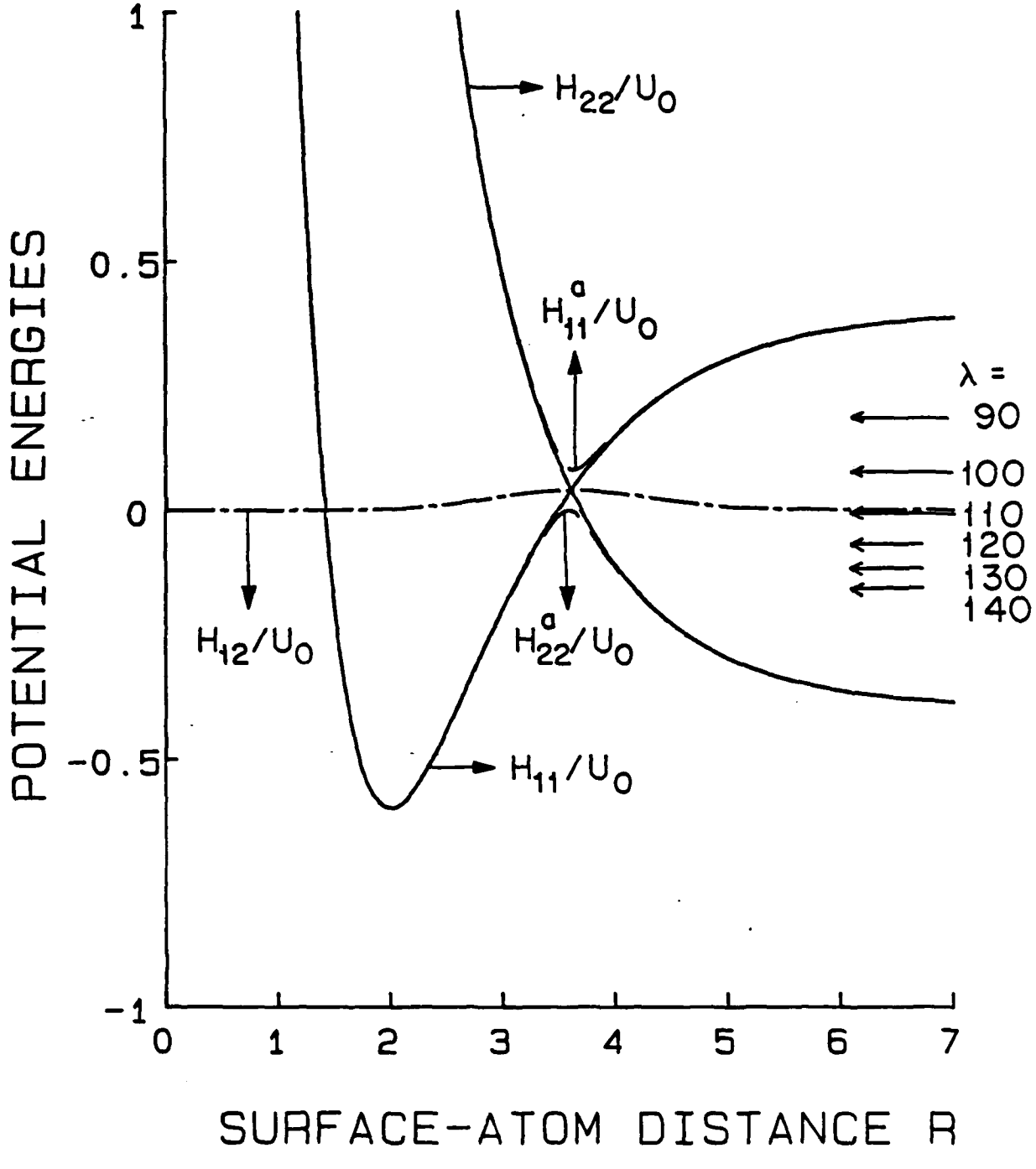
1
0.5
0
-0.5
-1
0
1
2
3
4
5
6
7
POTENTIAL ENERGIES
SURFACE-ATOM DISTANCE R
H_{22}/U_0
H_{11}^a/U_0
H_{12}/U_0
H_{22}^a/U_0
H_{11}/U_0
λ =
90
100
110
120
130
140

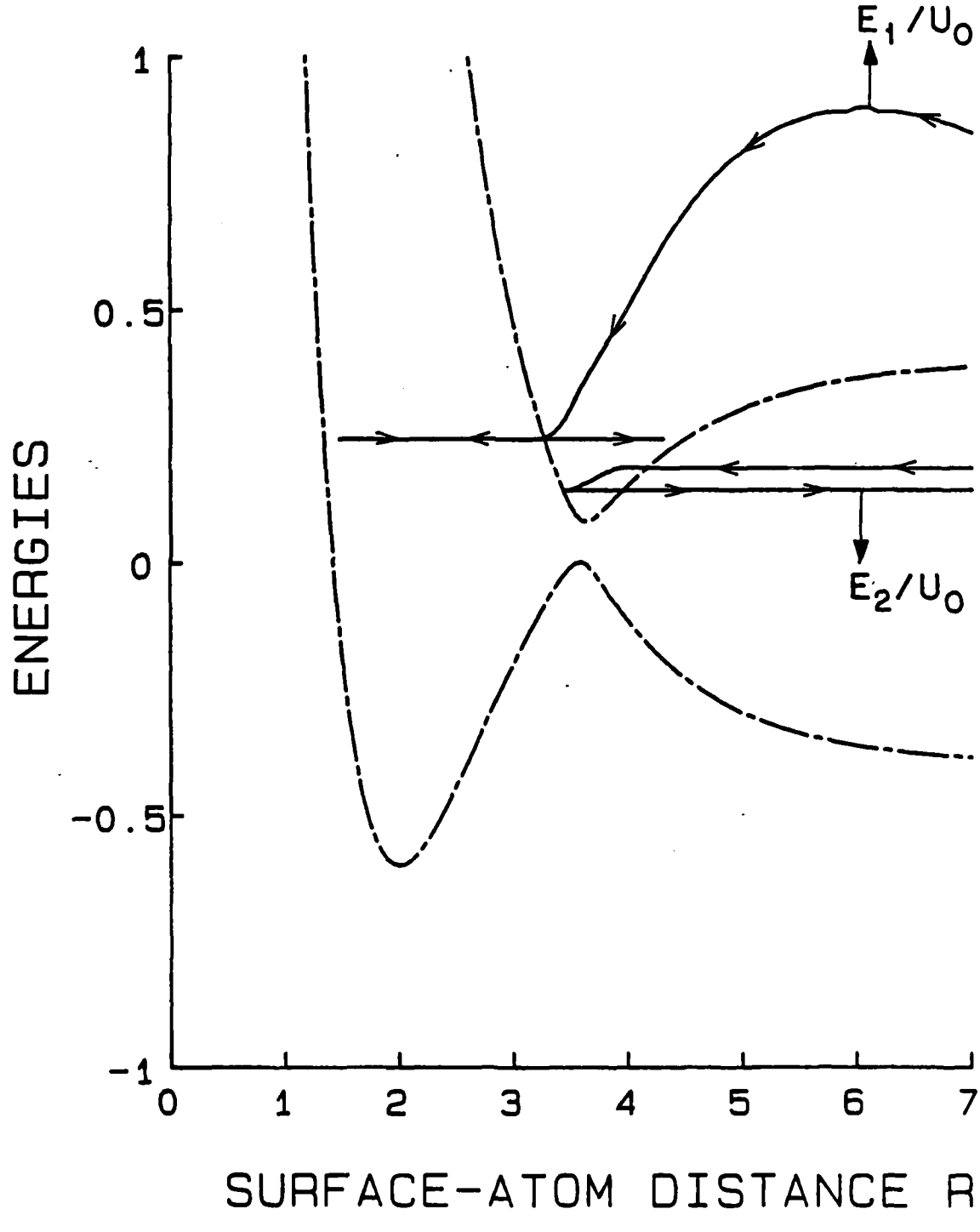
E1/U0
E2/U0
ENERGIES
1
0.5
0
-0.5
-1
0
1
2
3
4
5
6
7
SURFACE-ATOM DISTANCE R

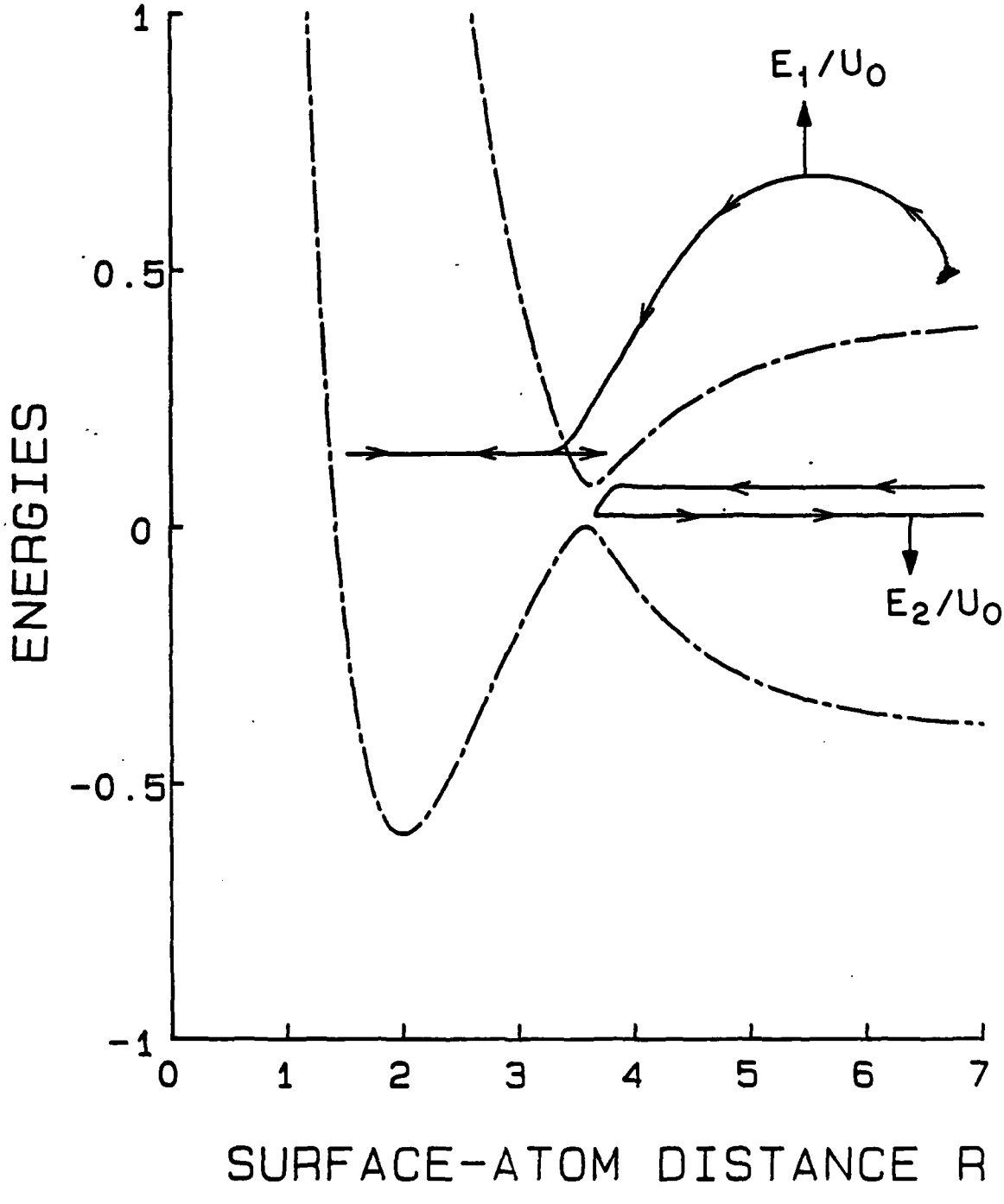
1
0.5
0
-0.5
-1
ENERGIES
E_1/U_0
E_2/U_0
0
1
2
3
4
5
6
7
SURFACE-ATOM DISTANCE R

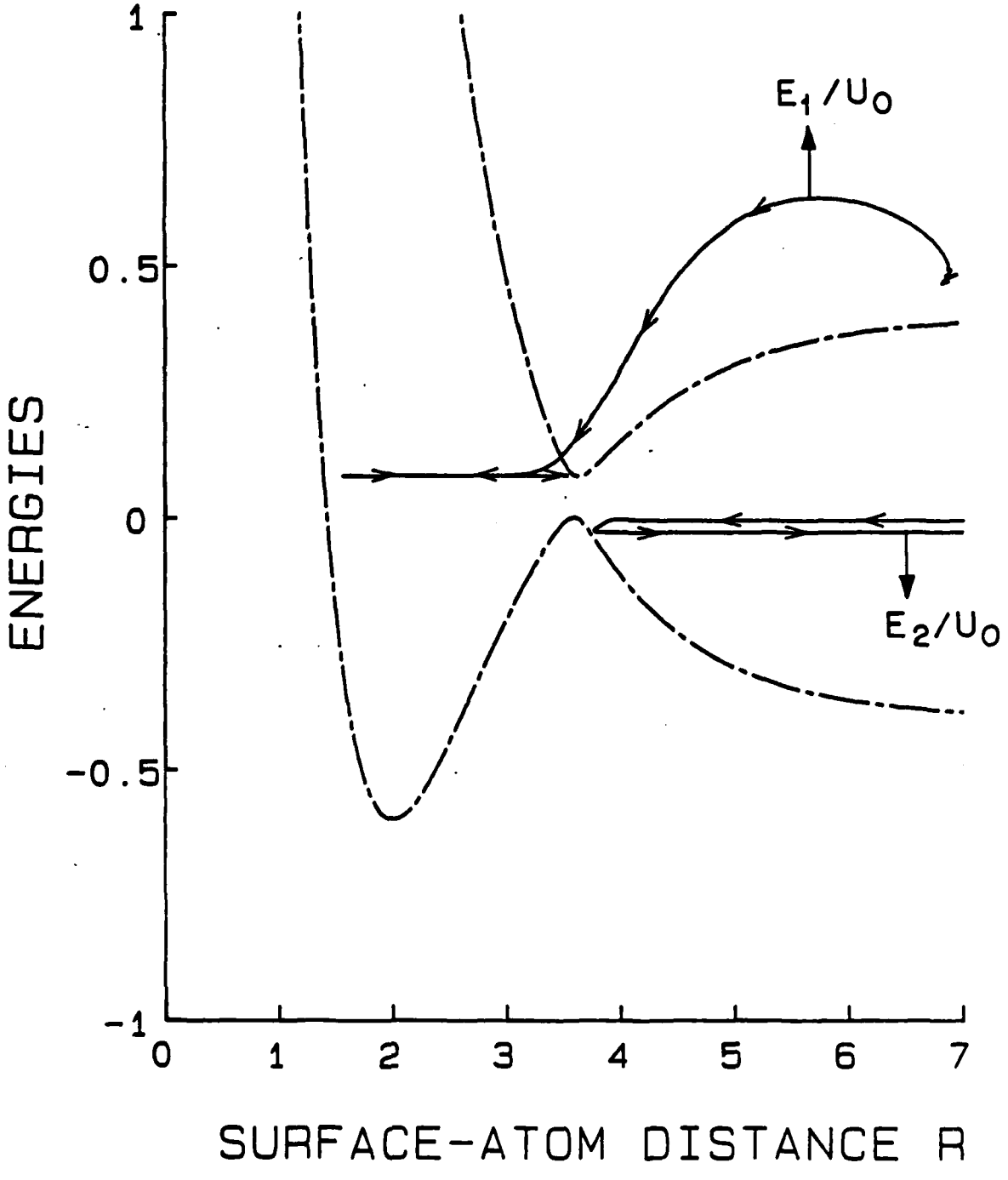
1
0.5
0
-0.5
-1
ENERGIES
E_1/U_0
E_2/U_0
0
1
2
3
4
5
6
7
SURFACE-ATOM DISTANCE R

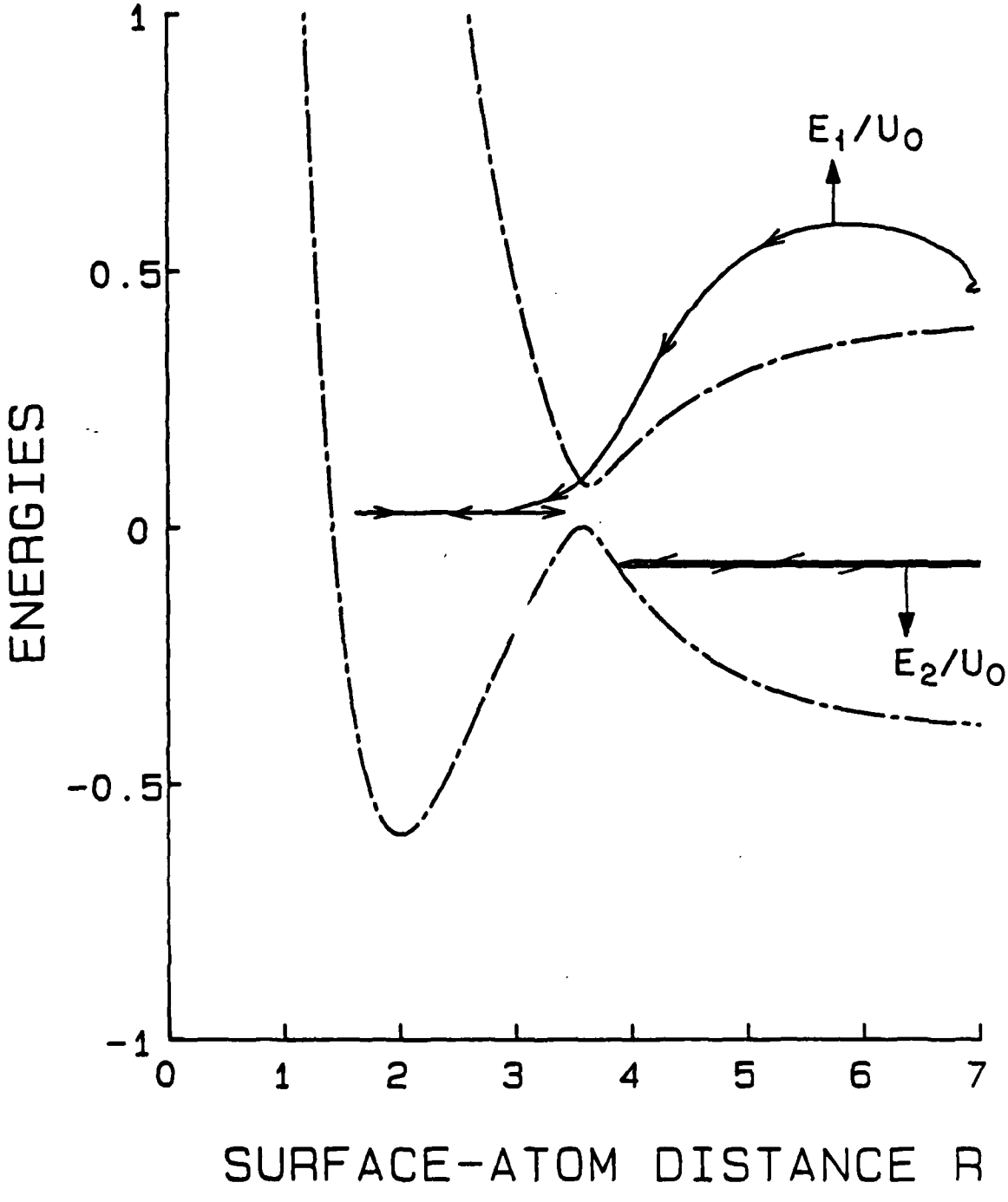
1
0.5
0
-0.5
-1
ENERGIES
E_1/U_0
E_2/U_0
0
1
2
3
4
5
6
7
SURFACE-ATOM DISTANCE R

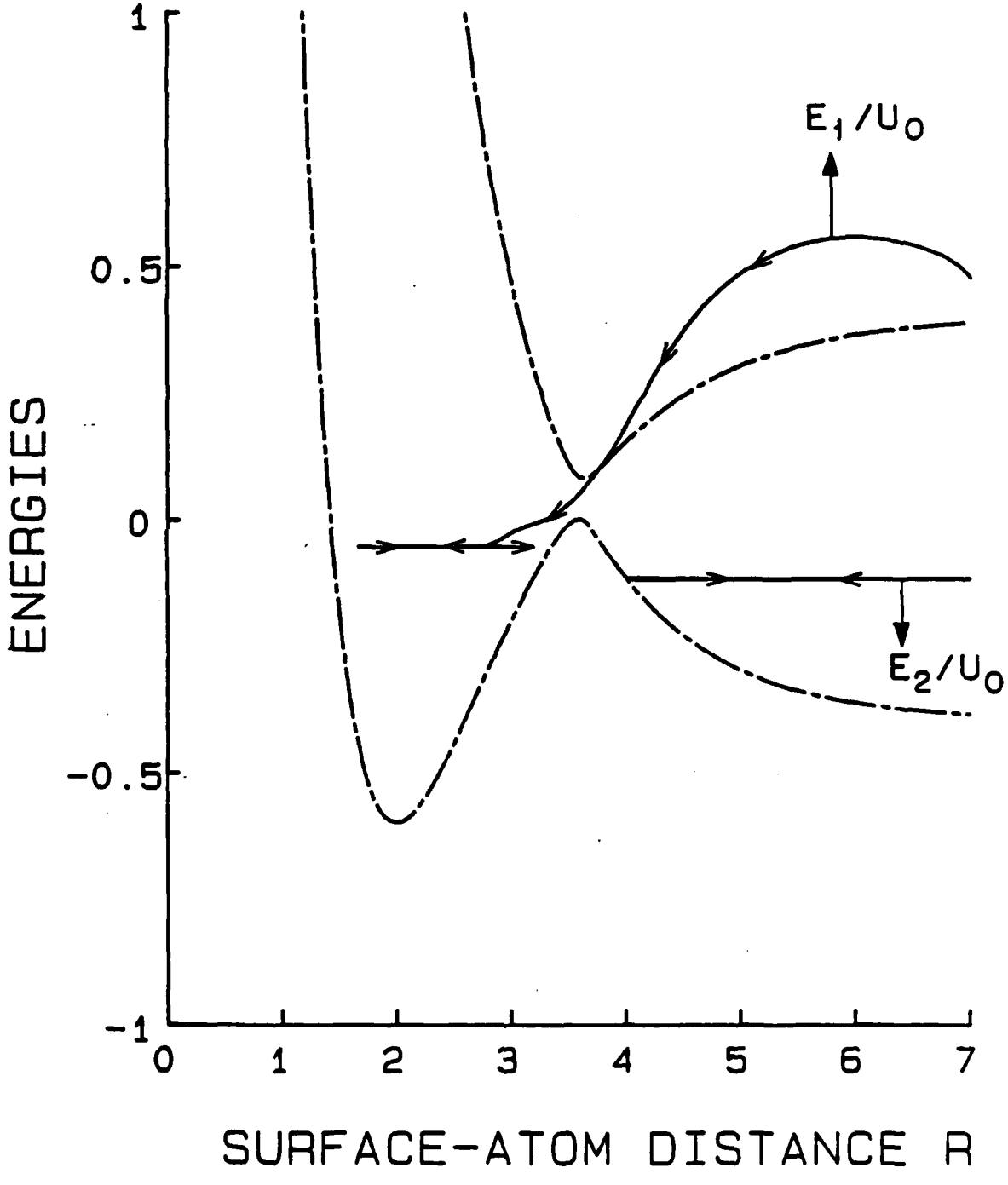
1
0.5
0
-0.5
-1
ENERGIES
E_1/U_0
E_2/U_0
0
1
2
3
4
5
6
7
SURFACE-ATOM DISTANCE R

Fig 3.1

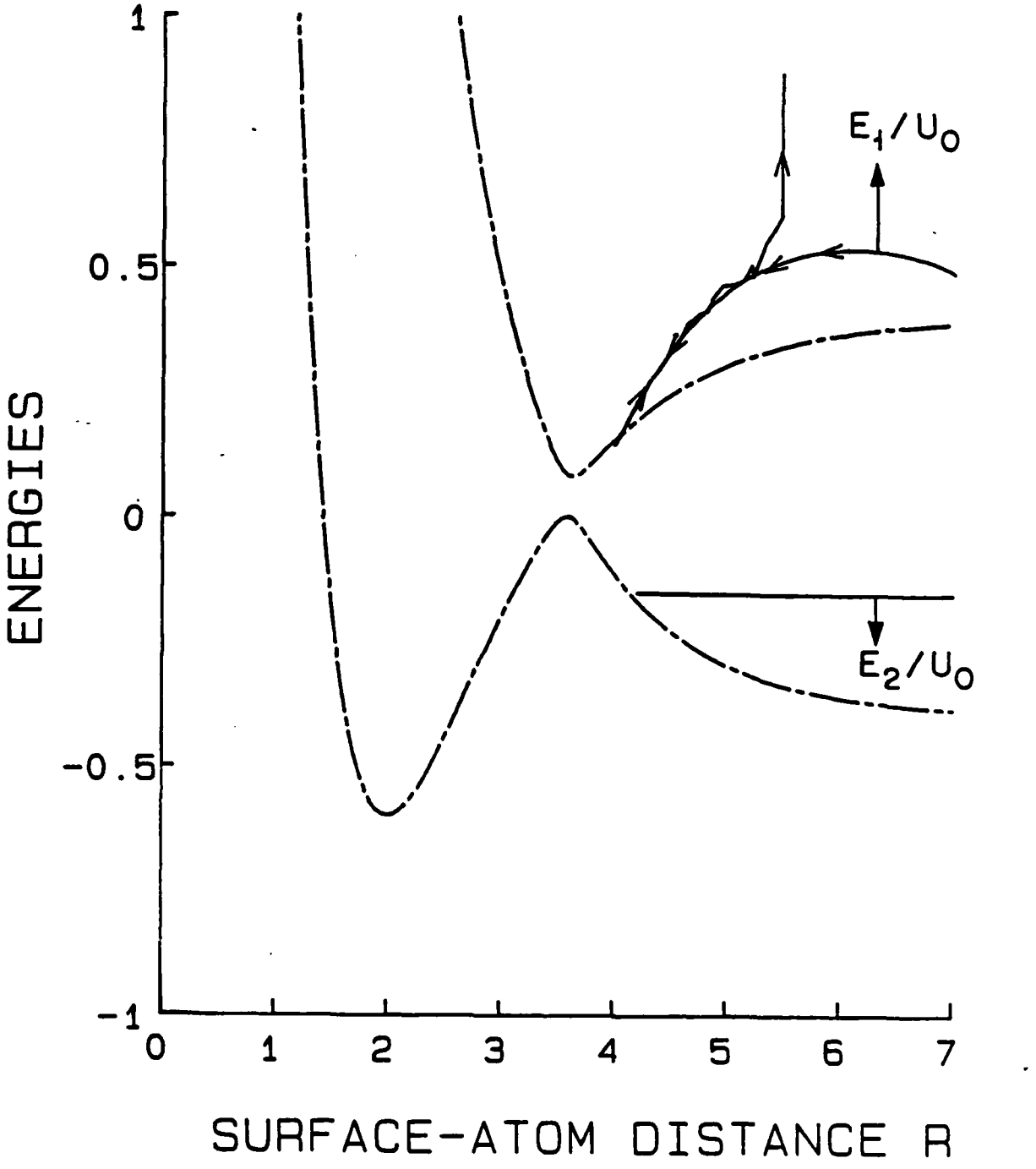
1
0.5
0
-0.5
-1
ENERGIES
E_1/U_0
E_2/U_0
0
1
2
3
4
5
6
7
SURFACE-ATOM DISTANCE R

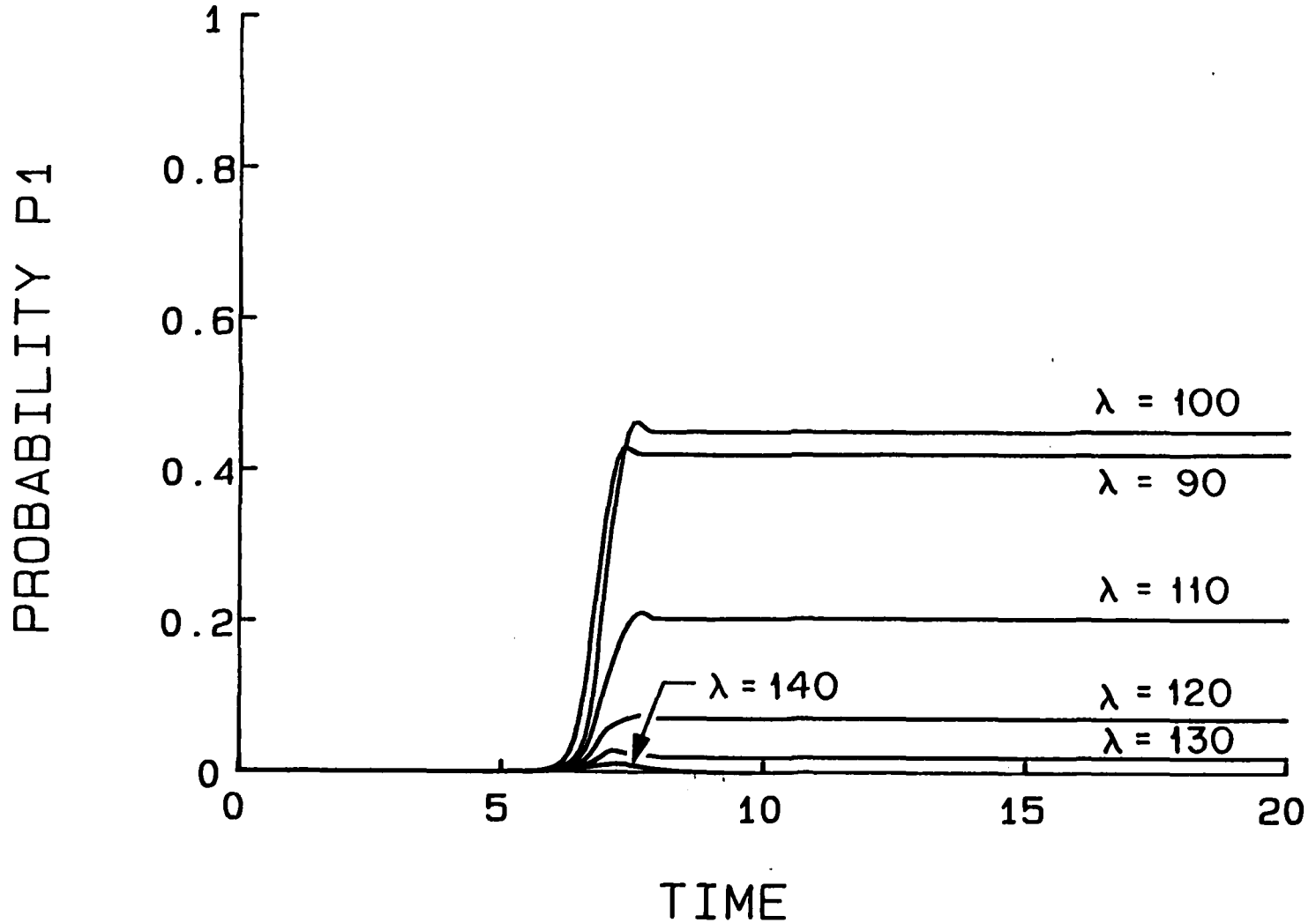
PROBABILITY P1
1
0.8
0.6
0.4
0.2
0
0
5
10
15
20
TIME
λ = 100
λ = 90
λ = 110
λ = 140
λ = 120
λ = 130

1
2
1
2
1
2
1
2

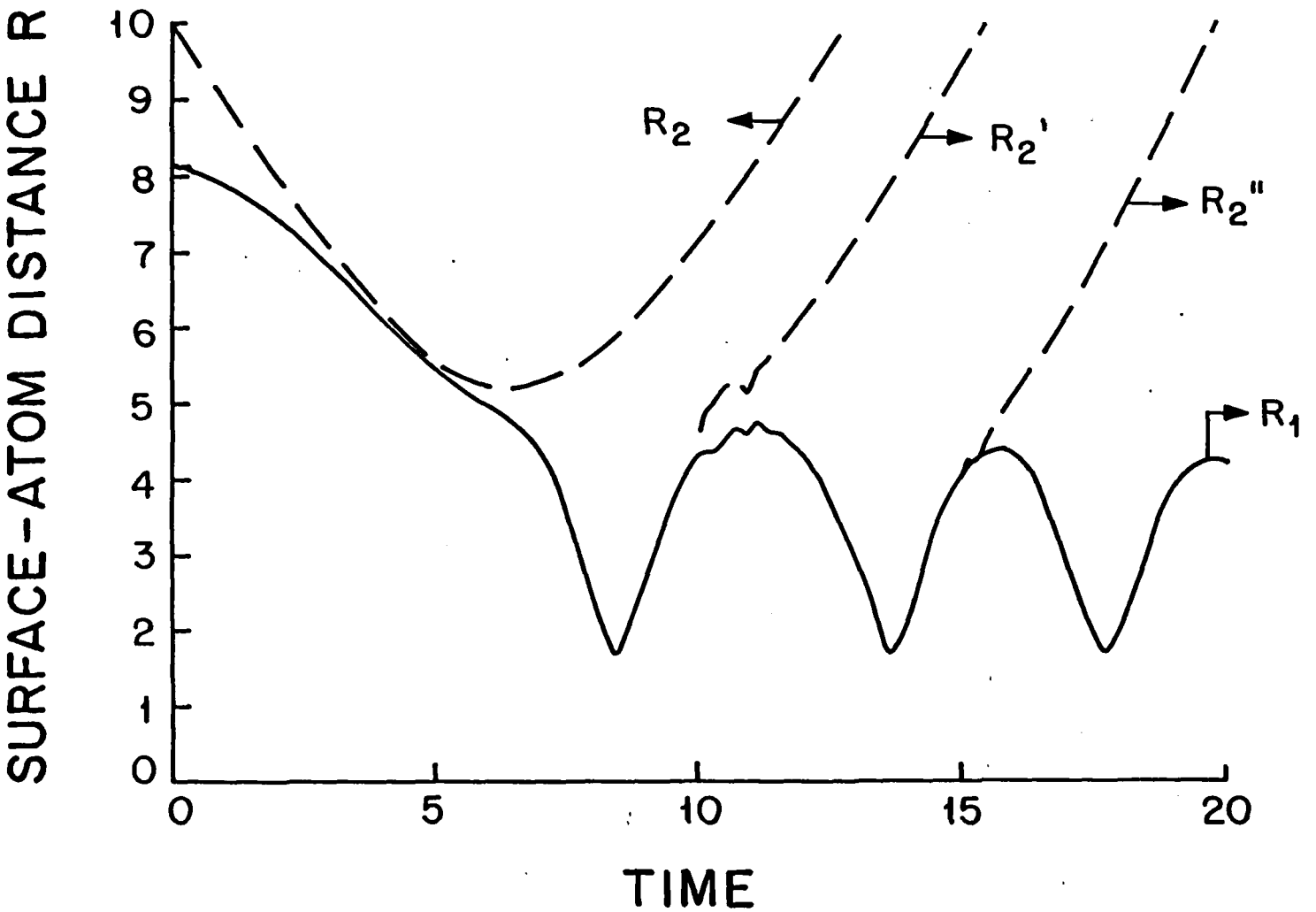
SURFACE-ATOM DISTANCE R
10
9
8
7
6
5
4
3
2
1
0
0
5
10
15
20
TIME
R2
R2'
R2"
R1

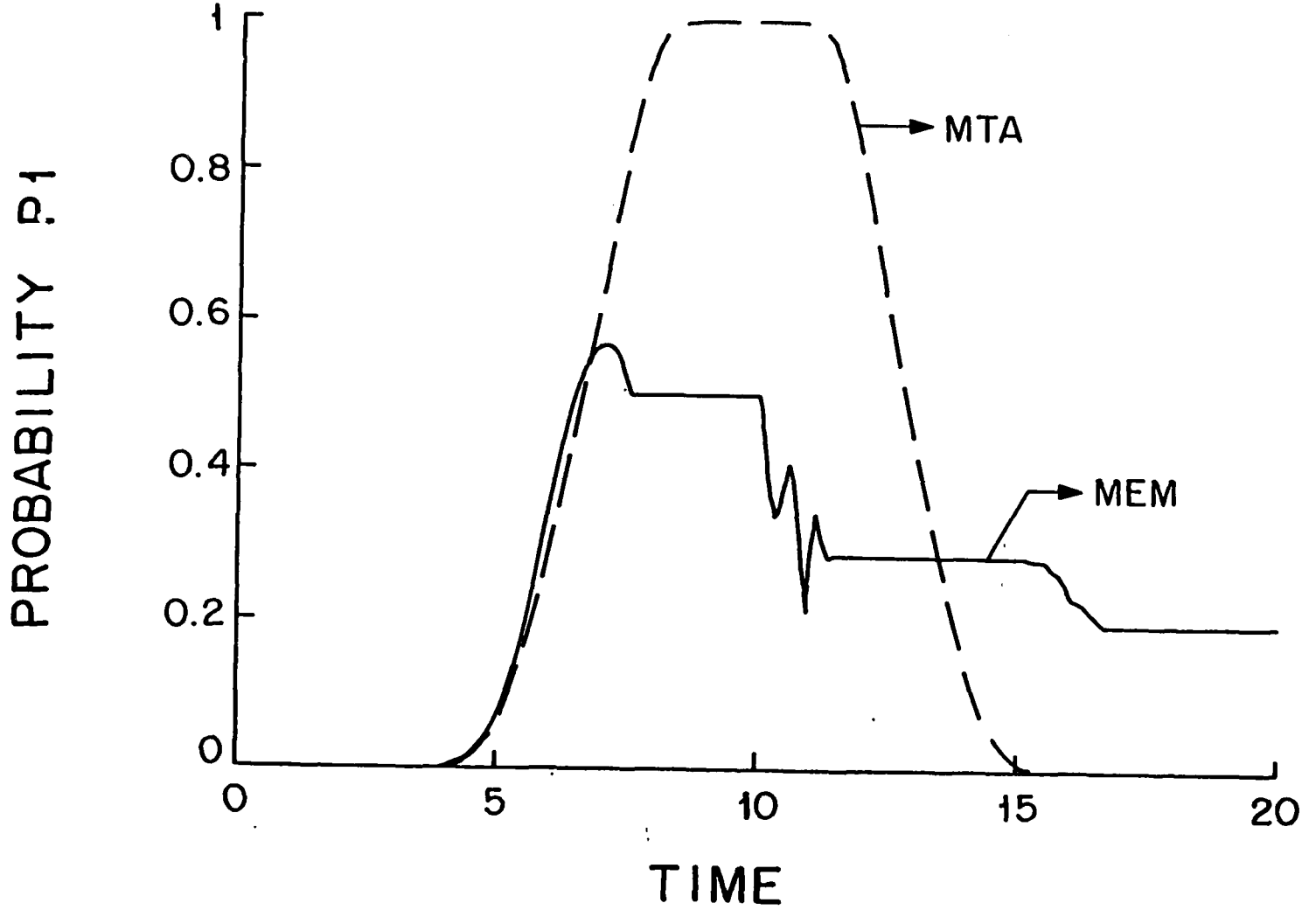
PROBABILITY P1
1
0.8
0.6
0.4
0.2
0
0
5
10
15
20
TIME
MTA
MEM

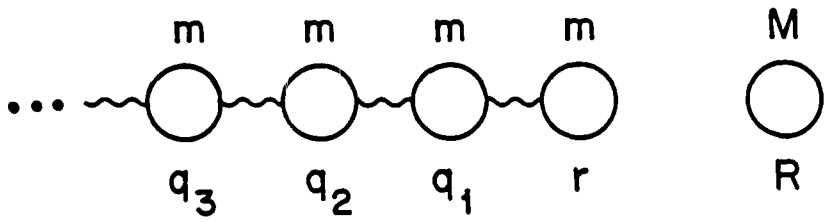
m
m
m
m
M
q_3
q_2
q_1
r
R

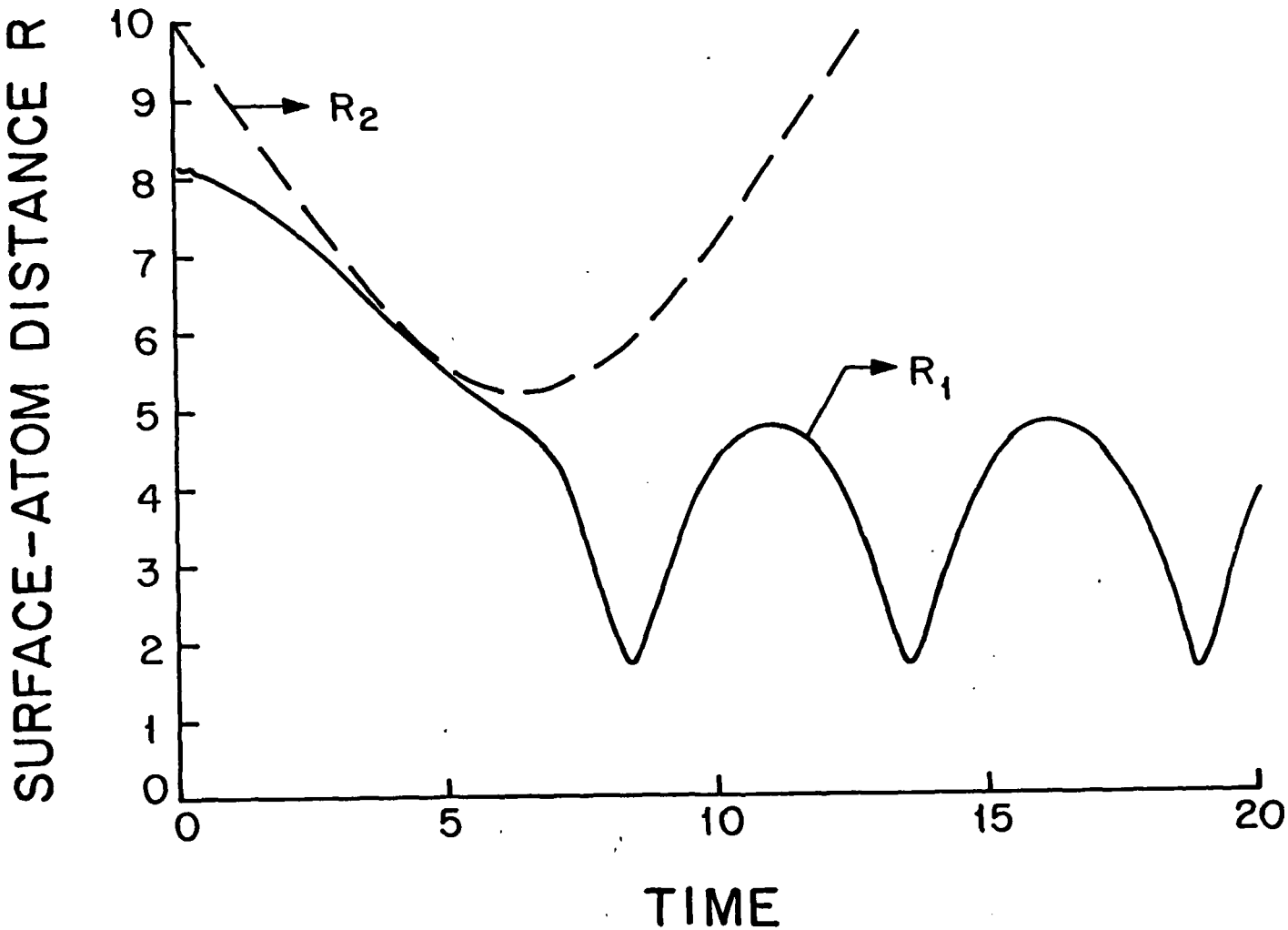
SURFACE-ATOM DISTANCE R
10
9
8
7
6
5
4
3
2
1
0
R_2
R_1
0
5
10
15
20
TIME

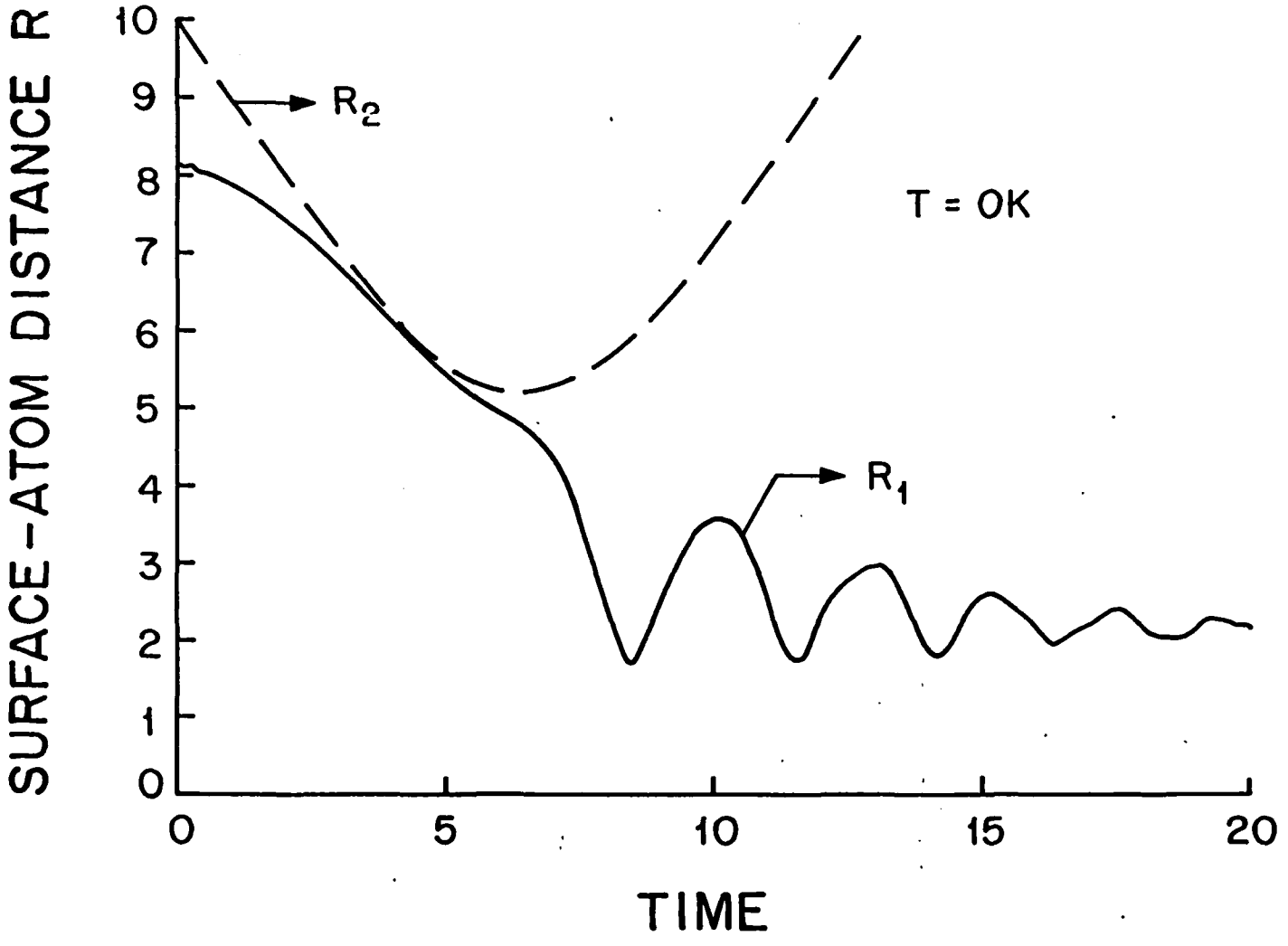
SURFACE-ATOM DISTANCE R
10
9
8
7
6
5
4
3
2
1
0
R_2
R_1
T = OK
0
5
10
15
20
TIME

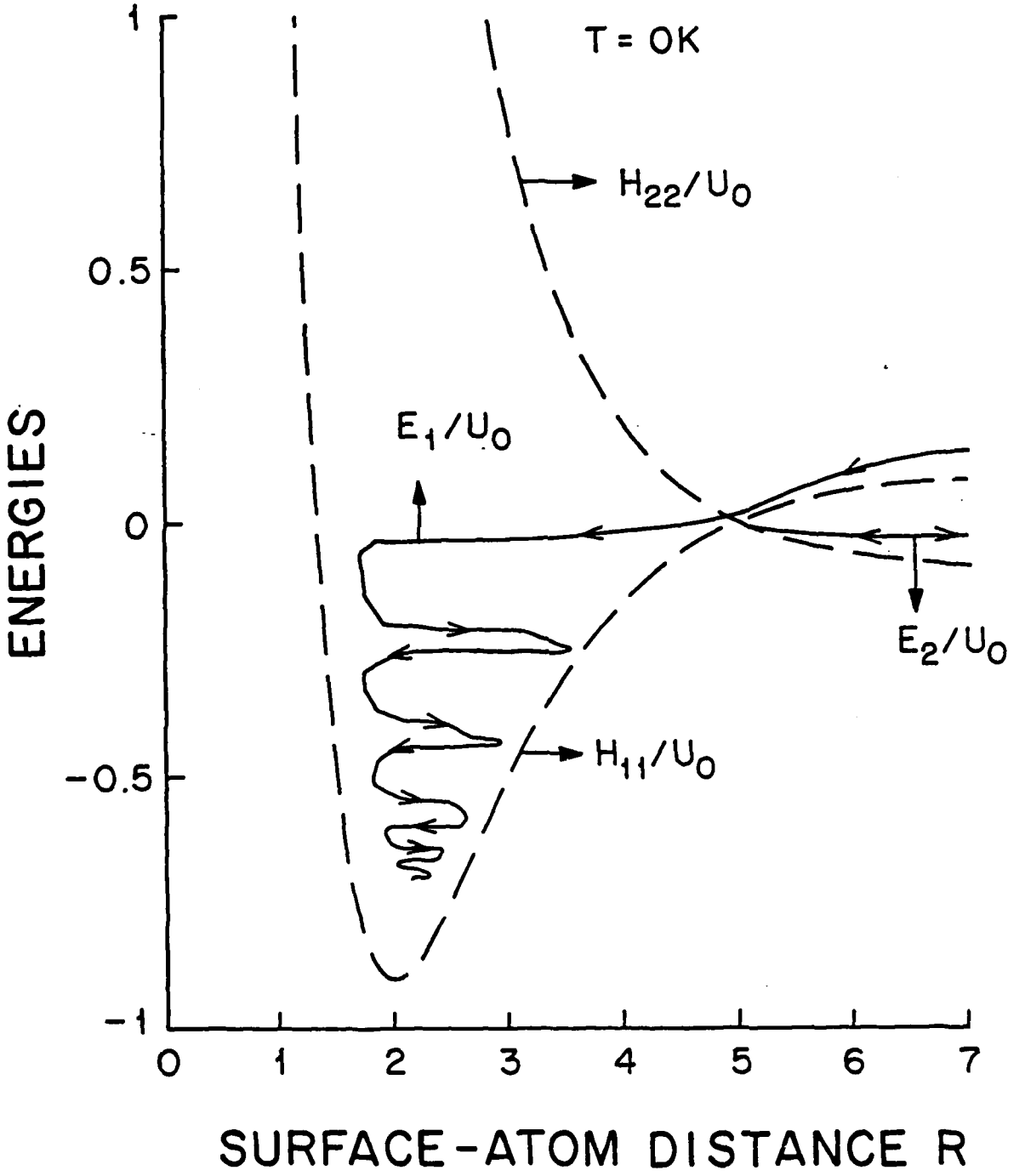
T = OK
H_{22}/U_0
E_1/U_0
E_2/U_0
H_{11}/U_0
ENERGIES
1
0.5
0
-0.5
-1
0
1
2
3
4
5
6
7
SURFACE-ATOM DISTANCE R

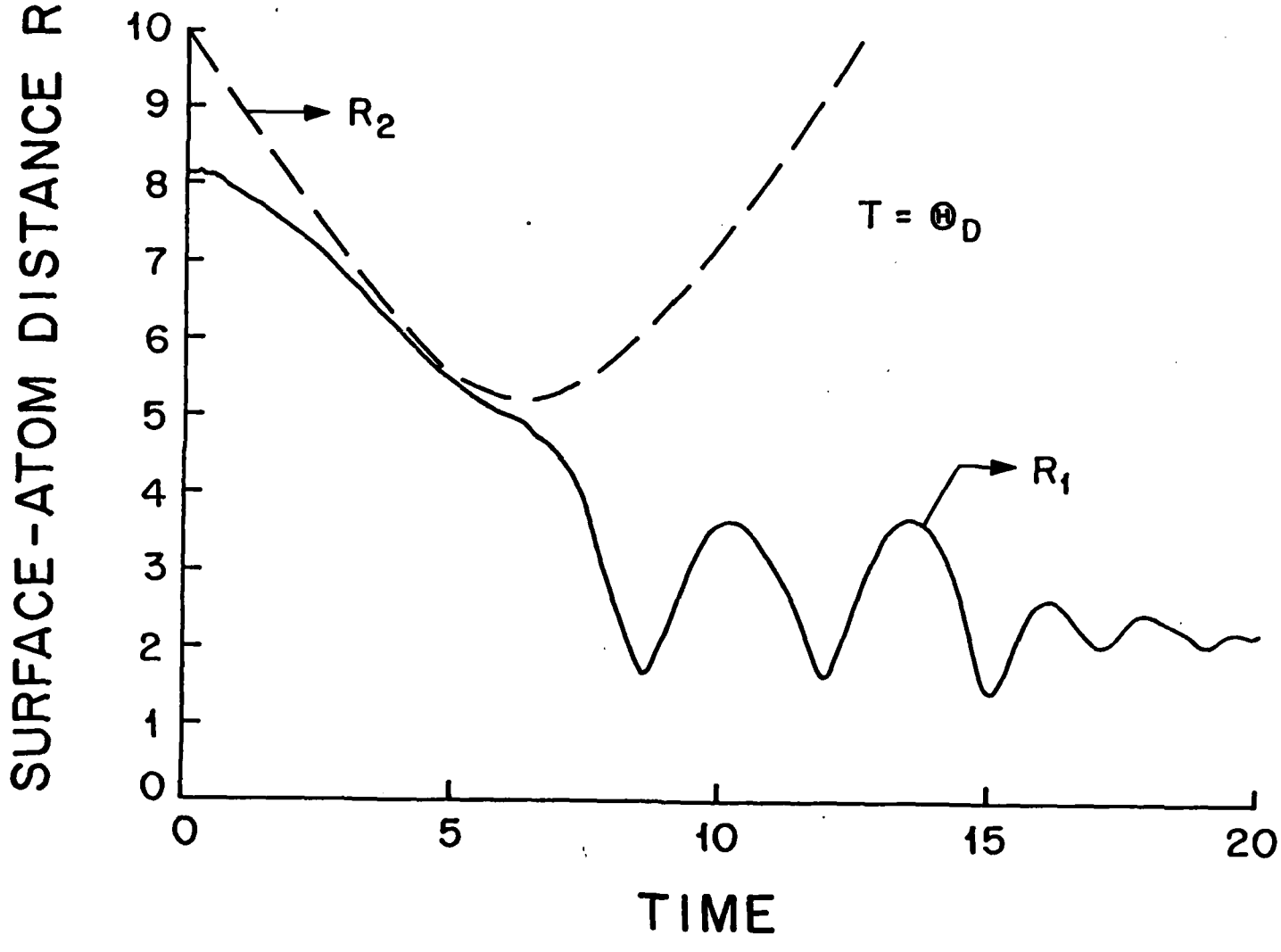
SURFACE-ATOM DISTANCE R
10
9
8
7
6
5
4
3
2
1
0
R_2
$T = \Theta_D$
R_1
0
5
10
15
20
TIME

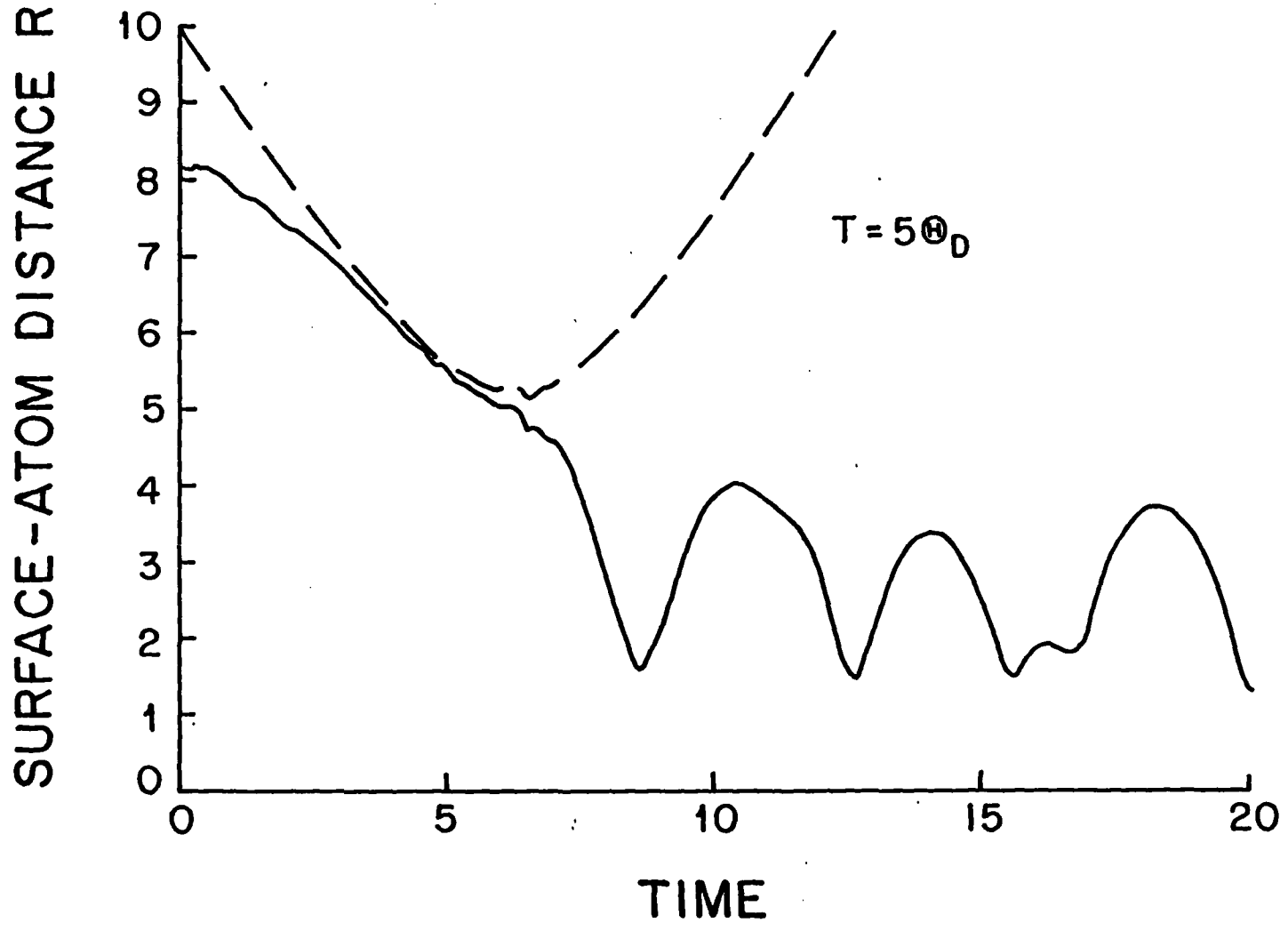
SURFACE-ATOM DISTANCE R
10
9
8
7
6
5
4
3
2
1
0
0
5
10
15
20
TIME
T = 5Θ_D

END

FILMED

5-86

DTIC